Epigenetic Regulation in Trained and Tolerized Macrophages

Miss Salisa Benjaskulluecha

จุฬาลงกรณ์มหาวิทยาลัย
CHULALONGKORN UNIVERSITY

A Dissertation Submitted in Partial Fulfillment of the Requirements

for the Degree of Doctor of Philosophy in Medical Microbiology

Medical Microbiology,Interdisciplinary Program

GRADUATE SCHOOL

Chulalongkorn University

Academic Year 2022

บทบาทของการควบคุมเชิงอิพิเจเนติกในแมโครฝาจชนิด Trained และชนิด Tolerized

น.ส.สลิษา เบญจสกุลลือชา

Thesis Title   Epigenetic Regulation in Trained and Tolerized Macrophages

By   Miss Salisa Benjaskulluecha

Field of Study   Medical Microbiology

Thesis Advisor   Professor TANAPAT PALAGA, Ph.D.

Thesis Co Advisor   Associate Professor ASADA LEELAHAVANICHKUL, M.D., Ph.D.

Accepted by the GRADUATE SCHOOL, Chulalongkorn University in Partial Fulfillment of the Requirement for the Doctor of Philosophy

-- Dean of the GRADUATE SCHOOL

(Associate Professor YOOTTHANA CHUPPUNNARAT, Ph.D.)

DISSERTATION COMMITTEE

-- Chairman

(Professor NATTIYA HIRANKARN, M.D., Ph.D.)

-- Thesis Advisor

(Professor TANAPAT PALAGA, Ph.D.)

-- Thesis Co-Advisor

(Associate Professor ASADA LEELAHAVANICHKUL, M.D., Ph.D.)

-- Examiner

(TEERAWUT NEDUMPUN, D.V.M., Ph.D.)

-- Examiner

(Associate Professor ORANART MATANGKASOMBUT, D.D.S., Ph.D.)

-- External Examiner

(Associate Professor Patompon Wongtrakoongate, Ph.D.)

สลิษา เบญจสกุลลือชา : บทบาทของการควบคุมเชิงอิพิเจเนติกในแมโครฟาจชนิด Trained และชนิด Tolerized.
(Epigenetic Regulation in Trained and Tolerized Macrophages) อ.ที่ปรึกษาหลัก : ศ. ดร.ธนาภัทร ปาลกะ,
อ.ที่ปรึกษาร่วม : รศ. นพ. ดร.อัษฎาศ์ ลีฬหวนิชกุล

ความทรงจำของภูมิคุ้มกันที่มีมาแต่กำเนิด (Innate immune memory) เป็นปรากฏการณ์ที่เซลล์ในระบบภูมิคุ้มกันที่
มีมาแต่กำเนิดสามารถเพิ่ม (trained) หรือยับยั้ง (tolerized) การตอบสนองของระบบภูมิคุ้มกันต่อการกระตุ้นครั้งที่สอง จาก
การศึกษาก่อนหน้าแสดงให้เห็นว่าการควบคุมเชิงอิพิเจเนติกส์ (epigenetic) เป็นกลไกหลักในการควบคุมความทรงจำทั้งสองชนิด
อย่างไรก็ตามความเข้าใจกลไกการควบคุม innate immune memory อย่างรอบด้านยังไม่ครบถ้วน ในการศึกษานี้ผู้วิจัยจึงได้คัด
กรองสารที่ออกฤทธิ์ต่อกลไกทางอิพิเจเนติกส์ เพื่อค้นหาโปรตีนที่มีผลต่อการควบคุมภูมิคุ้มกันแบบ trained ที่เหนี่ยวนำด้วยเบต้า
กลูแคน (BG-trained) และ แบบ tolerized ที่เหนี่ยวนำด้วย LPS (LPS-tolerized) ในแมโครฟาจ จากสารประกอบจำนวนทั้งหมด
181 สารได้รับการทดสอบ พบว่าสารประกอบที่ออกฤทธิ์ต่อโปรตีน Aurora kinase, histone methyltransferase PRMT และ
EZH2, histone demethylase LSD1 และ JMJD2, histone deacetylase 6 และ sirtuin-1, และ PARP แสดงฤทธิ์ยับยั้งต่อการ
กดภูมิคุ้มกันจากการเหนี่ยวนำด้วย LPS โดยส่งเสริมการผลิต TNFα ในการศึกษานี้มุ่งเน้นการทดสอบบทบาทของ LSD1 ในการ
ควบคุมภูมิคุ้มกันแบบ LPS-tolerized จากผลการทดลองพบว่าการยับยั้งการทำงานด้วยสารที่ออกฤทธิ์ต่อ LSD1 และการยับยั้ง
การแสดงออกของยีน LSD1 ด้วย siRNA เพิ่มการผลิตไซโตไคน์ในแมโครฟาจที่เหนี่ยวนำด้วย LPS อย่างไรก็ตามไม่พบการ
เปลี่ยนแปลงระดับของเครื่องหมาย H3K4me3 ที่บริเวณ *Tnf* promoter เมื่อการทำงานของ LSD1 ถูกยับยั้ง ในภูมิคุ้มกันแบบ
BG-trained พบว่าสารที่ออกฤทธิ์ยับยั้งโปรตีน O^6-methylguanine DNA methyltransferase (MGMT) ซึ่งเป็นเอนไซม์
เมทิลทรานสเฟอเรสซ่อมแซมดีเอ็นเอที่ได้รับบาดเจ็บที่เกิดจากสารอัลคาไลต์ สามารถควบคุมภูมิคุ้มกันแบบ BG-trained ในแมโคร
ฟาจ ระดับการแสดงออกของ MGMT เพิ่มขึ้นอย่างมีนัยสำคัญหลังจากถูกกระตุ้นด้วย BG และเมื่อยับยั้งหรือกดการแสดงออกของ
MGMT หลังจากกระตุ้นด้วย BG นำไปสู่การเพิ่มการอักเสบใน BG-trained c,แมโครฟาจ อย่างไรก็ตาม การขาดยีน MGMT ทำให้
การผลิตไซโตไคน์ที่ส่งเสริมการอักเสบลดลงทั้งในการศึกษาจากหลอดทดลองในแมโครฟาจ และในหนูทดลองที่มีการขาดยีนอย่าง
จำเพาะในเซลล์มัยดีลอยด์ โดยการขาดยีน MGMT เหนี่ยวนำให้เกิดการลดลงของสัญญาณภายใต้การทำงานของ TLR4 receptor
เช่น p38 และ SAPK/JNK และสัญญาณภายใต้การทำงานของ Dectin-1 receptor เช่น mTOR และ glycolysis ในแมโครฟาจที่
เหนี่ยวนำด้วย BG จากข้อมูลทางทรานสคริปโตมบ่งชี้ว่า MGMT อาจควบคุม trained immunity ผ่านทาง farnesoid X
receptor (*Nr1h4*) และ PR domain zinc figure protein 5 (*Prdm5*) เป็นต้น ผลลัพธ์เหล่านี้บ่งชี้ถึงบทบาทใหม่ของโปรตีน
MGMT ในการควบคุมภูมิคุ้มกันแบบ BG-trained นอกเหนือจากบทบาทในการซ่อมแซมดีเอ็นเอ ผลลัพธ์ที่ได้จากการศึกษาเหล่านี้
บ่งชี้ว่า innate immune memory ถูกควบคุมด้วยกลไกหลายชนิด โปรตีนเป้าหมายใหม่ที่ค้นพบจากงานวิจัยนี้มีศักยภาพในการ
ควบคุม innate immune memory ซึ่งสามารถนำไปประยุกต์ใช้ในการรักษาโรคได้ในอนาคต

สาขาวิชา	จุลชีววิทยาทางการแพทย์ (สหสาขาวิชา)	ลายมือชื่อนิสิต ....
ปีการศึกษา	2565	ลายมือชื่อ อ.ที่ปรึกษาหลัก ....
		ลายมือชื่อ อ.ที่ปรึกษาร่วม ....

6087802020 : MAJOR MEDICAL MICROBIOLOGY

KEYWORD: Innate immune memory, Macrophages, Trained immunity, LPS tolerance, O6-methylguanine DNA methyltransferase

Salisa Benjaskulluecha : Epigenetic Regulation in Trained and Tolerized Macrophages. Advisor: Prof. TANAPAT PALAGA, Ph.D. Co-advisor: Assoc. Prof. ASADA LEELAHAVANICHKUL, M.D., Ph.D.

Innate immune memory is the phenomenon that can either enhance (trained) or suppress (tolerized) immune response by innate immune cells during the second encounter of the stimuli such as pathogens. Previous studies reported that epigenetic regulations critically regulate both types of innate immune memory. However, a complete understanding of the underlying mechanisms is still lacking. In this study, we performed a screening of an epigenetics compound library to identify inhibitors that affect ß-glucan (BG)-trained or LPS-tolerized macrophages. Among 181 compounds tested, various inhibitors targeting Aurora kinase, histone methyltransferase PRMT and EZH2, histone demethylase LSD1 and JMJD2, histone deacetylase 6 and sirtuin-1, and PARP showed inhibitory activity against LPS tolerance by promoting effects on TNFα production. The effect of LSD1 in LPS tolerance was validated in this study. Inhibition or silencing of LSD1 results in suppressed LPS tolerance by enhance cytokines production. However, no change was observed in H3K4me3 level associated with the *Tnf* promoter upon LSD1 inhibition. In trained immunity, we identified an inhibitor of O^6-methylguanine DNA methyltransferase (MGMT), a DNA repair enzyme of the lesion triggered by alkylating agent, as a novel regulator of trained immunity in macrophages. MGMT expression significantly increased after the priming with BG, and inhibition or silencing of MGMT expression during the priming resulted in increased trained immunity. To further investigate the role of MGMT in trained immunity, mice with myeloid specific deletion of MGMT were generated (LysM-cre$^{cre/+}$; MGMT$^{fl/fl}$ mice). However, targeted deletion of MGMT expression resulted in a decrease in proinflammatory cytokines production in trained immunity both *in vitro* and *in vivo*. Depletion of MGMT in trained macrophages resulted in decrease downstream signaling molecules of TLR4 receptor, such as p38 and SAPK/JNK. In addition, signaling downstream of dectin-1 receptor, such as mTOR, and glycolytic function was also damped. These results highlight the unexpected role of MGMT in regulation of trained immunity beyond its role in DNA repair. Based on transcriptomic data, MGMT may regulate trained immunity through farnesoid X receptor (*Nr1h4*) and PR domain zinc figure protein 5 (*Prdm5*). Taken together, this screening approach indicates that innate immune memory is regulated by numerous mechanisms and the novel target proteins identified from this research has the potential to regulate innate immune memory, which could be used as a target of therapeutic agents for several diseases.

Field of Study:	Medical Microbiology	Student's Signature ....
Academic Year:	2022	Advisor's Signature ....
		Co-advisor's Signature ....

ACKNOWLEDGEMENTS

TABLE OF CONTENTS

LIST OF ABBREVIATIONS

AP1	Activator protein 1
AURK	Aurora kinase
BCG	Bacillus Calmette-Guerin (BCG)
BG	β-glucan
Camp	Cathelicidin
DAMPs	Damage-associated molecular patterns
DNA MT	DNA methyltransferase
DNA/RNAsyn	DNA/RNAsyn: DNA/RNA synthesis
Dnmt3a/b	DNA (cytosine-5)-methyltransferase 3A
ECAR	Extracellular acidification rate
EZH2	Enhancer of zeste homolog 2
FXR	Farnesoid X receptor
H3ac	Acetylation of histone H4
H4ac	Acetylation of histone H4
H3K4me1	Mono-methylation of lysine 4 on histone 3
H3K4me3	Tri-methylation of lysine 4 on histone 3
H3K9me2	Di-methylation of lysine 9 on histone H3
H3K9me3	Tri-methylation of lysine 9 on histone 3
H3K27ac	Acetylation of lysine 27 on histone H3
H3S10ph	Phosphorylation of serine 10 on histone H3
H3S28ph	Phosphorylation of serine 28 on histone H3
HDAC	Histone deacetylase
HDM	Histone demethylase
HIF-1α	Hypoxia Inducible factor 1 subunit alpha
HMT	Histone methyltransferase

IGF1R	Insulin-like growth factor 1
IKK	I kappa B kinases
IPLs	Immune gene priming long non-coding RNA
lncRNA	Long non-coding RNA
IRF3	Interferon regulatory factor 3
IRF5	Interferon regulatory factor 5
JMJD2	Jumonji C domain-containing protein 2
LPS	Lipopolysaccharide
LSD1	Lysine specific demethylase 1
LysM-cre$^{cre/+}$	LysM-cre mice
LysM-cre$^{cre/+}$; MGMT$^{fl/fl}$	Myeloid specific MGMT knockout mice
LysM-Cre$^{+/+}$; MGMT$^{fl/fl}$	Littermate control mice
MAPK	Mitogen-activated protein kinases
MARCO	Macrophage receptor with collagenous structure
MGMT	O^6-methylguanine DNA methyltransferase
MGMT$^{fl/fl}$	MGMT-LoxP mice
mTOR	Mechanistic target of rapamycin
NcoR1	Nuclear receptor corepressor 1
NFAT	Nuclear factor of activated T-cells
NF-κB	Nuclear factor kappa B
NOC	N-nitroso compounds
NR1H4	Nuclear receptor subfamily 1 group H member 4
NT-genes	Non-tolerizeable genes
O^6-MeG	O^6-methylguanine
oxLDL	Oxidized low-density lipoprotein
PAMPs	Pathogen-associated molecular patterns
PARP	Poly (ADP-ribose) polymerase

PRC2	Polycomb repressive complex-2
PRDM5	PR domain zinc figure protein 5
PRMT	Protein arginine methyltransferase
SAM	S-adenosyl methionine
SHIP	SH2-containing inositol phosphatase
SIRT1	Sirtuin1
SOSC1	Suppressor of cytokine signaling-1
SOSC3	Suppressor of cytokine signaling-3
TCA cycle	Tricarboxylic acid cycle
T-genes	Tolerizeable genes
TIRAP	Toll receptor IL-1R domain-containing adaptor protein
TLR4	Toll-like receptor 4
TNFα	Tumor necrosis factor
TRAF3	Tumor necrosis factor receptor associated factor 3
TRAF6	Tumor necrosis factor receptor associated factor 6
TRAM	TRIF-related adaptor molecule
UMLILO	Upstream master long non-coding RNA of the inflammatory chemokine locus

CHAPTER I
BACKGROUND AND RATIONALES

Innate immune response, as the first line of defense mechanism, is generally nonspecific and was thought to have no memory. However, organisms lacking adaptive immune response such as plants and invertebrates exhibit characteristics of immune memory, by altering in innate immune response after previous infection, such as greater response to secondary infection and transplantation rejection. Innate immune memory has two main opposite outcomes which are "trained", the memory that enhances immune response against secondary infection, and "tolerance", the memory that suppresses immune response against the secondary infection that plays important role in post sepsis immune paralysis (1).

Previous studies reported that epigenetic is the main mechanism regulating innate immune memory. Epigenetic is the process that reprograms cellular phenotype without changing in DNA sequence. The mechanisms include histone modification, DNA methylation, micro and long non-coding RNA (2). Histone modification is the most widely studied epigenetic mechanism in innate immune memory. However, only a few histone marks have been studied and reported to be important for innate immune memory and the effect of others epigenetic mechanisms in innate immune memory induction is poorly characterized. Therefore, this project aimed to investigate other unappreciative epigenetic mechanism(s) that may control innate immune memory by using β-glucan (BG)-induced trained and lipopolysaccharide (LPS)-induced tolerized macrophages as a model. We performed a large-scale screening of the epigenetic modifying inhibitors to identify novel epigenetic mechanisms in trained and tolerance immunity. The effective target from the screening step were selected for further study using *in vitro* gene knock down and *in vivo* gene knock out

macrophages. Understanding the epigenetic mechanism of innate immune memory will provide novel strategies for improving efficiency of vaccines and developing a new therapeutic agent against cancer and immune paralysis in sepsis.

CHAPTER II

LITERATURE REVIEW

2.1 Innate immune memory

Innate immune memory is recently recognized as the phenomenon that the previous infection or vaccination has on innate immune cells, including macrophages, neutrophils, or innate lymphoid cells (2, 3). In contrast to an adaptive immune memory, innate immune memory persists for relatively short duration, limited specificity and does not involve antigen receptors generated by gene rearrangement (2-4). Currently, innate immune memory can be classified into two different types: "trained immunity" which produces heightened immune response that induce non-specific protection and "tolerance" which results in repressive immune response to prevent excessive damage to host that manifests in defective of immune response in cancer and sepsis (**Figure 2.1**, (2, 3, 5)). These two types of innate immune memory can be induced by specific stimuli as shown in **Table 2.1** (6).
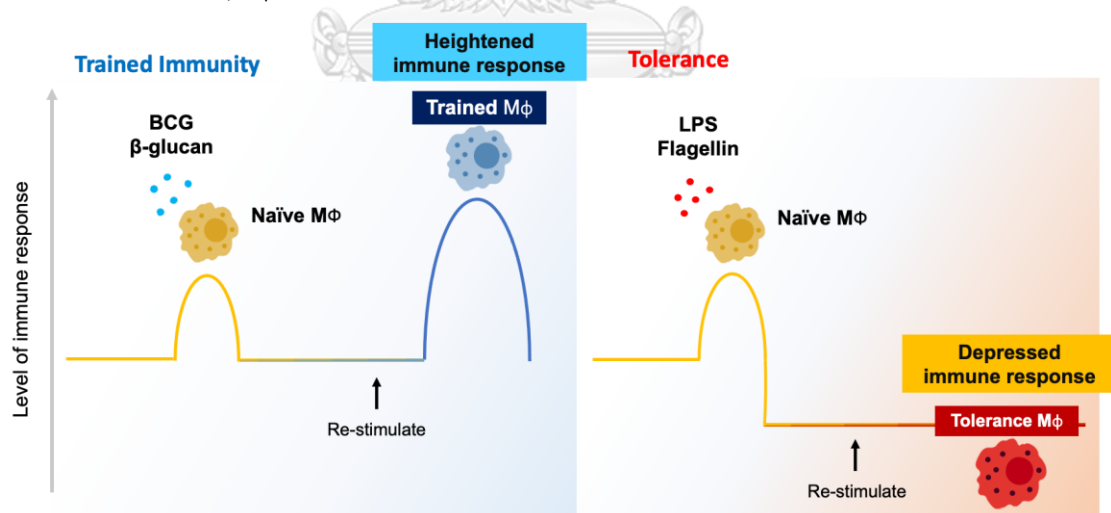
Figure 2.1 Innate immune memory in macrophages

The innate immune system possesses immune memory that can be induced by specific stimuli such as BG, Bacillus Calmette-Guerin (BCG) and others, resulting in

trained immunity, which induces a heightened immune response and non-specific protection. Alternatively, the innate immune memory induced by specific stimuli, such as LPS, flagellin and others, resulting in tolerance phenotype, which induces an immune repressive stage.

2.1.1 Trained immunity

Trained immunity is the heightened status of innate immune memory that enhances immune response and induces non-specific protection. The trained immunity can be generated by priming of innate immune cells with specific pathogen-associated molecular patterns (PAMPs) or damage-associated molecular patterns (DAMPs) such as BG, BCG and others metabolites such as oxidized low-density lipoprotein (oxLDL), and mevalonate (**Table 2.1**, (1, 5, 7)). These stimuli induce cellular reprograming leading to heightened immune response with non-specific secondary stimulation (2, 3, 5). The effect of trained immunity can be observed as the protective immune response against re-infection in plants (8) and invertebrates (9, 10), non-specific protection after vaccination in humans (11-13). Besides the protective role of trained immunity, the maladaptive trained immunity has been associated with numerous hyperinflammatory diseases such as allergy, atherosclerosis and Alzheimer's disease (1, 2, 7).

2.1.2 Tolerance

Tolerance is a hyporesponsive stage of innate immune response by innate immune cells which is induced after hyperinflammation or infection mainly to prevent over inflammatory response (14). Innate immune cells can be induced into tolerance stage by primary stimulation with potent inflammatory stimulators, most of which are activators of Toll-like receptor (TLR) such as LPS, Pam3CSK4 and others (**Table 2.1**). The stimulation can induce high level of cytokine production and others inflammatory genes in the primary stage. After primary stimulation, the immune responses are repressed upon stimulation with the same or different stimulants (14, 15). However,

the tolerance process has been associated with post sepsis immune paralysis which the immune response is repressed leading to susceptible to opportunistic infection (2, 16). On the other hand, it also plays important roles in mucosal tolerance and controls the tissue damage during infection (2, 14).

Table 2.1: Reported primary stimuli of trained and tolerance immunity

Phenotype	Primary stimuli	Target cells/ animals	References
Trained immunity	Bacillus Calmette-Guerin (BCG)	Monocyte	Arts et al., 2016 (11), Kleinnijenhuis et al., 2012 (17),
	β-glucan (BG)	Monocyte	Quintin et al., 2012 (18),
	Lipoprotein(a)	Monocyte	Van der Valk et al., 2016 (19),
	Oxidized low-density lipoprotein (oxLDL)	Monocyte	Bekkering et al., 2014 (20)
	Mevalonate	Monocyte/Human (mevalonate kinase deficiency)	Bekkering et al., 2018 (21)
	BG vaccination	C57Bl/6J mice	Garcia-Valtanen et al., 2017 (22)
	BCG vaccination	Human	Arts et al., 2016 (11),
	Plasmodium falciparum	PBMC	Schrum et al., 2018 (23)
Tolerance	Toll-like receptor (TLR) agonists: TLR 4: LPS, TLR 2: Pam3CSK4,	Macrophages /Monocyte	Foster et al., 2007 (14), Van der Heijden et al., 2018 (5), Novakovic et al., 2016 (24),

	TLR 3: poly(I:C), TLR 5: flagellin		Ifrim et al., 2014 (25), Lachmandas et al., 2016 (26)
	Systemic infection with bacteria	Mice and human	Foster et al., 2007 (14),

2.2 Regulation of innate immune memory in macrophages

2.2.1 Epigenetic regulation of the innate immune memory

After previous infections or vaccinations, it was shown that epigenetic changes accompany gene expression profiles in innate immune cells (2, 27). The discovery that epigenetic regulation is the key mechanism of innate immune memory stemmed from the report in the LPS-tolerized macrophages, which many of inflammatory genes induced by TLR4 stimulation such as *Tnf* and *Il6* are repressed (14). It was showed that the recruitment of RNA polymerase to the regulatory regions of these repressed genes was reduced after successive LPS stimulation. It was hypothesized that the chromatin structures of these genes are altered during tolerance process. However, the expression of antimicrobial genes such as cathelicidin (*Cnlp*) and macrophage receptor with collagenous structure (*Marco*) which also under the regulation by TLR4 stimuli, were maintained in tolerized macrophages. These group of genes were characterized as non-tolerizeable genes (NT-gene) in LPS tolerance. This observation emphasized that changes in chromatin structures occur at specific positions (14). The up-stream mechanisms that can control the change of chromatin structure in specific region is histone modification. This mechanism relies on modification of the N-terminus of the tail in histone subunit by adding or removing functional groups to specific amino acids on the histone tail. These mechanisms create histone marks which can change the chromatin structure into opened or closed structure, depending on the type of modification (28). As expected, the level of active histone marks, such

as acetylation of histone H4 (H4ac) and acetylation of histone H3 (H3ac), are decreased in the promoters of inflammatory genes after successive LPS stimulation (14).

In trained macrophages, it has an increased active histone mark in the promoter of pro-inflammatory cytokine genes and inhibition of the enzyme that control the induction of these active histone marks reduces the cytokine expression (18). These results emphasize that histone modifications are crucial for induction of both trained and tolerized macrophages (2, 5, 14, 18). However, besides histone modifications, other mechanisms of epigenetics, such as DNA methylation and non-coding RNA expression, also play important role in innate immune memory. The effect of these epigenetic mechanisms on trained and tolerized macrophages are summarized in **Table 2.2**

Epigenetics regulation in trained immunity

Histone modification has been reported to be the major epigenetic regulation that control the induction of genes in trained immunity. Previous studies showed an enrichment of active histone marks, such as acetylation of lysine 27 on histone H3 (H3K27ac) and tri-methylation of lysine 4 on histone 3 (H3K4me3), in the promoter of genes associated with trained immunity, such as pro-inflammatory cytokines and intracellular signaling molecules, after priming with BG and re-stimulation with LPS (2, 18, 29). In addition, the enrichment of these active epigenetic marks was supported by the decrease in repressive epigenetic marks such as tri-methylation of lysine 9 on histone 3 (H3K9me3) and DNA methylation. After removing BG, the enrichment of mono-methylation of lysine 4 on histone 3 (H3K4me1), is observed which represent an enhancer characteristic mark in genomic regions that are unmarked in unstimulated cells. These reports indicate that the generation of latent enhancers is induced which functions as an immunological scar to promote faster and higher magnitude of response after re-stimulation (1, 2, 5, 7, 30).

Besides histone modification, the expression of long non-coding RNA (lncRNA), such as immune gene priming lncRNA (IPLs) and upstream master long non-coding RNA of the inflammatory chemokine locus (UMLILO), has been identified as a collaborative mechanism that regulate trained immunity with histone modification by perform 3D looping contact between the histone modifying enzyme and specific DNA region (1, 7, 31, 32). These findings emphasize that trained immunity is tightly regulated by several epigenetic mechanism (**Table 2.2**).

Epigenetics regulation in tolerance immunity

The repression of inflammatory genes in tolerized macrophages has been reported to associated with the failure to deposit active histone marks the H3ac, H4ac and H3K4me3 in the promoters of inflammatory genes after two successes stimulation with LPS, which is observed in a single LPS stimulation. Moreover, the level of repressive histone marks, such as di-methylation of lysine 9 on histone H3 (H3K9me2), were increased in the promoters of inflammatory genes after successive LPS stimulation (14, 33).

Besides the histone modification, DNA methylation also plays important role in the repression of tolerized genes as it has higher level of CpG methylation in the promoters of proinflammatory cytokine genes. DNA methylation is mediated by DNA (cytosine-5)-methyltransferase 3A (Dnmt3a/b) which is recruited after the enrichment of H3K9me2. This finding emphasizes the epigenetics crosstalk between histone modification and DNA methylation during the induction of tolerance (**Table 2.2**, (34-36)).

Table 2.2 Epigenetic mechanisms reported to control innate immune memory

Phenotype	Epigenetic Mechanism	Function	References
Trained immunity	Histone modification	Increase active histone marks: H3K27Ac, H3K4me3	Quintin et al., 2012 (18), Saeed et al., 2014 (29),
		Generation of latent enhancer marks: H3K4me1	Saeed et al., 2014 (29), Ostuni et al., 2013 (30)
		Decrease repressive histone marks: H3K9me3	Netea et al., 2016 (2),
	DNA methylation	Loss of DNA Methylation in the promoter of inflammatory genes	Das et al., 2019 (37) Verma et al., 2017 (38)
	lnRNA expression	Expression of UMLILO and IPLs	Fanucchi et al., 2019 (31, 32)
Tolerance	Histone modification	Decrease active histone marks in cytokine promoter: H3ac, H4ac, and H3K4me3	Foster et al., 2007 (14), Sun et al., 2019 (39)
		Increase repressive histone marks in cytokine promoter: H3K9me2	El Gazzar et al., 2008 (34)
	DNA methylation	CpG methylation in cytokine promoter	El Gazzar et al., 2008 (34)

2.2.2 Metabolic reprogramming of innate immune memory

Metabolic reprogramming is one of the mechanisms that regulates the induction of innate immune memory. Several metabolites in metabolic pathway have specific roles in modulating inflammation modulation and epigenetic regulation in innate immune cells.

Metabolic reprogramming in trained immunity

Trained macrophages induce the shift of metabolic pathway from oxidative phosphorylation to aerobic glycolysis. As glycolysis can produce energy faster than the conventional pathway, this metabolic reprogramming allows trained macrophages to meet their high demand of energy consumption in a short time and inhibition of metabolic shift in trained macrophages has been reported to interfere with in trained immunity (1, 7, 40).

Besides up regulation of glycolysis pathway, several metabolites in the tricarboxylic acid (TCA) cycle, including α-ketoglutarate and its derivative such as 2-hydeoxyglutarate, succinate and fumarate, are accumulated in trained macrophages. These metabolites can inhibit KDM5 histone lysine demethylase enzyme that results in promote positive epigenetic modification in trained genes (7). The accumulation of these metabolites results from epigenetic changes that promote the expression of genes in TCA cycle such as succinate dehydrogenase (1, 40, 41). These findings indicate that metabolic and epigenetic are tightly regulated in trained immunity (**Table 2.3**).

Metabolic reprogramming in tolerance

In the priming step of LPS tolerance, macrophages are strongly activated and the switch of metabolic pathway to glycolysis is induced. However, re-stimulation of LPS results in defect of both glycolysis and oxidative phosphorylation (42). In addition, accumulation of some metabolites such as lactate (43), and itaconate (44) has been reported in LPS-tolerized macrophages. These metabolites can inhibit TLR4 signaling

molecules and activate epigenetic reprogramming which promote the tolerized phenotype (**Table 2.3,** (1, 7)).

Table 2.3 Metabolic reprogramming in innate immune memory

Phenotype	Function	References
Trained immunity	Increase glycolysis	Cheng et al., 2014(40)
	Increase metabolites in TCA cycle derivatives of α-ketoglutarate	Fanucchi et al., 2020 (7)
	Increase Mevalonate pathway	Bekkering et al., 2018 (21)
Tolerance	Decrease glycolysis	Gillen et al., 2021 (42)
	Decrease oxidative phosphorylation	Gillen et al., 2021 (42)
	Itaconate accumulation	Mills et al., 2018 (44)
	Lactate accumulation	Zhang et al., 2019 (43)

2.2.3 Signal transduction in trained and tolerized macrophages

TLR4 signaling

TLR4 is a cell surface receptor that recognizes LPS and numerous PAMPs/DAMPs that can induce tolerance memory. Activation of TLR4 during LPS-priming results in activation of tumor necrosis factor receptor associated factor 6 (TRAF6) through Toll receptor IL-1R domain-containing adaptor protein (TIRAP) and TRIF-related adaptor molecule (TRAM) signaling which results in activation of a complex of mitogen-activated protein kinases (MAPKs) and activator protein 1 (AP1) and a complex of I kappa B kinases (IKK) and nuclear factor kappa B (NF-κB) signaling (**Figure 2.2**). In addition, activation of tumor necrosis factor receptor associated factor

3 (TRAF3) also induce by TRAM signaling and activation of interferon regulatory factor 3 (IRF3). Ultimately, the activation of AP1, NF-κB and IRF3 results in pro-inflammatory cytokine production (45, 46). However, primary LPS stimulation also induces activation of several negative regulator of TLR4, such as SH2-containing inositol phosphatase (SHIP, (47)), suppressor of cytokine signaling-1 (SOSC1, (48)) and RelB (49, 50), that can dampen MAPKs and NF-κB activation (14, 46). Some of these negative regulators such as RelB collaborates with G9a histone methyltransferase which promotes the deposition of repressive histone mark in LPS tolerance (49, 50). Thus, epigenetic regulation is tightly linked with TLR4 signaling during the induction LPS tolerance.
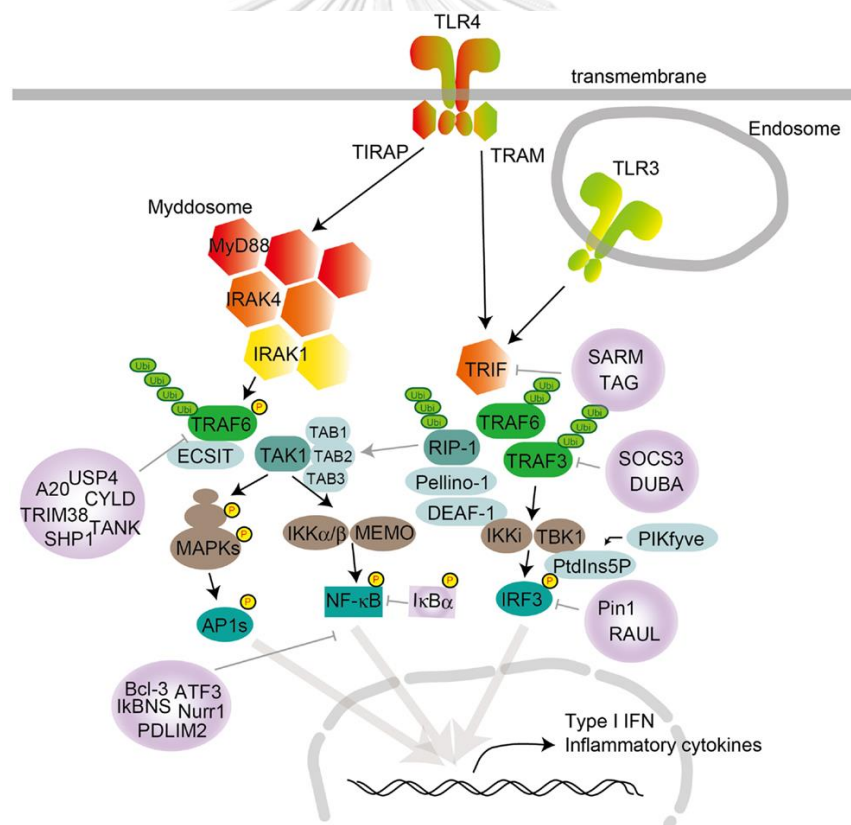
Figure 2.2 TLR4 signaling cascade (45)

TLR4 activation leads to activate intracellular signaling, such as MAPKs and NF-κB signaling pathway, which ultimately induce cytokines production.

Dectin-1 signaling

Dectin-1 is a receptor that mainly recognized β-(1→3)/(1→6)–glucans, which is the cell wall components of fungi and some bacteria. Besides BG, dectin-1 also act as a collaborative receptor for recognized BCG [51]. In trained immunity, activation of dectin-1 results in phosphorylation of AKT (ser473) which leads to activation of mechanistic target of rapamycin (mTOR) and induction of metabolic reprogramming in trained cells (**Figure 2.3)**. In addition, activation of dectin-1 also triggers calcium influx and NFAT leading to induction of the lncRNA such as IPLs and UMLILO which facilitates histone modification in trained immunity [1, 7, 31, 32]. As metabolic reprogramming induced by BG training accumulates several metabolites, such as mevalonate, which can enhance AKT and mTOR signaling by performing an amplification loop for enhance trained immunity through the activation of insulin-like growth factor 1 (IGF1R, [1, 21]). Moreover, some metabolites, such as fumarate and acetyl-coA, can act as repressor for KDM5 histone demethylase or co-factor for histone acetyltransferase, respectively [1, 7]. These findings indicate that epigenetic regulation and metabolic reprogramming regulate trained immunity through the up-stream dectin-1/AKT/mTOR signaling pathway.
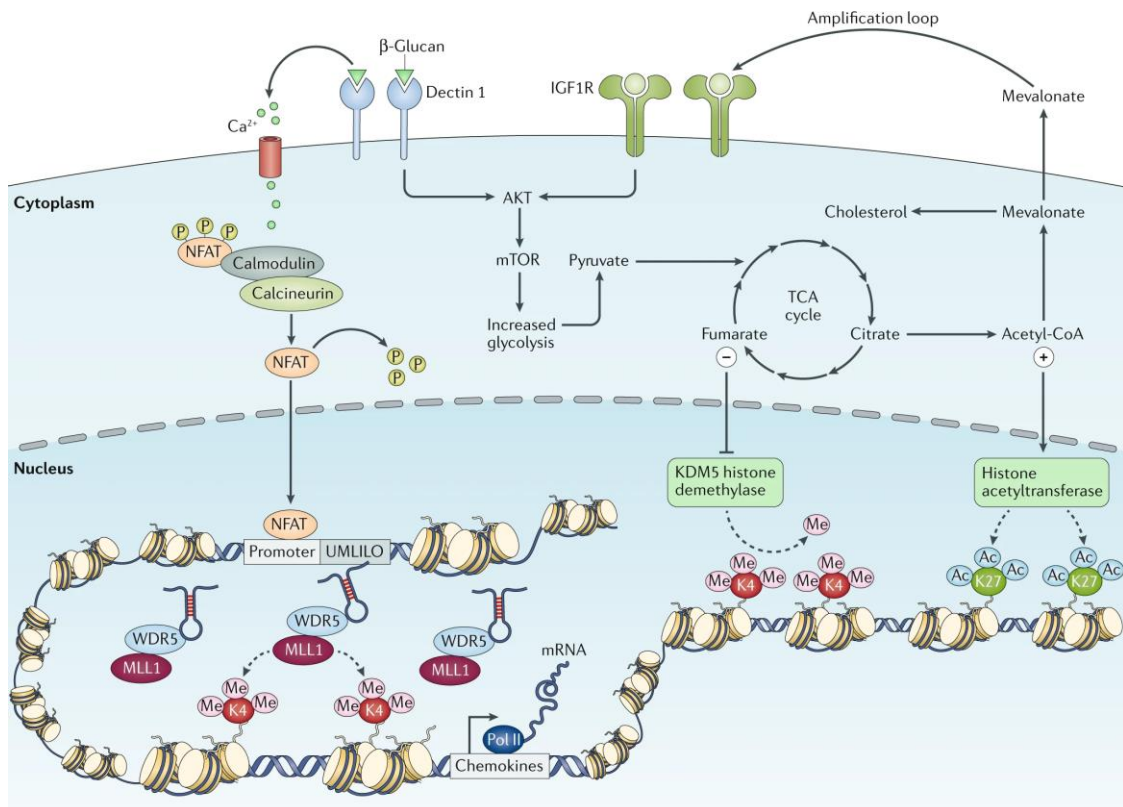
Figure 2.3 Dectin-1 signaling in BG-trained macrophages (1)

BG activated the dectin-1 signaling pathway, which induced metabolic reprogramming by AKT/mTOR activation, and the expression of lncRNAs by nuclear factor of activated T-cells (NFAT) activation.

2.3 Knowledge gaps in epigenetic mechanism of innate immune memory

Histone modification is the major epigenetic mechanism that control the induction of innate immune memory. However, only a few active and repressive histone marks, which mainly are acetylated and methylated lysine on histone 3 and histone 4, have been extensively studied to play the crucial role in innate immune memory. The effect of other unexplored histone marks and other epigenetic mechanisms may play an important role in regulation innate immune memory (2, 3, 5, 36). Therefore, detailed further investigations of other epigenetic mechanisms are needed to get broader view of innate immune memory and clarify the mechanism that control the induction of innate immune memory.

2.4 Novel target enzymes include in tolerance process in macrophages

From our preliminary screening results, we found that inhibitors against Aurora kinase, enhancer of zeste homolog 2 (EZH2), Histone deacetylase, Jumonji C domain-containing protein 2 (JMJD2), lysine specific demethylase 1 (LSD1), protein arginine methyltransferase (PRMT) and Poly (ADP-ribose) polymerase (PARP) increased cytokine expression in tolerized macrophages which can be assumed as inhibition of tolerance phenotype.

- **Aurora kinase**

Aurora kinase is a serine/threonine protein kinase that involved in the function of spindle fiber and centrosome during cell division. Aurora kinase has 3 subtypes: Aurora kinase A, B and C. Aurora A and Aurora B associate with mitotic division while Aurora C restricts to meiosis (52, 53). Only Aurora B has the epigenetic role in phosphorylation of serine 10 and serine 28 on histone H3 (H3S10ph and H3S28ph) and involves in H3K9me3 which are the repressive histone marks (54). Besides the role in histone modification and cell division, Aurora kinases also regulate the polarization of M1 macrophages by interact with NF-κB and interferon regulatory factor 5 (IRF5) (55). However, the role of Aurora kinase in the regulation of tolerized macrophages has not been investigated yet.

- **Enhancer of zeste homolog 2 (EZH2)**

EZH2 is the methyltransferase that is the component of polycomb repressive complex-2 (PRC2) which mediates H3K27me3, a repressive histone marks (56). EZH2 has been reported to regulate immune cells function through controls the expression of suppressor of cytokine signaling 3 (SOCS3) which attenuates inflammation process (38). However, the role of EZH2 and SOCS3 in tolerized macrophages are still exploded.

- **Histone deacetylase**

HDACs are the class of enzyme that remove acetyl group from acetylated lysine residue on histone and others cellular protein. HDACs can be divided in to four classes: class I (HDAC1, 2, 3 and 8), class II (HDAC4, 5, 6, 7, 9 and 10), class III (sirtuin1-7) and class VI (HDAC11). These HDACs mainly deacetylate acetyl group on histone protein except for HDAC6 and HDAC class III which mainly deacetylate acetyl group on cytoplasmic protein (57). In addition, several class of HDACs, such as HDAC1, HDAC3 and HDAC6, play an important role in inflammation (39, 58, 59) and HDAC6 has been reported to regulate LPS tolerance in astrocytes (59). However, the role of HDAC6 in LPS-tolerized macrophages remains to be explored.

- **Jumonji C domain-containing protein 2 (JMJD2)**

JMJD2 is a histone lysine demethylase that target H1.4K26me2, H3K9 and H3K36. JMJD2 compose of 5 subtypes: JMJD A, B, C, D and E. Besides the role in histone modification, JMJD can regulate inflammation by interact with other proteins such as TRAF6, mTOR and hypoxia Inducible factor 1 subunit alpha (HIF-1α). However, the role of JMJD in the regulation of tolerized macrophages has not been investigated yet (60).

- **Lysine specific demethylase 1 (LSD1)**

LSD1 is the histone demethylase that remove the methyl groups from both active and repressive mark, including H3K4, H3K9, H3K36, H3K79 and H4K20 (61). Besides the role in epigenetic regulation, LSD1 controls the inflammatory response during sepsis in myeloid cells. Deletion of LSD1 resulted in severe cytokine production and lethality in sepsis (62).

- **Protein arginine methyltransferase (PRMT)**

PRMTs are the class of enzyme that mediate methylation of arginine on cellular proteins, including histone, in order to control numerous cellular process such as chromatin remodeling, cellular proliferation and mRNA splicing (63, 64).

PRMTs can be divided in to four types: type I PRMTs (PRMT1, 2, 3, 4, 6 and 8), type II PRMTs (PRMT5 and 9), type III PRMTs (PRMT7, (63)). The epigenetic function of PRMTs is to mediate the methylation of arginine on histone H3 and H4 which mainly generate active histone marks (65). In addition, some subtypes of PRMTs, such as PRMT5, have been reported to associate with transcription repression as they are the component of histone deacetylase co-repressor complex (65).

- **Poly (ADP-ribose) polymerase (PARP)**

PARP is the protein family that mainly function in DNA repair process. PARP inhibitors normally use in cancer therapy as they can specifically induce apoptosis of breast cancer cells with BRCA1/2 mutation (66). In addition, PARPs also positively regulate inflammatory response by enhance NF-κB signaling. Several inflammatory molecules such as inflammatory cytokines also induce PARP activation (67). However, the role of PARPs in regulation of tolerized macrophages are still unexploded.

จุฬาลงกรณ์มหาวิทยาลัย

CHULALONGKORN UNIVERSITY

2.5 Novel target enzymes that may control trained immunity

From the preliminary results, we found that inhibitor against O^6-methylguanine DNA methyltransferase (MGMT) can modulate cytokine production in trained macrophages.

- **O^6-methylguanine DNA methyltransferase (MGMT)**

MGMT is a DNA repair enzyme that removes methylation at O^6 position of guanine (O^6-MeG, methylguanine) which is a DNA lesion caused by alkylating agents. The repairing process covalently transfer the methyl group to the active site of MGMT which permanently converts MGMT into an inactivated form and leads to its degradation. The unrepair O^6-methylguanine (O^6-MeG) scar can induce G to A transversion and single strand break which can induced mutation and cancer. Epigenetic modification of *Mgmt* promoter such as DNA methylation negatively regulates MGMT expression and is thought to be the cause of mutation and carcinogenesis. However, expression of MGMT in cancer cells can promotes the resistance to alkylating chemotherapy. Thus, MGMT inhibitors have been combined with chemotherapy to increase sensitivity to the treatment (68). Besides the role in carcinogenesis, in chronic inflammatory disease, MGMT promoter has been reported to be hypermethylated and repressed. Reduction of MGMT expression may accelerate the progression of these diseases (69-72). From our screening results, we found that inhibitor against MGMT enhanced cytokine production in trained macrophages. Besides MGMT, Ercc1 DNA repair enzyme has been reported to be involved in epigenetic regulation in trained immunity (73).

2.6 Therapeutic application potentials of innate immune memory

As innate immune memory has been associated with numerous immune-mediated diseases, understanding how to control the induction of the different memory may provide the new therapeutic strategy to balance immune response and alleviate the undesirable disease outcomes. For example, the inhibition of trained or the induction of tolerance could be the new therapeutic strategies against atherosclerosis and other hyperinflammation conditions which is a violent trained memory (2, 74). On the other hand, the induction of trained immune memory may improve immune response in immune-paralysis after sepsis and in cancer (2, 3, 5, 74, 75). Moreover, the molecules that induce trained immunity can be used as the vaccine component to induce broader response which may provide the better protection in multiple coinfections and when conventional vaccines are not available (76).

2.7 Research question

What are other essential mechanisms involved in trained and tolerized macrophages?

2.8 Objective

- To identify the uncharacterized mechanisms that regulate innate immune memory in BG-trained and LPS-tolerized macrophages

- To investigate the therapeutic potentials or molecular mechanism of the novel target protein identified in this study

CHAPTER III

MATERIALS AND METHODS

3.1 Generation of bone marrow-derived macrophages (BMM)

Eight-week-old female C57BL/6 mice purchased from Nomura Siam International, Thailand were used as a source of bone marrow in this study. BMMs were generated from bone marrow cells extracted from the tibia and femur of C57BL/6 mice. Bone marrow cells were cultured in Dulbecco's modified Eagle's medium (DMEM) (HyClone, USA) supplemented with 10% (v/v) fetal bovine serum (Gibco, USA), 10 mM HEPES (HyClone), 1 mM sodium pyruvate (HyClone), 100 U/ml penicillin, and 0.25 mg/ml streptomycin (DMEM complete media) with 20% L929 culture supernatant and 5% horse serum (HyClone, USA), and fresh media was added at day 4. After 7 days in culture, cells were detached with cold PBS and stored at -80°C until use. BMMs were confirmed by flow cytometry using the macrophage specific surface markers F4/80 and CD11b. Experimental procedures involving laboratory animals were approved by the Institutional Animal Care and Use Committee (IACUC) of the Faculty of Medicine, Chulalongkorn University (approval protocol No. 025/2562). All experiments were performed according to the guidelines issued by the IACUC.

3.2 Induction of β-glucan (BG)-trained and LPS-tolerant macrophages

For the induction of BG-trained or LPS-tolerized macrophages, BMMs were cultured in complete DMEM and primed with 50 μg/ml pachyman BG (Megazyme, USA) for trained macrophages or 100 ng/ml *Escherichia coli* LPS (L2880, Sigma Aldrich, USA) for tolerized macrophages. After 24 hr of priming, the medium was replaced with fresh DMEM complete medium and the cells were rested for 48 hr. The resting step was followed by LPS 10 ng/ml stimulation for the indicated times.

Culture supernatant, RNA or cell lysates were harvested at the indicated times for analysis. The amount of TNFα in the culture supernatant was measured by a mouse TNFα ELISA kit (Biolegend, USA) according to the manufacturer's protocol.

3.3 Quantitative reverse transcription realtime-PCR (qRT-PCR)

Total RNA of macrophages treated as indicated was harvested with the TRIzol reagent (Invitrogen, USA) and extracted with direct-zol RNA kits (Zymo Research, USA). The quality and concentrations of RNA were measured by a NanoDrop^{TM} 2000 spectrophotometer (Thermo Fisher Scientific, USA). One hundred nanograms of RNA per sample was converted to cDNA, which was used for quantitative PCR using iQ^{TM} SYBR Green SuperMix (Bio-Rad, USA) according to the manufacturer's instructions. The primers used in this study are shown in **Table 3.1**. The relative expression of all target genes was normalized to the expression of *Actb* by the $2^{-\Delta\Delta CT}$ method and calculated by comparison with that of ctrl LPS or unstimulated cells (77).

3.4 Western blot

Macrophages were treated to become BG-trained or LPS-tolerized macrophages as described above. Cell lysates were collected at the indicated times using RIPA buffer (50 mM Tris HCl pH 7.4, 150 mM (for other proteins) or 500 mM (for histone and LSD1 extraction) NaCl, 5 mM EDTA, 1% nonidet P-40, 0.5% sodium deoxycholate supplemented with protease and phosphate inhibitors (Cell Signaling Technology, USA)). The protein concentrations were measured by a bicinchoninic acid assay using the Pierce BCA Protein Assay Kit (Thermo-Fisher Scientific, USA). Proteins were resolved by 8% (mTOR, LSD1, AKT, and NF-κB signaling proteins), 10% (Aurora kinase or SETD7) or 15% (histone) SDS-PAGE and subjected to Western blot as described elsewhere. The antibodies were diluted in PBS with 3% (w/v) skim milk for probing. All antibodies used in this study and the dilutions were summarized in **Table 3.2**. The signal was detected by the ECL chemiluminescent detection method. Relative intensity was analyzed by ImageJ analysis.

3.5 Epigenetics compound library screening

The Epigenetics Compound Library with a unique collection of 181 epigenetics compounds (Cat L1900, Selleckchem, USA) was used as the inhibitor source. The library was purchased and obtained in January 2018 and the list of compounds in the library was shown in **Appendix B**. For the screening assay, BG-trained or LPS-tolerized macrophages were pretreated with the inhibitors at two concentrations of inhibitory concentration 50 (IC50) indicated by the manufacturer's data for 1 h during the priming or stimulation phase. Control cells received vehicle control DMSO and were subjected to the same priming. Cells were cultured in the presence of inhibitors during priming or stimulation for 24 h. The culture supernatant was subjected to ELISA to measure TNFα. The relative amount of TNFα produced by inhibitor treated cells was calculated as the fold change, by normalized with that from the vehicle control-treated cells. The inhibitors that showed enhancing or suppressing effects with the fold changes of 1.5-fold or higher and 0.75-fold or lower, respectively, were chosen for further confirmation. Interaction of the potential targets identified in this study was performed with STRING version 11.0 (https://string-db.org/, (78)).

3.6 MTT assay

Macrophages were treated with indicated inhibitors. After 20 h of LPS stimulation, MTT reagent was added to a final concentration of 0.5 mg/ml and the cells were further incubated for 4 h. After incubation, 200 μl of DMSO was added to each well to dissolve the MTT formazan pellet. The intensity of the pellet was measured by a microplate reader at a wavelength of 540 nm.

3.7 Apoptotic assay

Macrophages were treated with inhibitor as indicated. After 24 h of LPS stimulation, cells were collected using cold PBS. Apoptotic and necrotic cells were detected by flow cytometry using PE Annexin V Apoptosis Detection Kit with 7-

AAD (Biolegend, USA). Macrophages cultured with 1% DMSO for 24 h were used as positive control.

3.8 *In vitro* knock down of specific genes by siRNA

SMARTpool siRNA targeted murine *Lsd1* (ON-TARGET*plus*™), *Mgmt* (Accell™) or control non-targeting siRNA (NT) were purchased from Dharmacon™ (Horizon Discovery, UK). Lipofectamine 2000 (Thermo Fisher Scientific, USA) were used as transfection reagent. Lipid-siRNA complex was prepared in warmed Opti-MEM™ I Reducing-Serum Media (Gibco, USA) and incubate for 15 min with gentle rotation before topping up with BMMs in antibiotic free DMEM complete media. The final concentrations of siRNA and Lipofectamine were 50 nM and 0.6%v/v, respectively. After 6 h of incubation, transfection media were replaced with fresh BMM media with antibiotic. The reduction of mRNA and protein was confirmed at 48 hr after siRNA transfection by qRT-PCR and Western blot as described above.

3.9 Chromatin immunoprecipitation assay

Approximately 7.0×10^6 cells of BMMs were prepared and activated as indicated. The SimpleChIP® Enzymatic Chromatin IP Kit (Cell Signaling Technology, USA) was used to perform ChIP according to the manufacturer's instructions. Samples were subjected to immunoprecipitation using either rabbit anti-H3K4me3 antibody or a control IgG antibody (Cell Signaling Technology, USA). Fragmented DNAs were purified using spin columns (Cell Signaling Technology) and was used as the templates for qPCR using indicated primer sets spanning the *Tnf* and *Il6* promoters (**Table 3.3**). Fold enrichments were normalized and calculated based on the total amount of 10% input presented in relative quantification using $2^{-\Delta\Delta ct}$ method (77).

3.10 Generation of myeloid specific MGMT knockout mice (LysM-cre^cre/+; MGMT^fl/fl)

In this study, specific knock out of *Mgmt* in macrophages was generated by the Cre/loxP system which is a site-specific genetic modification technique by Cyagen (China). This system contains two components: Cre recombinase and its recognition

site loxP. The specific gene knock out in macrophages requires two different types of mice: the LysM-Cre (LysM-cre$^{cre/+}$) the strain that cre recombinase is inserted under the lysozyme M (LysM) promoter which will drive the expression of this enzyme in macrophages and neutrophil, and the MGMT-loxP (MGMT$^{fl/fl}$), the strain that *Mgmt* allele is flanked with the loxP sequence in exon 3 region. When the two components are combined in myeloid cells of LysM-cre$^{cre/+}$; MGMT$^{fl/fl}$ mice (MGMT knockout mice), Cre recombinase recombines the loxP sequence lead to deletion of exon 3 of MGMT (**Figure 3.3** ,(79)). All experimental procedures involving laboratory animals were approved by IACUC of Chulalongkorn University Laboratory Animal Center (approval protocol No. 2073016). All experiments were performed according to the guidelines issued by the IACUC.
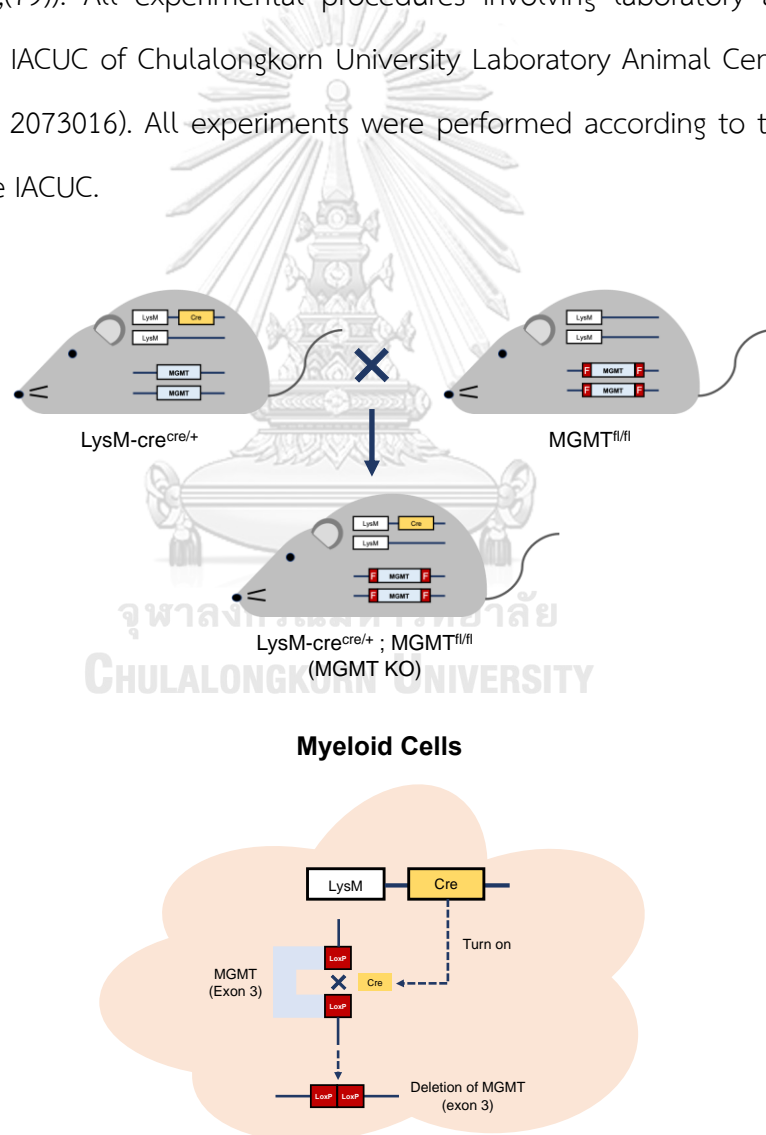
Figure 3.1 Germline of myeloid (LysM+) specific MGMT knockout mice

3.11 Breeding scheme to generate myeloid specific MGMT KO mice

        Macrophages specific MGMT knockout mice were generated from crossbreeding between LysM-cre strain (LysM-cre$^{cre/+}$) and MGMT-LoxP strain (MGMT$^{fl/fl}$) (all purchased from Cyagen, China, **Figure 3.4**).

Breeding Pair I: LysM-Cre$^{cre/+}$ x   MGMT$^{fl/fl}$

        F1:   LysM-Cre$^{cre/+}$; MGMT$^{fl/+}$ (50%)

                    LysM-Cre$^{+/+}$; MGMT$^{fl/+}$ (50%)

Breeding Pair II: LysM-Cre$^{cre/+}$; MGMT$^{fl/+}$ x   MGMT$^{fl/fl}$

        F2:   LysM-Cre$^{cre/+}$; MGMT$^{fl/fl}$ (KO) (25%)

                    LysM-Cre$^{+/+}$; MGMT$^{fl/fl}$ (25%)   ⎤ use for further colony maintenance

                    LysM-Cre$^{cre/+}$; MGMT$^{fl/+}$ (25%, Euthanized)

                    LysM-Cre$^{+/+}$; MGMT$^{fl/+}$ (25%, Euthanized)

The F2 progeny MGMT KO mice and littermate control were used as parental strains to obtain higher percentage of KO and littermate WT control progeny.

Breeding Pair III: LysM-Cre$^{cre/+}$; MGMT$^{fl/fl}$ x   MGMT$^{fl/fl}$

        F3:   LysM-Cre$^{cre/+}$; MGMT$^{fl/fl}$ (KO) (50%)

                    LysM-Cre$^{+/+}$; MGMT$^{fl/fl}$ (littermate control) (50%)
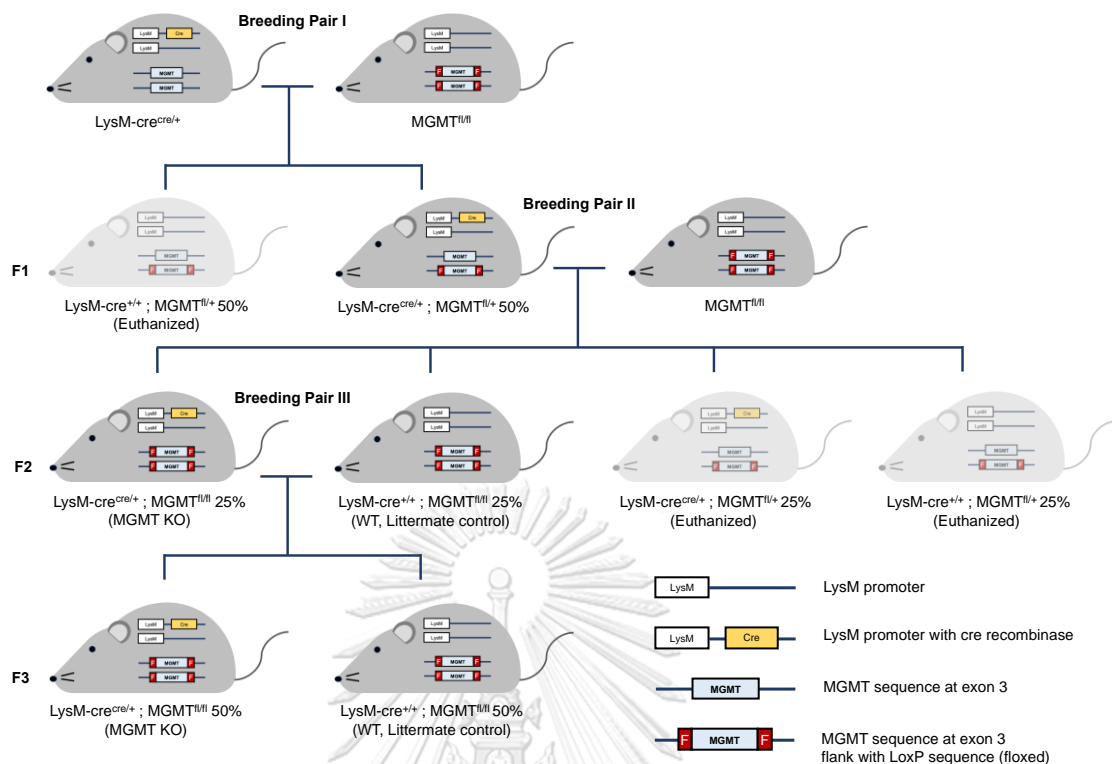
Figure 3.2 Breeding scheme of LysM-cre strain and MGMT-LoxP strain

3.12 Genotyping

To check the genotype of LysM-Cre mice and MGMT floxed mice, ear patch tissues from ear punching were collected as a source of DNA for genotyping. The DNA were extracted by incubation in tissue digestion buffer (50 mM KCl and 10 mM Tris-HCl pH 9.0) supplemented with 0.1% Triton X-100 and 0.4 mg/ml proteinase K (Promega, USA) at 56°C O/N. The genotypes of mice were validated by PCR following the company's instruction. The primer set for genotyping were listed in **Table 3.4**.

3.13 *In vivo* model for trained immunity

Trained immunity in eight to ten weeks old MGMT KO and littermate control mice were induced by intraperitoneal injection with 1 mg of pachyman BG (PBS as control). After 5 days, all mice will be intraperitoneal injected with 10 μg of *E. coli* LPS (PBS as control, (41)). Blood cytokines were detected at 3 h after LPS injection by LEGENDplex™ Mouse Inflammation Panel (Biolegend, USA) following the company's

instruction. Level of cytokine production was measured by flow cytometry. Data were analyzed using The LEGENDplex™ Data Analysis Software Suite (https://www.biolegend.com /ja-jp/legendplex#software).

3.14 Transcriptome study

Unstimulated, BG-primed (BG24) and BG-primed with LPS stimulation (BG/LPS) macrophages were prepared as described above. Total RNA from each sample were extracted using RNeasy Mini Kit (Qiagen, USA) following the manufacturer's protocol. 0.5-1 µg of total RNAs were subjected to RNA quality assessment using the 2100 Bioanalyzer (Agilent Technology, USA). All RNA sample in this study acquired RNA integrity number (RIN) scores greater than 7.0 and 28S/18S ratio greater than 1. RNA sequencing was carried out using a DNBSEQ sequencing technology at BGI sequencing center, Hong Kong (paired end read with 150 bp/read).

3.15 Transcriptomic analysis

RNA-Seq analysis Sequencing reads were mapped against the *Mus musculus* reference genome GRCm39. Reads were mapped and aligned with Hisat2 (80) and counted using the R package Rsubread, featureCounts (81, 82). Then, differential expressed genes (DEGs) were compared and analyzed using the R package DESeq2 with the *p*-value cut off < 0.05 (44). To focus on the effect of MGMT KO in trained immunity, the normalized counts of DEGs in BG24 and BG/LPS were normalized to the normalized counts unstimulated WT macrophages. Then, heatmap of DEGs in BG24 and BG/LPS were created using the R package pheatmap (https://cran.r-project.org/web/packages/pheatmap/index.html). Lists of up-down regulated DEGs in each condition were compared using Venn Diagram (https://bioinformatics. psb.ugent.be/webtools/Venn/). DEGs that specifically upregulated in each condition were subjected to perform Gene Set Enrichment Analysis (GSEA) using GSEA version 4.3.2 (83, 84). DEGs and its log2FoldChange from DESeq2 were used as input for GSEA pre-rank analysis. Mouse Gene Symbol Remapping Human Orthologs MSigDB version

2022.1.HS was selected as chip platform. Wikipathway version 2022.1 was selected as searching database (85, 86). Significant GSEA pathway were selected with p-value < 0.05 and FDR < 0.25.

3.16 Glycolysis stress assay

Approximately 1×10^5 cells of BMMs were plated in XFp Cell Culture Miniplate (Agilent Technologies, USA) overnight in BMMs media. The medium was replaced with fresh DMEM complete medium and the cells were rested for 1 h before stimulation with BG for 24 h. After resting for 48 h, glycolytic function was detect using Agilent Seahorse XF Glycolysis Stress Test Kit (Agilent Technologies, USA) following the manufacturer's protocol. The glycolysis signal was detected as extracellular acidification rate (ECAR) by Agilent Seahorse XFp Analyzer (Agilent Technologies, USA). In brief, BMMs were incubated in glucose free assay medium and non-glycolysis acidification was measured. This step was followed by addition of glucose to the system (final concentration = 10 mM) to induce glycolysis function. Oligomycin, an ATP synthase inhibitor (final concentration = 50 mM) was added to inhibit the mitochondria function leading to induce the maximum glycolysis. Finally, 2-DG, a glycolysis inhibitor (final concentration = 500 mM) was added to confirm that ECAR signal in this system represent the glycolytic function. The data were analyzed using Agilent Seahorse Wave (Agilent Technologies, USA, **Figure 3.2**).
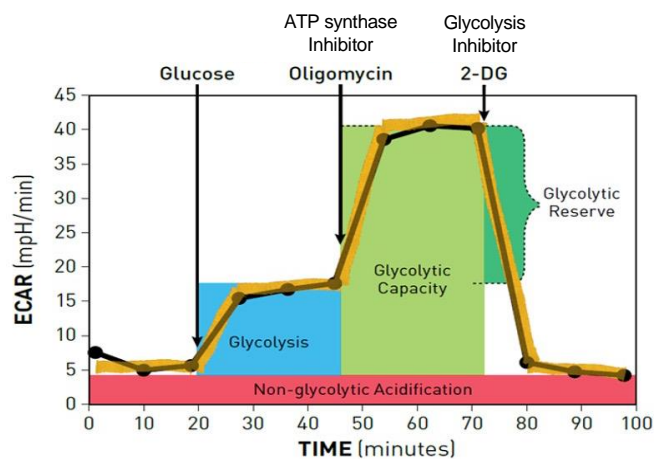
Figure 3.3 Glycolysis stress test (Agilent Technologies, USA)

3.17 Statistical analysis

All experiments were performed in triplicate and at least twice independently, except for the primary screening. Statistical analyses were performed using GraphPad Prism version 9.0. One-way ANOVA with Dunnett's or Tukey's multiple comparison test and two-tailed unpaired and paired t-test (α=0.05) were used when comparing the two conditions. This study is reported in accordance with ARRIVE guidelines.

Table 3.1 List of primers used in this study.

Gene	Forward (F) and Reverse (R) Primers	Annealing Temperature	Reference
Tnf	F: 5'-AGC CCA CGT CGT AGC AAA CCA C-3' R: 5'-ATC GGC TGG CAC CAC TAG TTG GT-3'	55 °C	Viceconte *et al.*(87)
Il6	F: 5'-CTC TGG GAA ATC GTG GAA ATG-3' R: 5'-AAG TGC ATC ATC GTT GTT CAT ACA-3'	57 °C	Minashima *et al.*(88)
Il1b	F: 5'-TAT ACC TGT CCT GTG TAA-3 R: 5'-TTG ACT TCT ATC TTG TTG A-3'	53 °C	Lai *et al.* (89)
Il10	F: 5'-TCA AAC AAA GGA CCA GCT GGA CAA CAT ACT GC-3' R: 5'-CTG TCT AGG TCC TGG AGT CCA GCA GAC TCA A-3'	58 °C	Palaga *et al.*(90)
Cd40	F: 5'-GTT TAA AGT CCC GGA TGC GA-3' R: 5'-CTC AAG GCT ATG CTG TCT GT-3'	64 °C	Magner *et al.*(91)
Serpine1	F: 5'-TCA TCA ATG ACT GGG TGG AA-3' R: 5'-TGC TGG CCT CTA AGA AAG GA-3'	62 °C	Syed *et al.*(92)
Marco	F: 5'-GAA GAC TTC TTG GGC AGC AC-3' R: 5'-CTT CTT GGG CAC TGG ATC AT-3'	62 °C	Jing *et al.*(15)
Camp	F: 5'-CGA GCT GTG GAT GAC TTC AA-3' R: 5'-CAG GCT CGT TAC AGC TGA TG-3'	68 °C	Kin *et al.*(93)
Lsd1	F: 5'-CGA TAC TGT GCT TGT CCA CCG A-3'	60 °C	Hwang et al.,

	F: 5'-CCA AGC CAG AAA CAC CTG AAC C-3'		2018 (94)
Mgmt	F: 5'- GCT CTC CAT CAC CCT GTG TT-3'	60 ℃	Designed by
	F: 5'-ATG AGG ATG GGG ACC GGA TTG-3'		this study
Actb	F: 5'-ACC AAC TGG GAC GAC ATG GAG AA-3'	55 ℃	Wongchana
	R: 5'-GTG GTG GTG AAG CTG TAG CC-3'		*et al.*(95)

Table 3.2 List of antibodies used in this study.

Antibody	Company	Dilution	Detection time
Primary Antibody			
rabbit anti-H3K4me3 antibody	Cell Signaling Technology, USA	1:1000	5 min
rabbit anti-H3K27me3 antibody	Cell Signaling Technology, USA	1:1000	5 min
rabbit anti-total H3 antibody	Cell Signaling Technology, USA	1:4000	1 min
rabbit anti-phospho mTOR	Cell Signaling Technology, USA	1:1000	2 min
rabbit anti-total mTOR	Cell Signaling Technology, USA	1:1000	2 min
rabbit anti-phospho Aurora A/Aurora B/Aurora C	Cell Signaling Technology, USA	1:1000	30 min
rabbit anti-LSD1	Cell Signaling Technology, USA	1:2000	2 min
rabbit anti-phospho AKT (ser473)	Cell Signaling Technology, USA	1:1000	10 min
rabbit anti-phospho AKT (Thr308)	Cell Signaling Technology, USA	1:1000	10 min
rabbit anti-total AKT	Cell Signaling Technology, USA	1:1000	5 min

rabbit anti-phospho mTOR	Cell Signaling Technology, USA	1:1000	2 min
rabbit anti-total mTOR	Cell Signaling Technology, USA	1:1000	2 min
rabbit anti-GAPDH antibody	Cell Signaling Technology, USA	1:4000	1 min
rabbit anti-phospho NF-кB p65	Cell Signaling Technology, USA	1:2000	1 min
rabbit anti-phospho p38	Cell Signaling Technology, USA	1:2000	1 min
rabbit anti-phospho ERK	Cell Signaling Technology, USA	1:2000	1 min
rabbit anti-phospho SAPK/JNK	Cell Signaling Technology, USA	1:2000	1 min
rabbit anti-total NF-кB p65	Cell Signaling Technology, USA	1:4000	1 min
rabbit anti-total p38	Cell Signaling Technology, USA	1:4000	1 min
rabbit anti-total ERK	Cell Signaling Technology, USA	1:4000	1 min
rabbit anti-total SAPK/JNK	Cell Signaling Technology, USA	1:4000	1 min
mouse anti-SETD7 antibody	Bio-Rad, USA	1:1000	1 min
mouse anti-MGMT antibody	1:2000	1:2000	2 min
mouse anti-actin antibody	Merck Millipore, USA	1:10000	30 sec
Secondary Antibody			
goat anti-rabbit IgG HRP	Cell Signaling Technology, USA	1:4000	-

sheep anti-mouse IgG HRP	1:4000	1:4000	-

Table 3.3 List of primers used in chromatin immunoprecipitation assay.

Gene	Forward (F) and Reverse (R) Primers	Annealing Temperature	Reference
mTnf promoter	F: 5'-CAA CTT TCC AAA CCC TCT GC-3' R: 5'-CTG GCT AGT CCC TTG CTG TC-3'	59 ℃	Saz-Leal *et al.*(96)
mIl6 promoter	F: 5'-CAC TTC ACA AGT CGG AGG CT-3' R: 5'-AAT GAA TGG ACG CCC ACA CT-3'	61 ℃	Hu *et al.*(97)

Table 3.4 List of primers used for genotyping.

Gene	Forward (F) and Reverse (R) Primers	Annealing Temperature	Reference
Cre genotyping	F: 5'-GAA CGC ACT GAT TTC GAC CA-3' R: 5'-GCT AAC CAG CGT TTT CGT TC-3'	60 ℃	Cyagen, China
MGMT-floxed genotyping	F3: 5'-TGG GCT TCA AAT CAA GGA ACA GAA-3' R5: 5'-AAC TAT CCT GCT CACT CTC TGT AG-3'	60 ℃	Cyagen, China

จุฬาลงกรณ์มหาวิทยาลัย

CHULALONGKORN UNIVERSITY

CHAPTER IV

RESULTS

4.1 Generation and characterization of BG-trained and LPS-tolerized macrophages

4.1.1 Generation of BG-trained or LPS-tolerized macrophages

To generate BG-trained or LPS-tolerized macrophages, BMMs were first primed with BG or LPS for 24 hr and allowed to rest in fresh media for 48 h, as indicated in **Figure 4.1.1a**. The resting step was followed by LPS stimulation (10 ng/ml) for 24 h. The amount of TNFα in the culture supernatant was measured by ELISA, and the relative levels were calculated by normalization to the amount of TNFα produced by naïve BMMs that received only one dose of LPS stimulation (10 ng/ml). As shown in **Figure 4.1.1b**, BG priming alone minimally induced TNFα production, whereas priming with LPS at 100 ng/ml induced significantly higher TNFα than the BG priming. Stimulation of BG-primed macrophages with LPS resulted in 3.26-fold (3.26±0.96) higher TNFα than that in control LPS-stimulated macrophages. For LPS-tolerized macrophages, LPS-primed BMMs produced significantly lower TNFα upon LPS stimulation than naïve BMMs receiving LPS stimulation at 10 ng/ml. These results confirmed that priming of BG and LPS can induce trained and tolerized response in macrophages.
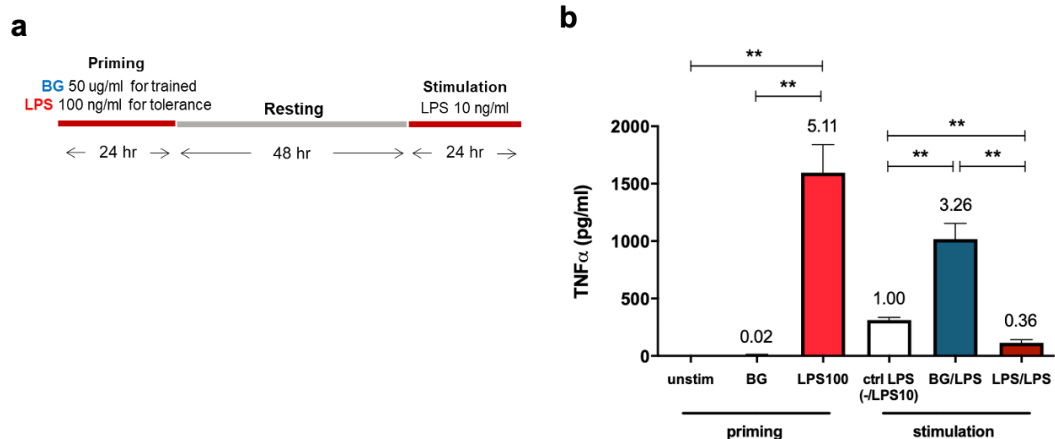
Figure 4.1.1 Generation BG-trained and LPS-tolerized macrophages (98)

(**a**) Protocol to induce BG-trained or LPS-tolerized macrophages using BMM. (**b**) TNFα production was detected by ELISA in unstimulated cells, BG-primed cells, or LPS-primed cells at 24 h after priming and in LPS-stimulated naïve cells (crtl LPS), LPS-stimulated BG-primed cells (trained, BG/LPS) or LPS-stimulated LPS-primed cells (tolerized, BG/LPS) after 24 h of LPS stimulation. The relative fold changes were calculated by normalizing to the amount obtained from LPS-stimulated naïve BMMs (10 ng/ml) and indicated on top of the bars. *, **, and *** indicate significant differences compared by two-tailed unpaired t-tests at $p < 0.05$, $p<0.01$ and $p<0.001$, respectively.

4.1.2 Expression profiles of pro-inflammatory and anti-inflammatory cytokines in BG-trained and LPS-tolerized macrophages

To investigate the expression profiles of pro-inflammatory and anti-inflammatory cytokines in BG-trained and LPS-tolerized macrophages, the macrophages were prepared as described above. The mRNA expression profiles of cytokines was examined at 6 h after priming, and stimulation as indicated in **Figure 4.1.2a**. Priming with BG minimally induced mRNA expression of both pro-inflammatory and anti-inflammatory cytokines, whereas stimulation of BG-primed macrophages with LPS enhanced mRNA expression of the pro-inflammatory cytokines *Tnf*, *Il6*, and *Il1b,* while no trained effect was observed at the level of mRNA for the anti-inflammatory cytokine *Il10.* The enhancement of pro-inflammatory cytokine expression strongly confirmed that priming of BG induced trained immunity in macrophages. In LPS-tolerized macrophages, pro-inflammatory and anti-inflammatory cytokines were significantly induced in the LPS priming, while re-stimulation with LPS repressed expression of these cytokines. These results indicated that induction of tolerized memory in BMMs was successfully established (**Figure 4.1.2b-e**).
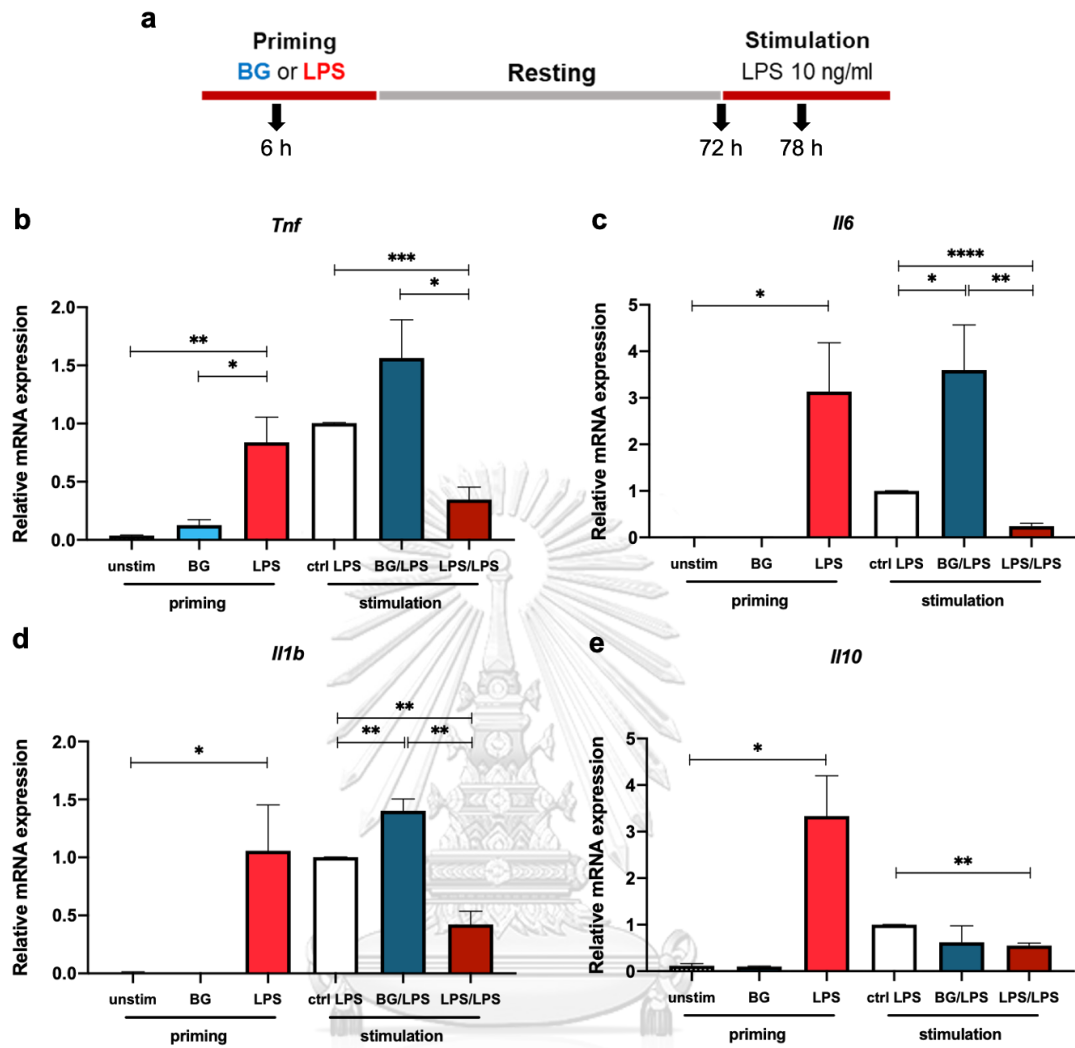
**Figure 4.1.2** mRNA expression profiles of pro-inflammatory and anti-inflammatory cytokines in BG-trained and LPS-tolerized macrophages (98)

(**a**) Protocol to induce BG-trained or LPS-tolerized macrophages using BMM and the indicated time for total RNA collection. (**b-e**) mRNA expression of proinflammatory cytokines *Tnf*, *Il6* and *Il1b* and anti-inflammatory cytokine *Il10* were detected after the priming and stimulation for 6 h as indicated in (**a**). The relative expression levels of cytokine genes was normalized to the expression of *Actb* by the $2^{-\Delta\Delta CT}$ method and calculated by comparing with the BMMs with LPS stimulation (ctrl LPS). *, **, and *** indicates statistically significant difference by two-tailed unpaired *t*-test at $p < 0.05$, $p < 0.01$ and $p < 0.001$, respectively.

4.1.3 Global histone modifications in BG-trained and LPS-tolerized macrophages

As histone modifications are one of the key mechanisms in regulating innate immune memory, we investigated the global changes of some key histone marks during BG-trained or LPS-tolerized treatment. BMMs were treated as indicated in **Figure 4.1.3a**, and the total cell lysates were analyzed for the representative active and repressive histone marks, H3K4me3 and H3K27me3. Priming with LPS or BG did not significantly alter the levels of H3K4me3 and H3K27me3 compared to the unstimulated condition. During LPS stimulation in LPS-tolerized macrophages, these marks completely disappeared in LPS-tolerized cells. In contrast, these marks were still detectable but with lower intensity in BG-trained macrophages (**Figures 4.1.3 d-g**). Taken together, BMM-derived macrophages were successfully conditioned to become BG-trained and LPS-tolerized macrophages, and drastic changes in global representative histone marks after priming or during stimulation were evident.
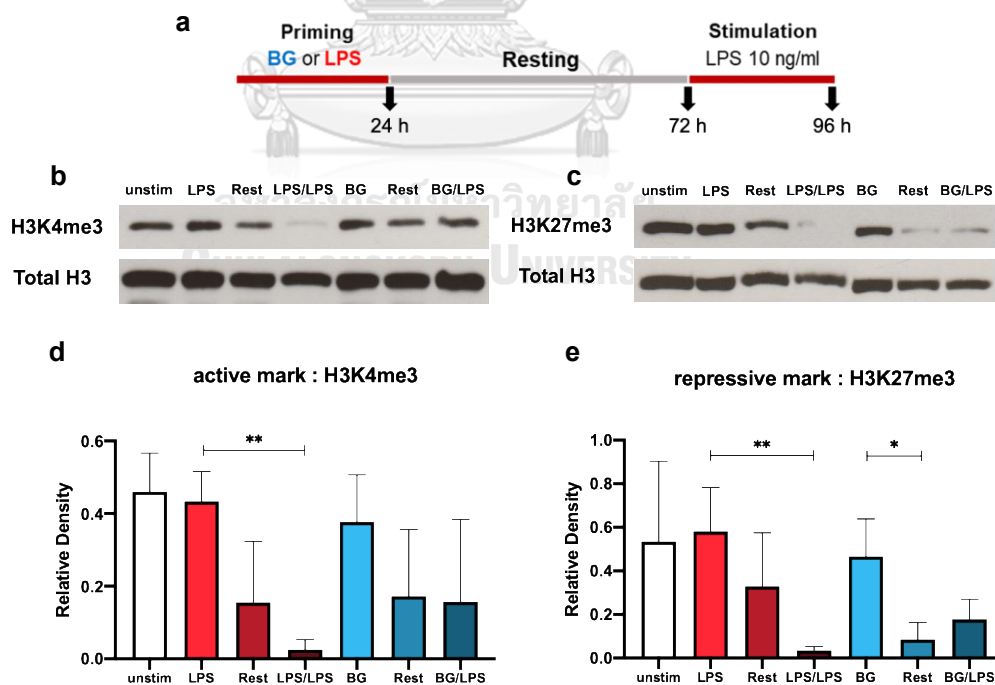
Figure 4.1.3 The representative of active (H3K4me3) and repressive (H3K27me3) histone profiles in BG-trained and LPS-tolerized macrophages (98)

(**a**) A protocol to induce BG-trained or LPS-tolerized macrophages using BMM and the indicated time for cell lysate collection. (**b-e**) Levels of H3K4me3 (**b and d**) and H3K27me3 (**c and e**) normalized to total histones in BMMs treated as indicated in (**a**) as detected by Western blot. *, **, and *** indicate significant differences compared by two-tailed unpaired *t*-tests at *p*< 0.05, *p*<0.01 and *p*<0.001, respectively.

4.1.4 Characterization of BG-trained macrophages

Besides epigenetic regulation, trained immunity has been reported to be controlled by mTOR signaling pathway. To validate our training system, phosphorylation of mTOR protein was investigated by Western blot assay. Total cell lysates were collected from BG-trained macrophages after priming, resting and LPS stimulation. As shown in **Figure 4.1.4a-b**, phosphorylation of mTOR was clearly induced after LPS stimulation of BG-trained macrophages. This result strongly confirmed that priming of BG resulted in induction of trained immunity in macrophages as reported in previous study (40, 98).
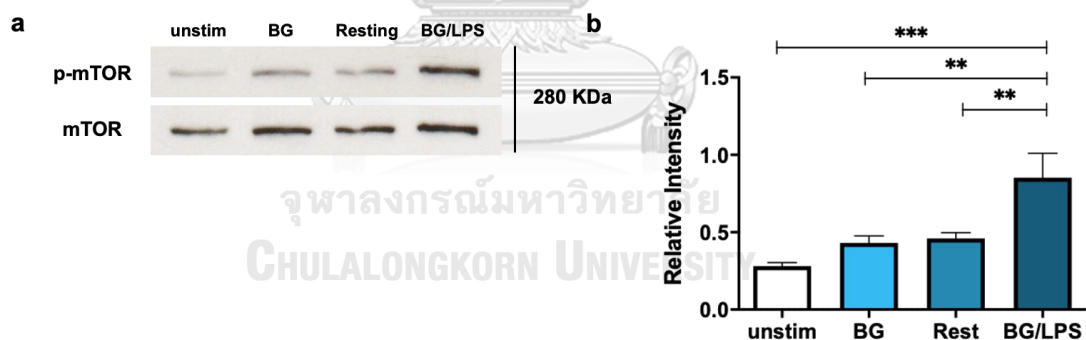
Figure 4.1.4 mTOR signaling in BG-trained macrophages (98)

BG-trained macrophages were prepared, and cell lysates were collected at indicated time point as described in **Figure 4.1.3a**. (**a**) The phosphorylated and total mTOR protein were detected by Western blot. (**b**) The relative intensity of phosphorylated mTOR from Western blot was quantitated by ImageJ analysis and normalized to total mTOR (**b**). *, **, *** and **** indicate statistical significant differences by one-way ANOVA with Tukey's multiple comparison test at *p*< 0.05, *p*<0.01, *p*<0.001 and *p*<0.0001, respectively.

4.1.5 Characterization of LPS-tolerized macrophages

According to the previous study (14), LPS tolerance alters expression of numerous genes during stimulation. Besides cytokine genes, LPS priming also repressed the expression of other inflammatory genes that are characterized as tolerizeable genes (T-gene), such as *Cd40* and *Serpine1*. In contrast, the expression of specific gene set involved in antimicrobial activity are characterized as non-tolerizeable genes (NT-gene), including cathelicidin antimicrobial peptide (*Camp*) and macrophage receptor with collagenous structure (*Marco*), was enhanced during LPS tolerance. To validate this finding, the expression of both T and NT-genes were investigated in LPS-tolerized macrophages. As shown in Figure 4.1.5, LPS-tolerized macrophages induced by our protocol significantly repressed *Cd40* and *Serpine1* T-gene expression and enhanced the expression of NT-gene *Camp* and *Marco* compared to the control LPS stimulation (-/LPS). These results are consistent with the specific pattern of gene regulation in LPS-tolerized macrophages in a previous study.
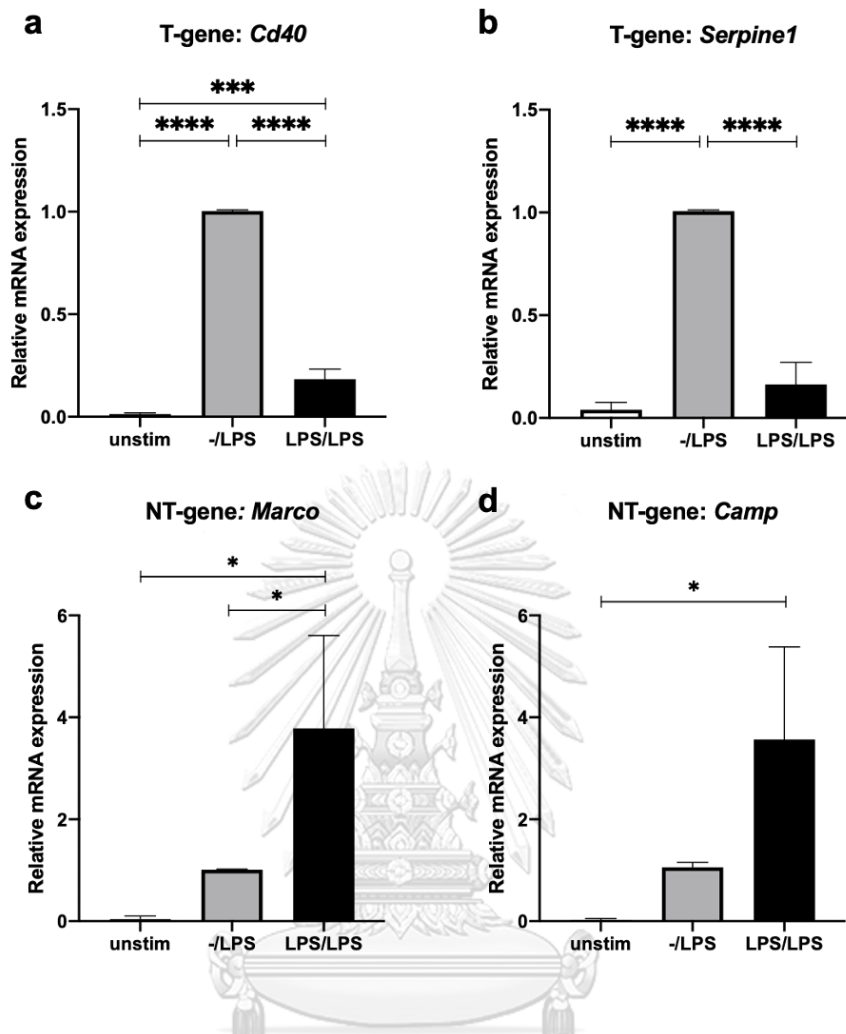
Figure 4.1.5 Expression profile of T and NT genes in LPS-tolerized macrophages (98)

(**a-d**) Expression profiles of tolerizeable genes (T-gene) *Cd40* (**a**) and *Serpine1* (**b**), and non-tolerizeable genes (NT-gene) *Marco* (**c**) and *Camp* (**d**) were detected in LPS-tolerized macrophages after LPS stimulation for 6 h as indicated in **Figure 4.1.2a**. The relative mRNA expression was normalized to the expression of *Actb* by the $2^{-\Delta\Delta CT}$ method and calculated by comparing with LPS-stimulated BMM (-/LPS). *, **, *** and **** indicate statistical significant differences by one-way ANOVA with Tukey's multiple comparison test at $p < 0.05$, $p < 0.01$, $p < 0.001$ and $p < 0.0001$, respectively.

4.2 Inhibitor screening

    4.2.1 Epigenetic compound library screening in BG-trained macrophages

        To identify epigenetic modifier(s) that target molecules with a role in regulating innate immune memory in macrophages, screening assays were performed using an epigenetics compound library in BG-trained or LPS-tolerant macrophages as described in 4.1. The detailed categories of the compounds in the library are listed in **Figure 4.2.1a-b** and **Appendix Table 1**. The inhibitor targets included histone modifying enzymes (38%), epigenetic reader domains (9%), DNA methyltransferases (4%), the JAK/STAT pathway (12%) and other kinases (13%). The screening aimed to identify compounds that affect at the priming or stimulating step during BG-trained or LPS tolerance induction. The screening protocol is summarized in **Figure 4.2.1c-d**. The readout for the screening assay was the amount of TNFα, compared with the control trained macrophages with vehicle control treatment. Compounds that induced TNFα production higher than 1.5-fold or lower than 0.75-fold when compared with the control were summarized in **Figure 4.2.1e**. Among the 181 compounds tested, two compounds showed enhancing effects, while only one compound showed an inhibitory effect on the BG-trained responses. PFI-2 HCl, a histone methyltransferase inhibitor, reduced trained TNFα production when applied during the priming step. An O^6-methylguanine-DNA methyltransferase (MGMT) inhibitor and a DNA/RNA synthesis inhibitor enhanced TNFα production when applied during the priming step. However, none of the compounds had an effect when applied during the stimulation phase (**Figure 4.2.1e and Table 4.2.1**).
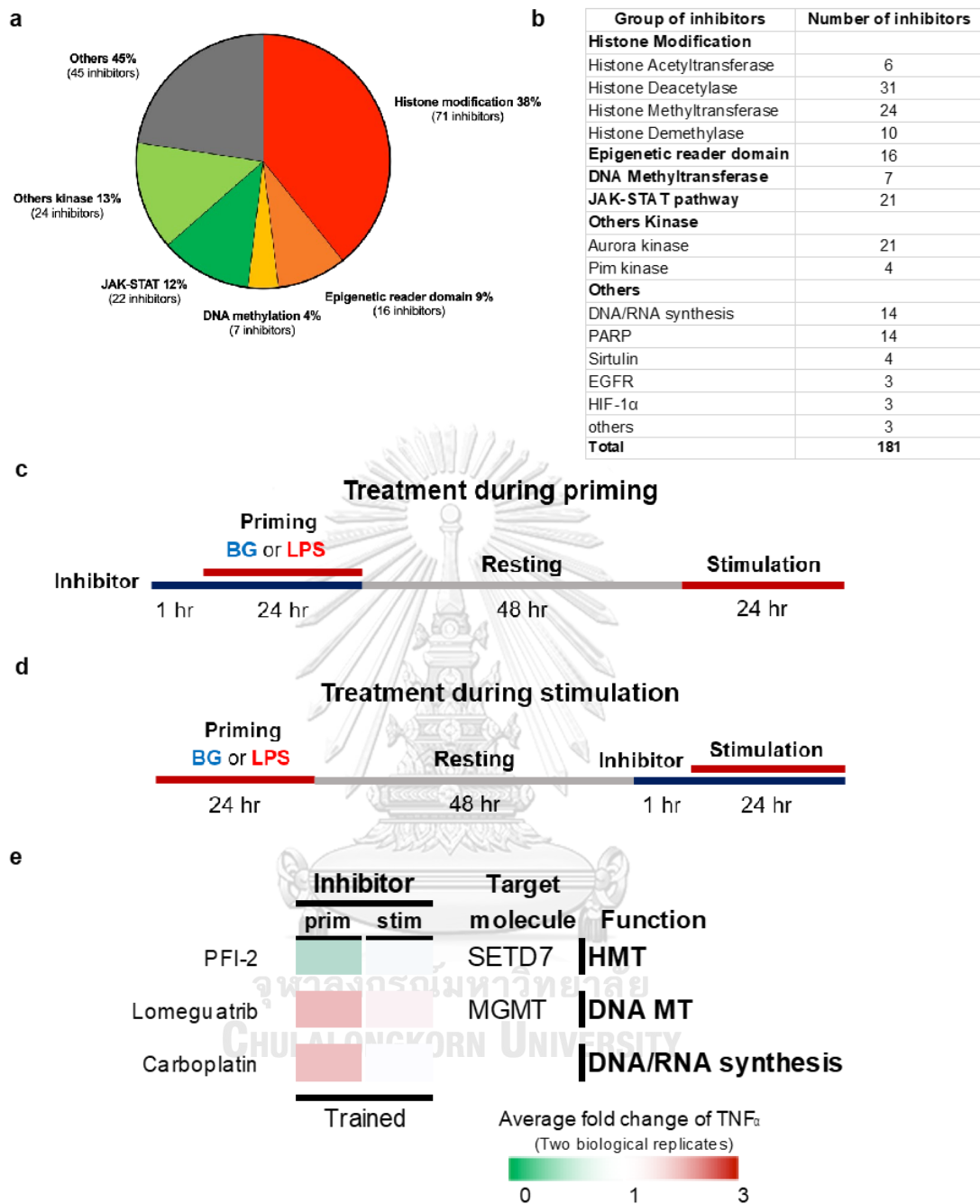
Figure 4.2.1. Compounds that showed enhanced or suppressed TNFα production in BG-trained macrophages (98)

(**a-b**) Categories of the compounds in epigenetic compound library. (**c-d**) The screening protocols to identify compounds with enhancing or suppressing TNFα production in BG-trained or LPS-tolerized macrophages. (**e**) The relative fold changes of TNFα produced from compound-treated BG-trained macrophages (priming step or

stimulation step) were calculated by normalizing to the amount of TNFα produced from vehicle control treated BG-trained macrophages. Average fold changes from two biological replicates are shown in the heatmap format. Only compounds that increased the relative fold changes of TNFα more than 1.5-fold or lower than 0.75-fold are shown. HMT: Histone methyltransferase, DNA MT: DNA methyltransferase

Table 4.2.1. Dose of effective inhibitors and concentration of TNFα from BG-trained macrophages according to **Figure 4.2.1** (98)

Trained Inhibitor	Group	Target	IC50*	Inhibitor treatment	TNFα fold over ctrl	TNFα conc. (pg/ml)
PFI2	HMT	SETD7	2 nM	Inh+prim	0.72 ± 0.07	633 ± 99
Lomeguatrib	DNA MT	MGMT DNA repair	5 nM	Inh+prim	1.53 ± 0.07	2485 ± 470
Carboplatin	DNA/RNASyn	DNA synthesis inhibitor	35 uM	Inh+prim	1.49 ± 0.16	2238 ± 372

Average TNFα concentration in BG-trained macrophages = 1017.17 ± 237.20 pg/ml

HMT: Histone methyltransferase, DNA MT: DNA methyltransferase, DNA/RNAsyn: DNA/RNA synthesis

* inhibitory concentration 50 (IC50) from the manufacturer's data

4.2.2 Epigenetic compound library screening in LPS-tolerized macrophages

In LPS-tolerized macrophages, 28 compounds showed suppressive effects against LPS tolerance, which resulted in increased TNFα production after LPS stimulation. A clear inhibitory effect was observed with inhibitors targeting Aurora kinases, histone methyltransferases, histone deacetylases (HDAC), sirtuin, poly ADP-ribose polymerase (PARP), DNA methyltransferase and DNA/RNA synthesis. Most inhibitors rescued TNFα production under LPS tolerance conditions when added during the LPS stimulation phase (78.6%). The HDAC6 inhibitors ricolinostat and nexturastat and the HDAC1 and HDAC3 inhibitors entinostat showed inhibitory effects when added during the priming step. However, the effect of the enhancer of zeste homolog 2 (EZH2) inhibitor EPZ011989 and the DNA/RNA synthesis inhibitors carboplatin and nedaplatin were detected when treated at either the priming or the stimulating step (**Figures 4.2.2a-b and Table 4.2.2**). The compounds that showed

enhancing effects against LPS tolerance were not further validated because the levels of TNFα were already extremely low in LPS-tolerized macrophages.
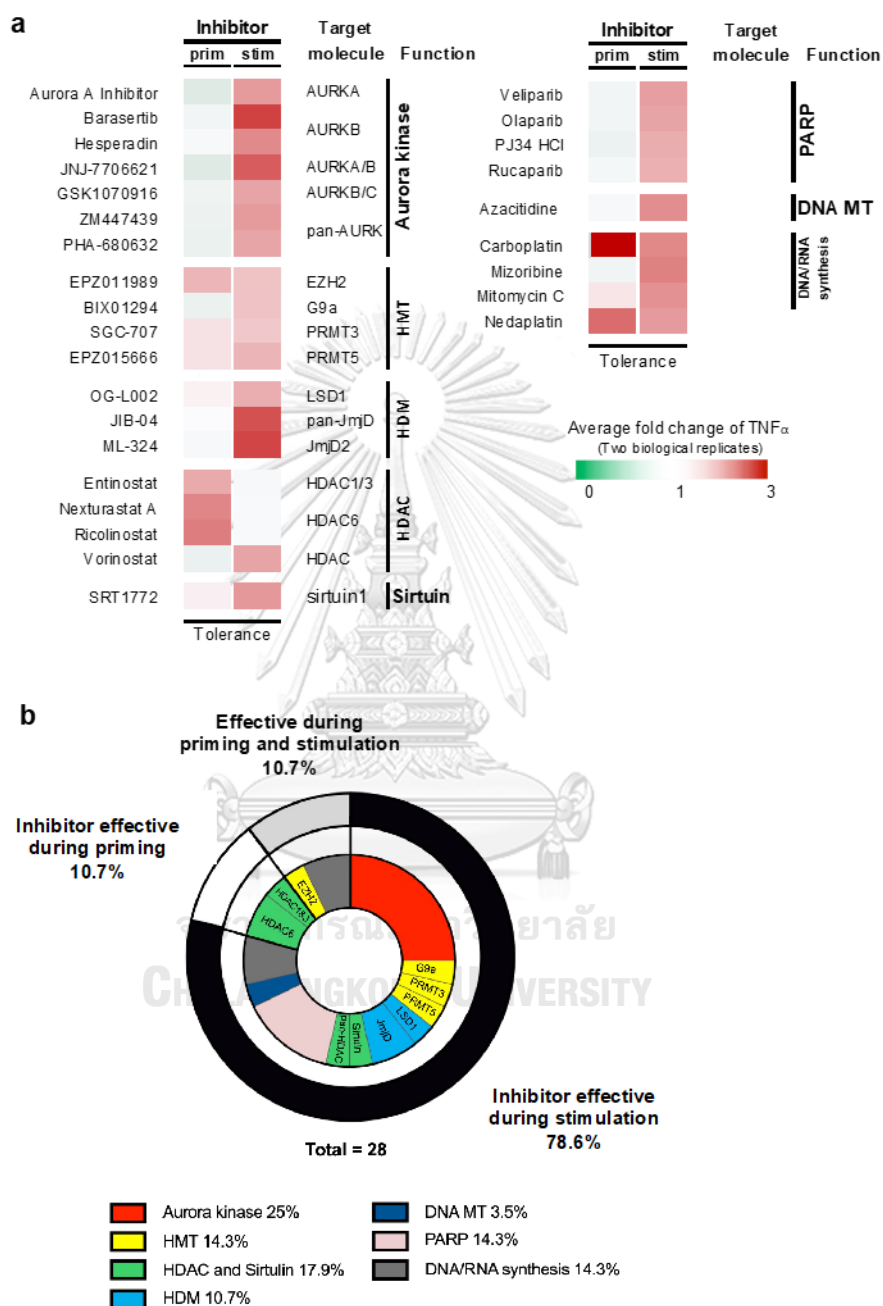

Figure 4.2.2 Compounds that showed enhanced TNFα production in LPS-tolerized macrophages (98).

(**a**) The relative fold changes of TNFα produced from compound-treated LPS-tolerized macrophages (priming step or stimulation step) were calculated by normalizing to the amount of TNFα produced from vehicle control treated LPS-tolerized macrophages. The fold changes are the average from two biological replicates and shown in the heatmap format. Only compounds that increased the relative fold changes of TNFα more than 1.5-fold are shown. (**b**) Summary of the targets of suppressing inhibitors based on target and protocol. HMT: Histone methyltransferase, HDM: Histone demethylase, HDAC: Histone deacetylase, PARP: Poly (ADP-ribose) polymerase, DNA MT: DNA methyltransferase, DNA/RNAsyn: DNA/RNA synthesis

Table 4.2.2 Doses of effective inhibitors and concentration of TNFα from LPS-tolerized macrophages shown in **Figure 4.2.2** (98)

Tolerance Inhibitor	Group	Target	IC50*	Inhibitor treatment	TNFα fold over ctrl	TNFα conc. (pg/ml)
Aurora A Inhibitor	AURK	Aurora A	3.4 nM	Inh+stim	1.84 ± 0.39	121 ± 50
Barasertib	AURK	Aurora B	0.37 nM	Inh+stim	2.51 ± 0.81	167 ± 86
Hesperadin	AURK	Aurora B	0.25 nM	Inh+stim	1.96 ± 0.69	158 ± 32.53
JNJ-7706621	AURK	Aurora A/B + panCDK	9 nM	Inh+stim	2.31 ± 1.21	199 ± 49.5
GSK1070916	AURK	Aurora B/C	6.5 nM	Inh+stim	1.77 ± 0.39	145 ± 9
ZM447439	AURK	pan-Aurora	0.13 uM	Inh+stim	1.84 ± 0.23	205 ± 77.78
PHA-680632	AURK	pan-Aurora	0.135 uM	Inh+stim	1.76 ± 0.41	124 ± 39
EPZ011989	HMT	EZH2	3 nM	Inh+prim	1.63 ± 0.25	162 ± 96.17
EPZ011989	HMT	EZH2	3 nM	Inh+stim	1.54 ± 0.04	210 ± 55.15
BIX01294	HMT	G9a/GLP	2.7 uM	Inh+stim	1.53 ± 0.01	207.5 ± 48.79
SGC-707	HMT	PRMT3	31 nM	Inh+stim	1.5 ± 0.03	204.5 ± 53.03
EPZ015666	HMT	PRMT5	5 nM	Inh+stim	1.65 ± 0.11	222.5 ± 38.89
OG-L002	HDM	LSD1	20 nM	Inh+stim	1.69 ± 0.23	161 ± 84
JIB-04	HDM	Pan-JmjD	0.85 uM	Inh+stim	2.39 ± 0.43	166 ± 17
ML-324	HDM	JmjD2	0.92 uM	Inh+stim	2.48 ± 0.54	644.5 ± 692.26
Entinostat	HDAC	HDAC1/3	1.7 uM	Inh+prim	1.72 ± 0.29	164.75 ± 63.99
Nexturastat A	HDAC	HDAC6	5 nM	Inh+prim	1.99 ± 0.3	190 ± 70.71
Ricolinostat	HDAC	HDAC6	5 nM	Inh+prim	2.06 ± 0.22	192.5 ± 24.75
Vorinostat	HDAC	HDAC	10 nM	Inh+stim	1.77 ± 0.01	205 ± 100.41
SRT1720	Sirtulin	SIRT1 activator	0.16 uM	Inh+stim	1.86 ± 0.53	295 ± 72.12
Veliparib	PARP	PARP1/2	5.2 nM	Inh+stim	1.81 ± 0.05	211 ± 107.48
Olaparib	PARP	PARP1/2	5 nM	Inh+stim	1.77 ± 0.03	203 ± 94.75
PJ34 HCl	PARP	PARP1/2	20 nM	Inh+stim	1.7 ± 0.1	194 ± 83.44
Rucaparib	PARP	PARP inhibitor	1.4 nM	Inh+stim	1.68 ± 0.25	186.5 ± 64.35
Azacitidine	DNAMT	cytidine analogue	20 uM	Inh+stim	1.94 ± 0.48	282.5 ± 101.12
Carboplatin	DNA/RNASyn	DNA synthesis inhibitor	35 uM	Inh+prim	4.49 ± 1.09	171 ± 5
Carboplatin	DNA/RNASyn	DNA synthesis inhibitor	35 uM	Inh+stim	1.98 ± 0.41	134 ± 58
Mizoribine	DNA/RNASyn	DNA synthesis inhibitor	100 uM	Inh+stim	2.04 ± 0.72	140 ± 79
Mitomycin C	DNA/RNASyn	DNA synthesis inhibitor	13 nM	Inh+stim	1.85 ± 0.31	214 ± 78.15
Nedaplatin	DNA/RNASyn	DNA synthesis inhibitor	94 uM	Inh+prim	2.08 ± 0.47	316 ± 125
Nedaplatin	DNA/RNASyn	DNA synthesis inhibitor	94 uM	Inh+stim	1.77± 0.55	176 ± 13

(Average TNFα concentration of LPS-tolerized macrophages is 113.86 ± 46.82 pg/ml)

AURK: Aurora kinase, HMT: Histone methyltransferase, HDMT: Histone demethylase, HDAC: Histone deacetylase, PARP: Poly (ADP-ribose) polymerase, DNAMT: DNA methyltransferase, DNA/RNAsyn: DNA/RNA synthesis

* Inhibitory concentration 50 (IC50) from the manufacturer's data

4.2.3 Potential interacting networks of the targets of the compounds identified in the screening

To investigate the potential interaction (direct interaction or functional interaction) among the targets of the compounds identified by this screening, the STRING database was used to generate a protein-protein interaction network. As shown in **Figure 4.2.3a**, the interaction network generated from the targets identified in LPS-tolerized macrophages revealed the following three distinctive clusters: the Aurora kinase (cell division) related interacting network, the histone modifying enzyme network and the base-excision repair network. In contrast, for the target proteins of compounds identified in the BG-trained macrophages, the network revealed a link with Trp53, Foxo3, Hist2h3c2 and Msh16, which share common features related to apoptosis, DNA repair and polycomb repressive complex 2 (PRC2) (**Figure 4.2.3b**). These analyses suggest that proteins involved in apoptosis, DNA repair, cell division and histone modification may play roles in innate immune memory in macrophages.
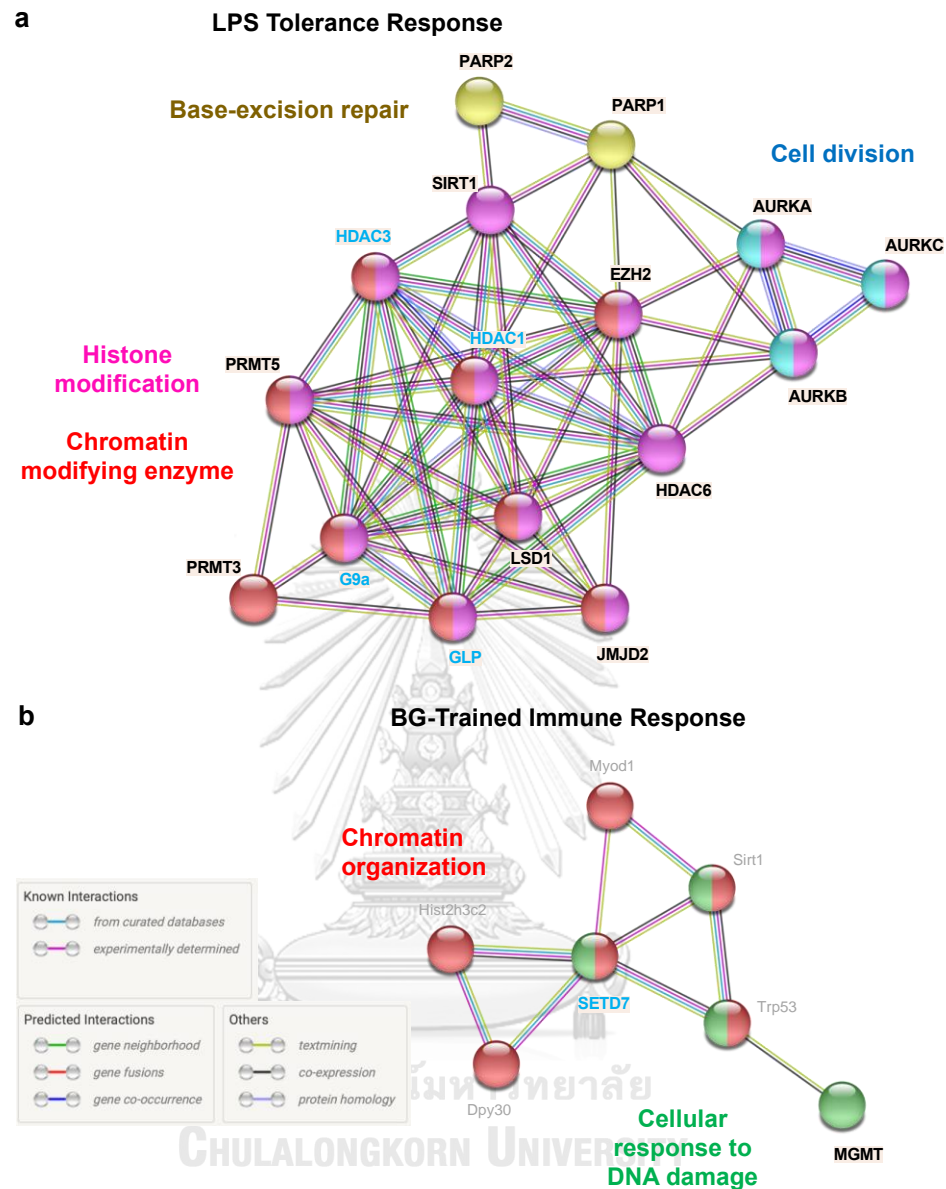
Figure 4.2.3 Possible interactions among the targets of the identified inhibitors (98).
Potential interactions among targets of inhibitors identified in the screening for
tolerance (**a**) and trained immunity (**b**) by STRING. The target proteins of inhibitors
identified in this study are shown in black text while the potential functional partner
proteins are shown in gray text. The interactions among proteins that are
experimentally determined are linked with red lines while the interactions predicted
from curated database are shown in blue. The intensity of edges represents the

confidence of the interaction between two proteins. Effective targets related to previous studies are represented in blue text.

4.3 Inducement of histone lysine demethylase LSD1 in LPS-tolerized macrophages

4.3.1 The effect of suppressive compounds against LPS-tolerance on IL-6 production

To confirm the results from inhibitor screening described above, inhibitors identified in this study were selected to investigate for their effect on IL-6 production in LPS-tolerized macrophages. The selected inhibitors were HDAC inhibitor ricolinostat, Aurora kinase inhibitors barasertib, GSK1070916, and PHA680632, HDMT inhibitors ML324 and OGL002, and HMT inhibitor EPZ015666. As shown in **Figure 4.3.1a**, the inhibitor that enhanced the highest IL-6 production during LPS tolerance was the HDMT inhibitor OG-L002 (1.71-fold), followed by the Aurora-B/C inhibitor GSK1070916 (1.63-fold) and the Aurora-B-specific inhibitor barasertib (1.59-fold), respectively. The HMT inhibitor EPZ015666 and the HDMT inhibitor ML324 also increased IL-6 production, but the difference did not reach statistical significance. All inhibitors did not reduce cell viability to less than 80% after 24 h of incubation (**Figures 4.3.1a-c**).
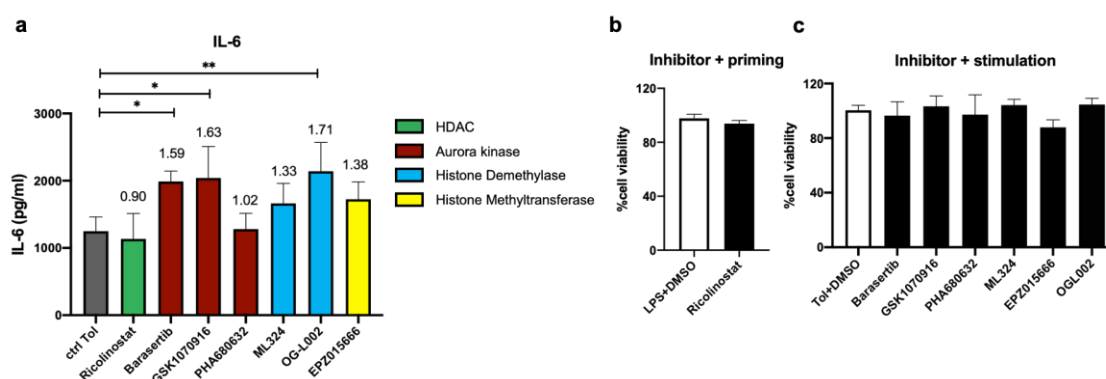
Figure 4.3.1 Effect of the compounds with inhibitory effect against LPS tolerance on IL-6 production (98)

(**a**) IL-6 production after treatment with selected inhibitors from Fig. 3a was measured by ELISA at 24 h after LPS stimulation. (**b, c**) Cell viability was detected by MTT assay at 24 h after treatment with inhibitors from (**a**). *, **, *** and **** indicate significant differences compared by one-way ANOVA with Dunnett's multiple comparison test (a) and two-tailed unpaired *t*-test (d) at $p < 0.05$, $p < 0.01$, $p < 0.001$ and $p < 0.0001$, respectively.

4.3.2 Effect of LSD1 inhibition by OG-L002 on LPS-tolerized macrophages

As the HDMT inhibitor OG-L002 decreased LPS tolerance by enhancing in both TNFα and IL-6 production, the effects of LSD1 inhibition by OG-L002 on TNFα and IL-6 production during LPS tolerance were confirmed (**Figure 4.3.2a-b**) at various concentrations of inhibitor treatment. The effect of TNFα production was found to be in a dose dependent manner up to 40 μM without reducing cell viability (**Figure 4.3.2c**). The highest concentration of OG-L002 increased the TNFα production to more than 2-fold of the control. However, IL-6 production was only slightly induced by this concentration, but the difference between control and inhibitor treatment did not reach statistical significance.
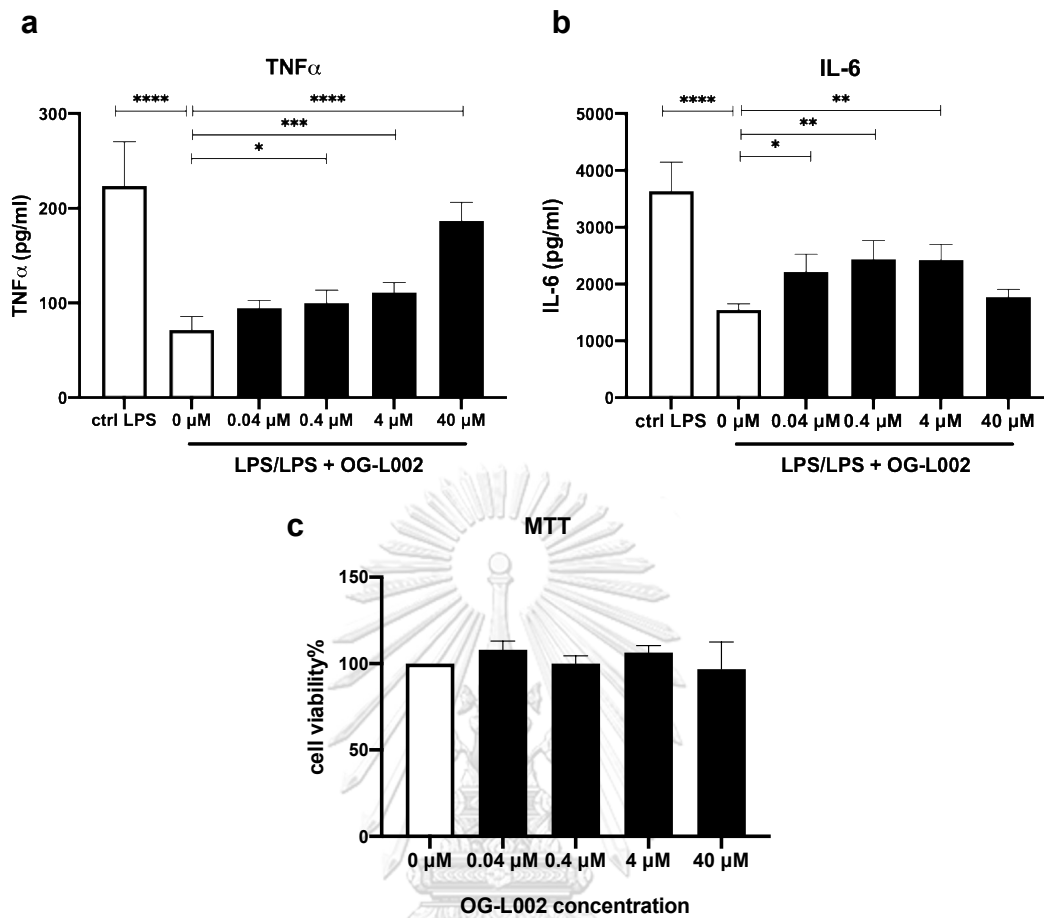
Figure 4.3.2 Effect of OG-L002 on TNFα and IL-6 production in LPS-tolerized macrophages (98).

(**a-b**) The level of TNFα (**a**) and IL-6 (**b**) production in LPS-tolerized macrophages that were treated with the different concentration of LSD1 inhibitor OG-L002. (**c**) Cell viability from the MTT assay in LPS-primed macrophages after treatment with different concentrations of OG-L002 for 24 hr. *, **, *** and **** indicate significant differences compared by one-way ANOVA with Tukey's multiple test at $p < 0.05$, $p < 0.01$, $p < 0.001$ and $p < 0.0001$, respectively.

4.3.3 Expression profile of LSD1 in LPS-tolerized macrophages

To investigate the involvement of LSD1 in LPS-tolerized macrophages, protein expression profiles of LSD1 was detected by Western blot. Total cell lysates were collected after LPS priming, resting and LPS stimulation. Protein profile revealed increased LSD1 expression during LPS priming whereas its level declined after the resting period and LPS stimulation (**Figure 4.3.3a-b**).
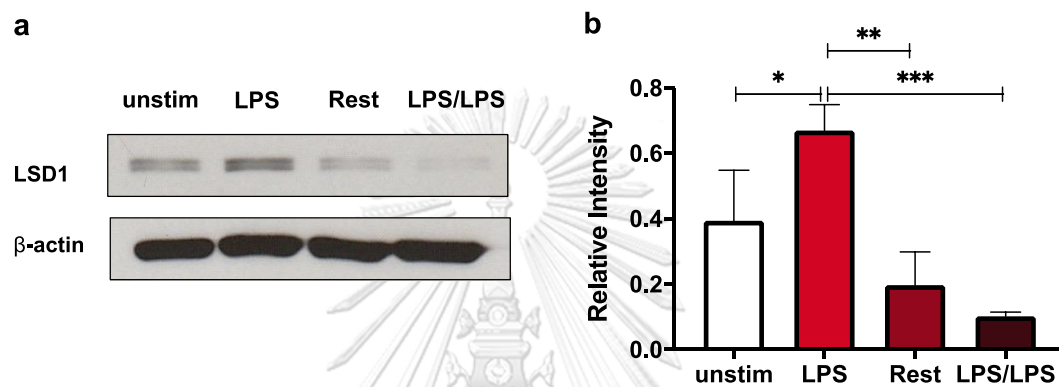
Figure 4.3.3 LSD1 expression profile during LPS-tolerance (98)
(**a-b**) Expression pattern of LSD1 protein were analyzed by Western blot. The relative intensity of LSD1 from Western blot was quantitated by ImageJ analysis and normalized to β-actin. *, **, *** and **** indicate significant differences compared by one-way ANOVA with Tukey's multiple test at $p < 0.05$, $p < 0.01$, $p < 0.001$ and $p < 0.0001$, respectively.

4.3.4 The impact of LSD1 inhibition on enrichment of H3K4me3 in *Tnf* and *Il6* promoter during LPS tolerance

As LSD1 or KDM1A is an epigenetic modifying enzyme that plays important role in demethylation of mono- or di- methyl from H3K4 and H3K9, we hypothesized that LSD1 inhibition should increase the enrichment of active histone mark during LPS-tolerance. To answer this question, the level of H3K4me3 active histone mark, one of LSD1 targets, was investigated by ChIP-qPCR at the *Tnf* and *Il6* promoter. As shown in **Figure 4.3.4a-b**, to our surprise, treatment with 40 μM OG-L002 did not significantly alter the level of H3K4me3 at the *Tnf* promoter but significantly reduced H3K4me3 enrichment in the *Il6* promoter, this result suggests that LSD1 may selectively alter IL-6 production through reducing H3K4me3 that result in decreased *Il6* transcription (**Figure 4.3.2b**).
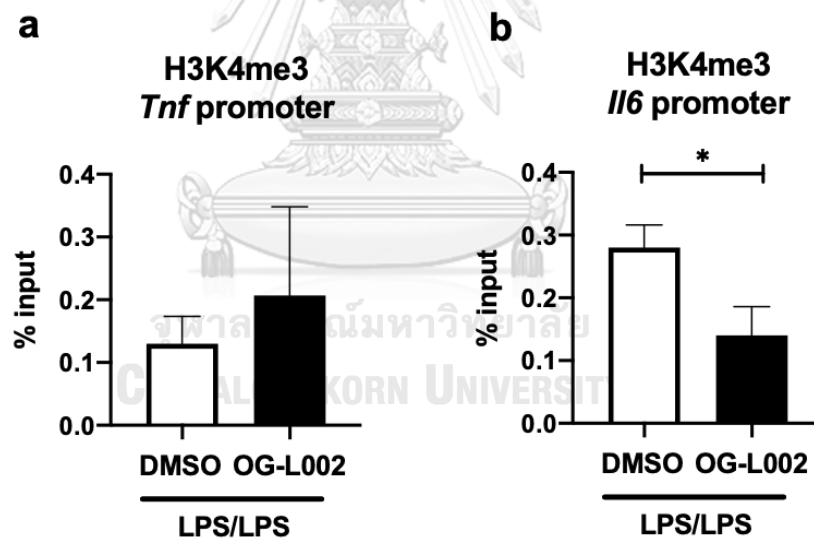
Figure 4.3.4 Effect of OG-L002 on H3K4me3 enrichment on *Tnf* and *Il6* promoter of LPS-tolerized macrophages (98)

(**a-b**) The enrichment of H3K4me3 modification on *Tnf* (**a**) and *Il6* (**b**) promoter of LPS-tolerized macrophages treated with 40 μM OG-L002 at 6 h after LPS stimulation. *, **, *** and **** indicate significant differences compared by two-tailed unpaired *t*-test at $p < 0.05$, $p < 0.01$, $p < 0.001$ and $p < 0.0001$, respectively.

4.3.5 Impact of siRNA-mediated *Lsd1* silencing by siRNA on LPS-tolerance

Finally, we performed siRNA-mediated gene silencing of *Lsd1* to confirm the results obtained by the use of inhibitor. As shown in **Figure 4.3.5a-b**, siRNA targeting *Lsd1* effectively reduced LSD1 protein to approximately 50%. This siRNA was transfected to BMMs 48 h before LPS priming, followed by resting for 48 h and stimulation by LPS for 6 hr. As shown in **Figure 4.3.5d**, the level of *Il1b* mRNA significantly increased when *Lsd1* was silenced in comparison to the control non-targeting siRNA, an indicator that LPS tolerance is compromised. Increased mRNA level of inflammatory genes, *Tnf* and *Il6*, were observed but the difference did not reach statistical significance (**Figure 4.3.5c and e**). Thus, inhibiting LSD1 by inhibitor or reducing its expression by siRNA treatment consistently interferes with LPS tolerance by increasing some tolerizeable gene expression.
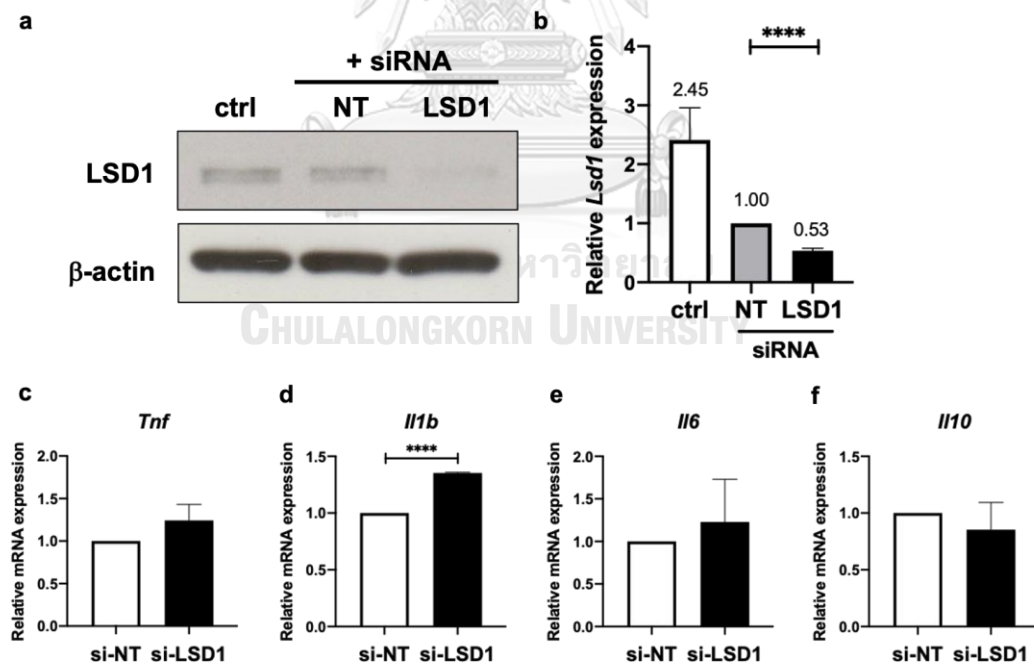
Figure 4.3.5 Effect of *Lsd1* silencing on LPS-tolerized macrophages (98)

BMMs were transfected with 50 nM of LSD1 siRNA or Non-Target (NT) siRNA as described above. (**a-b**) Level of LSD1 expression at 48 h after siRNA transfection was detected by Western blot and qRT-PCR. (**c-f**) Expression profiles of pro-inflammatory (**c**) *Tnf*, (**d**) *Il1b*, and (**e**) *Il6*, and anti-inflammatory cytokines (**f**) *Il10* in *Lsd1* silencing LPS-tolerized macrophages at 6 h after LPS stimulation. *, **, *** and **** indicate significant differences compared by two-tailed unpaired *t*-test at $p < 0.05$, $p < 0.01$, $p < 0.001$ and $p < 0.0001$, respectively

4.4 Role of O^6-methylguanine DNA methyltransferase (MGMT) in BG-trained macrophages

4.4.1 Effect of MGMT inhibition on BG-trained macrophages

To confirm the results from inhibitor screening, the effects of MGMT inhibition by lomeguatrib on TNFα and IL-6 production in BG-trained macrophages were confirmed by various concentration of inhibitor treatment (0.01 µM - 10 µM) prior to the BG-priming as indicated in **Figure 4.4.1a**. TNFα and IL-6 production was induced to be in a dose dependent manner. However, level of IL-6 production in BG-trained macrophages slightly decreased after treatment with the highest concentration of MGMT inhibitor (**Figure 4.4.1b and c**). As MGMT is DNA repair enzyme, inhibition of this target protein may interfere cell viability and induce apoptosis and necrosis of BG-trained macrophages. To clarify this point, level of apoptotic and necrotic cells induced by inhibitor treatment was measured by Annexin V and 7AAD staining. As shown in **Figure 4.4.1d**, treatment of lomeguatrib at 0.01 µM - 10 µM did not significantly induce apoptotic and necrotic cells, compared to the vehicle control. These results indicated that MGMT inhibition enhance TNFα and IL-6 production in BG-trained macrophages.
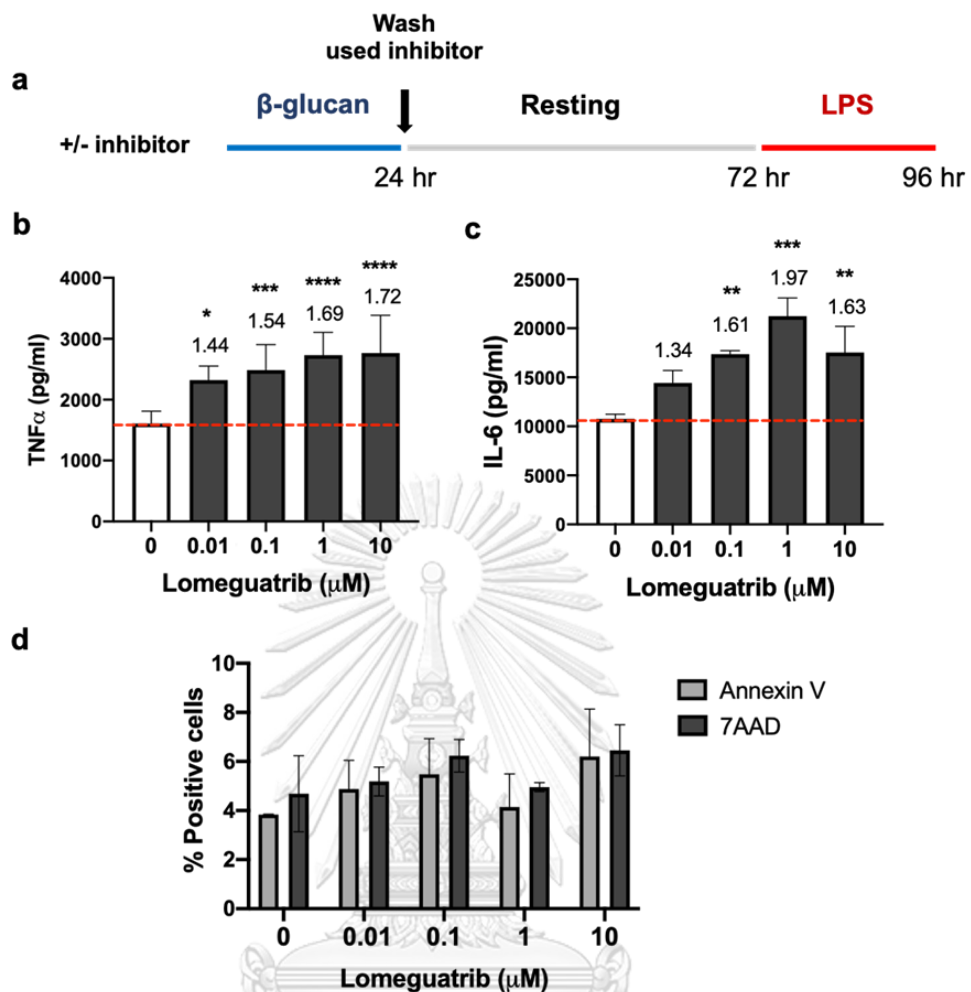
Figure 4.4.1 Effect of MGMT inhibitor lomeguatrib on TNFα and IL-6 production in BG-trained macrophages.

(**a**) Protocol to induce BG-trained macrophages and the indicated time for inhibitor treatment. (**b-d**) The level of TNFα (**b**) and IL-6 (**c**) production in BG-trained macrophages after LPS stimulation that were treated with the different concentration of MGMT inhibitor lomeguatrib. (**d**) Level of apoptotic cells (Annexin V positive) and necrotic cells (7AAD positive) was measured by flow cytometry after treatment with different concentrations of lomeguatrib. *, **, *** and **** indicate significant differences compared by one-way ANOVA with Dunnett's multiple test at $p < 0.05$, $p < 0.01$, $p < 0.001$ and $p < 0.0001$, respectively.

4.4.2 Effect of *Mgmt* silencing on BG-trained macrophages

To further confirm the results from inhibitor treatment and investigate the involvement of MGMT in trained immunity, we used small interference RNA (siRNA) to silent *Mgmt* expression. Silencing efficacy of siRNA were validated at 48 h after siRNA treatment (**Figure 4.4.2a**). The level of MGMT expression strongly decreased in si-MGMT treated macrophages. Trained immunity was induced in the macrophages as described above and TNFα and IL-6 production were measured at 24 h after LPS stimulation. As expected, *Mgmt* silencing macrophages enhance effect of trained immunity as the level of TNFα and IL-6 production are higher than the non-target control (**Figure 4.4.2b and c**). These results agree with the data from inhibitor treatment and strongly emphasized the effect of MGMT inhibition or silencing in enhancement of trained immunity.
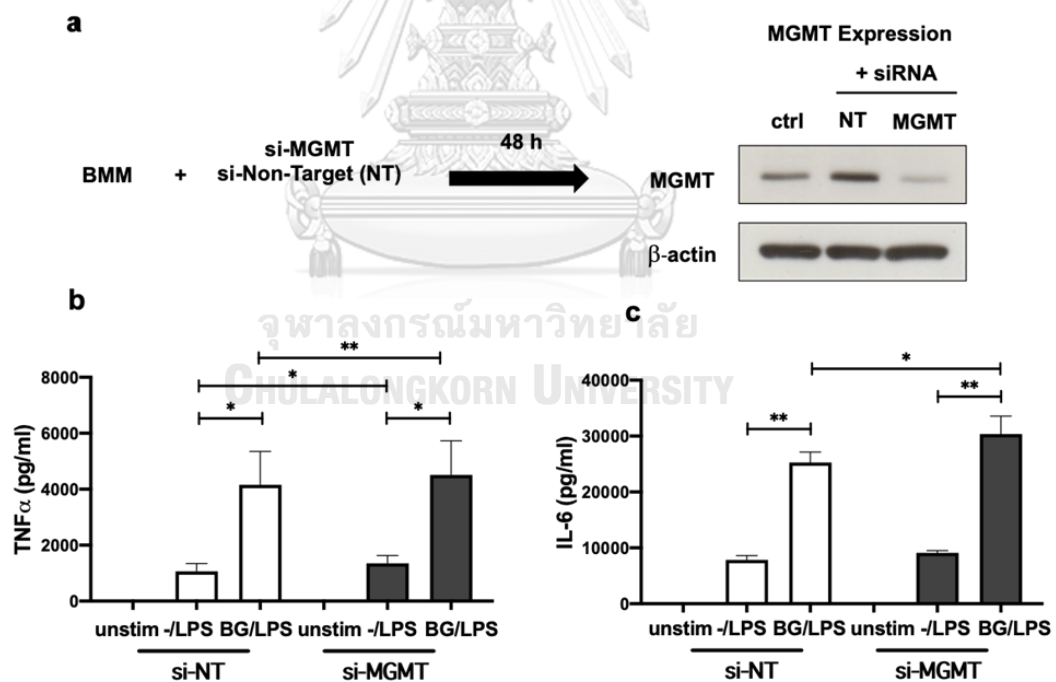
Figure 4.4.2 Trained immunity in *Mgmt* silencing macrophages

(**a**) Silencing efficacy of siRNA was measured in BMMs pretreated with 1 μM si-MGMT or non-targeting control for 48 h prior induction of trained immunity. (**b-c**) Trained immunity were induced as in **Figure 4.4.1a**. The level of TNFα (**b**) and IL-6 (**c**)

production from *Mgmt* silencing and non-targeting silencing macrophages was measured at 24 h after LPS stimulation. *, **, and *** indicates significant difference by two-tailed paired *t*-test at $p < 0.05$, $p < 0.01$ and $p < 0.001$, respectively.

4.4.3 Expression profiles of MGMT in BG-trained macrophages

As MGMT play important role in regulation of trained immunity, RNA and protein profiles of MGMT during induction of trained immunity were investigated. For the RNA profiles, total RNAs were collected after priming and LPS-stimulation for 6 h and the expression levels were measured by RT-PCR. As shown in **Figure 4.4.3a**, *Mgmt* expression significantly decreased after priming with BG, resting and LPS stimulation. As protein synthesis is the outcome of mRNA expression, the protein profiles were examined at 24 h after BG-priming and LPS stimulation. Interestingly, the protein level of MGMT significantly increased after priming with BG then significantly decreased at after 48 h of resting step and LPS stimulation (**Figure 4.4.3b-c**). The upregulation of MGMT protein during BG priming emphasizes the possible role of MGMT in regulation of trained immunity.

Figure 4.4.3 Expression profiles of MGMT in BG-trained macrophages

WT and MGMT KO macrophages were stimulated as in **Figure 4.4.1a**. (**a**) RNA expression profiles of *Mgmt* were detected after the priming and stimulation for 6 h. The data were normalized by *Actn* by $2^{-\Delta\Delta CT}$ method and calculated as fold changes compared to unstimulated cells. (**b**) Expression patterns of MGMT were detected by Western blot. (**c**) The relative intensity of MGMT expression from Western blot was

analyzed by ImageJ and normalized to GAPDH. *, **, and *** indicates significant difference compared by one-way ANOVA with Tukey's multiple test at $p < 0.05$, $p < 0.01$, $p < 0.001$ and $p < 0.0001$, respectively.

4.4.4 Expression profile of MGMT in WT and MGMT KO macrophages

Because the effect of MGMT has already been confirmed by inhibitor treatment and siRNA silencing, MGMT KO macrophages generated from bone marrow of the MGMT KO mice were used to further investigate the role of MGMT in trained immunity. Macrophages generated from bone marrow of the littermate control mice were used as the control WT macrophages. To assess the knockout efficacy, expression profiles of MGMT in WT and KO macrophages was observed by Western blot assay and RT-PCR. As expected, both protein and mRNA levels of MGMT expression were significantly decreased in MGMT KO macrophages (**Figure 4.4.6**).
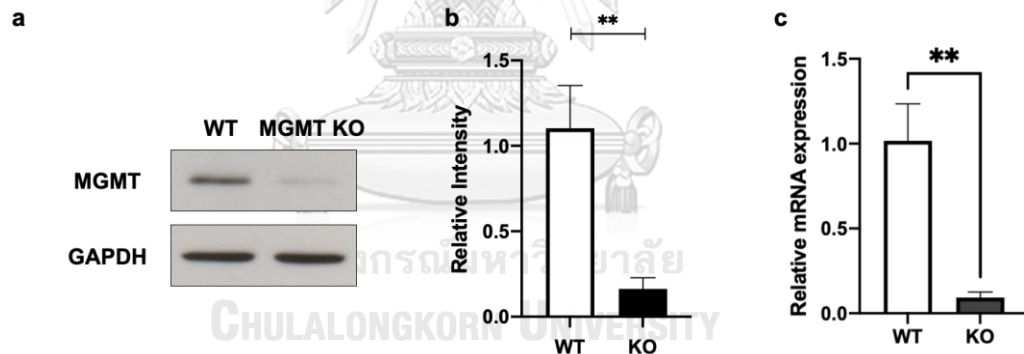
Figure 4.4.4 Generating MGMT KO macrophages

(**a**) MGMT expression profile in unstimulated WT and MGMT KO macrophages detected by Western blot. (**b**) Relative intensity of MGMT expression normalized to GAPDH analyzed by ImageJ analysis. (**c**) The relative mRNA level of *Mgmt* expression was normalized to *Actb* by $2^{-\Delta\Delta CT}$ method and calculated as fold changes compared to unstimulated WT macrophages. *, **, and *** indicates significant difference by two-tailed unpaired t-test at $p < 0.05$, $p < 0.01$ and $p < 0.001$, respectively

4.4.5 Trained immunity in MGMT KO macrophages

To investigate the effect MGMT in trained immunity, WT and MGMT KO macrophages were primed and stimulated as mentioned in **Figure 4.4.1a**. As shown in **Figure 4.4.5a and b**, both types of macrophages can induce training effect in both TNFα and IL-6 production when compared to the LPS stimulation alone. LPS stimulation alone did not result in different cytokine production. However, MGMT KO macrophages produced a lower training effect on both TNFα and IL-6 production, while the difference of cytokine production was not observed in response to the LPS stimulation. This finding contrasts with the result obtained from inhibitor treatment and siRNA silencing indicating that the effect of MGMT in regulation of trained immunity depended on specific time points.
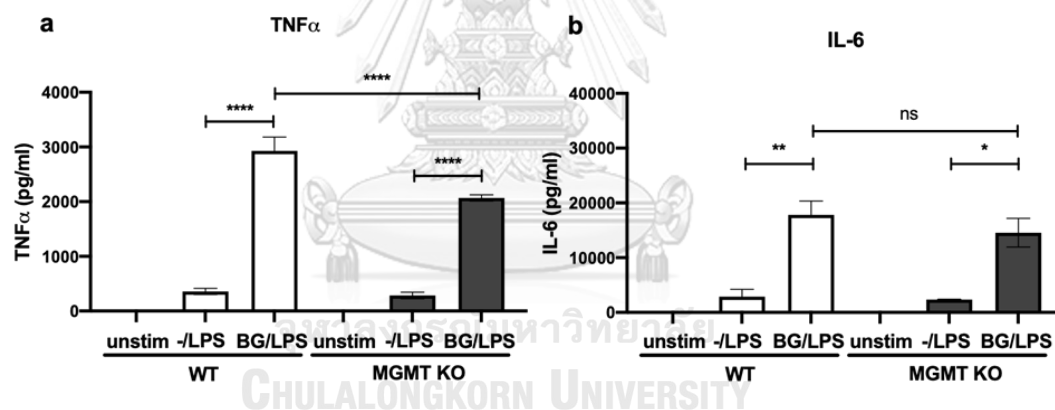
Figure 4.4.5 Decreased trained immunity in MGMT KO macrophages

WT and MGMT KO macrophages were induced to be trained macrophages as indicated **Figure 4.4.1a**. (**a-b**) The level of TNFα (**a**) and IL-6 (**b**) production from unstimulated, LPS-stimulated or BG-primed in WT and MGMT KO macrophages was detected by ELISA at 24 h after LPS stimulation. *, **, and *** indicates significant difference by two-tailed unpaired *t*-test at $p < 0.05$, $p < 0.01$ and $p < 0.001$, respectively.

4.4.6 Expression profiles of pro-inflammatory cytokines in WT and MGMT KO macrophages

As the results from the KO macrophages are different from the data obtained by inhibitor treatment and siRNA silencing, the expression profile of pro-inflammatory cytokines in was investigated to further confirm the effect of MGMT against cytokine production in BG-trained macrophages. As shown in **Figure 4.4.6b-d**, depletion of MGMT significantly decreased expression of *Tnf*, *Il6* and *Il1b* in trained macrophages without alter the cytokines expression in LPS stimulation which agrees with the results in **Figure 4.4.5**. Both WT and KO macrophages can induce training effect in *Tnf*, *Il6* and *Il1b* but the training effect in *Il1b* expression did not reach statistical significance.
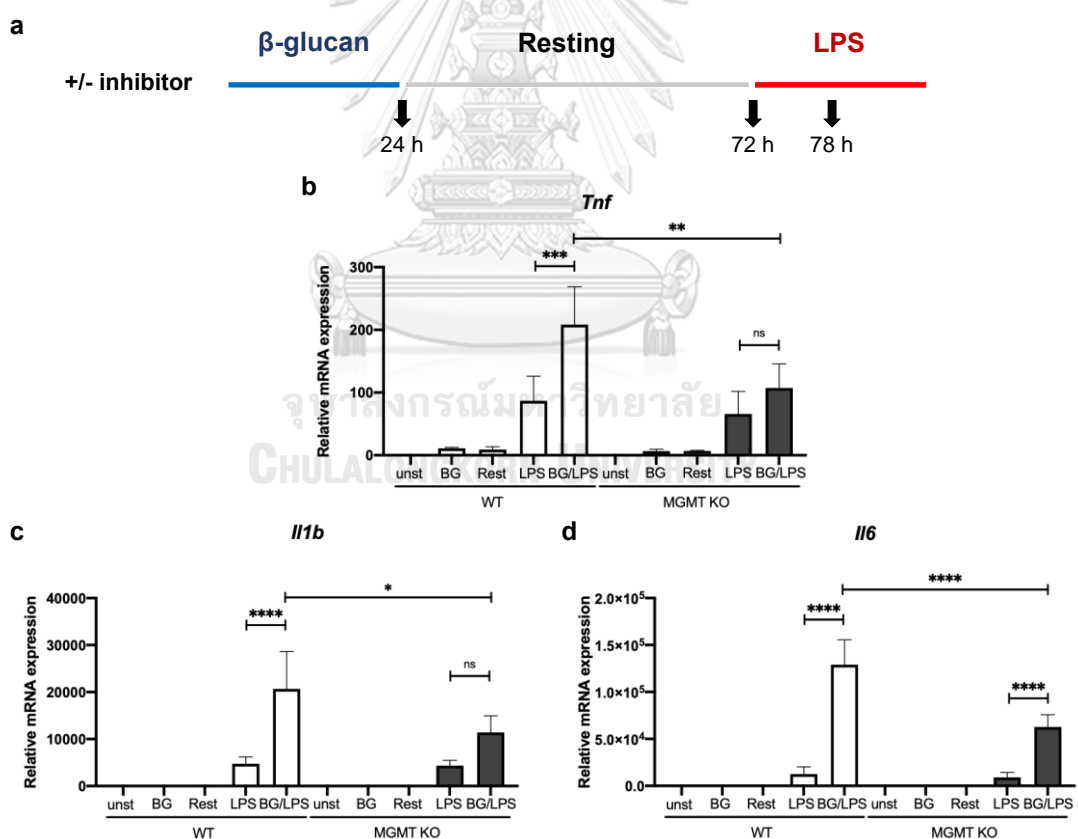
Figure 4.4.6 Decreased mRNA expression of pro-inflammatory cytokines in WT and MGMT KO macrophages

(**a**) Protocol to induce BG-trained macrophages and the indicated time for total RNA collection. (**b-d**) mRNA expression profile of pro-inflammatory cytokines *Tnf* (**b**), *Il6* (**c**) and *Il1b* (**d**) from WT and MGMT KO macrophages were detected after the priming and stimulation for 6 h. The relative mRNA expression was normalized to *Actb* by $2^{-\Delta\Delta CT}$ method and calculated by with unstimulated BMM. *, **, and *** indicates significant difference by two-tailed unpaired *t*-test at $p < 0.05$, $p < 0.01$ and $p < 0.001$, respectively.

4.4.7 Cell viability in LPS-stimulated or trained WT and MGMT KO macrophages

As MGMT is a DNA repair enzyme, the reduction of cytokine production in trained immunity of MGMT KO macrophages in the previous experiment may be due to failure in DNA repair and the decrease in cell viability. To validate this point, cell viability of BG-trained WT and MGMT KO macrophages were detected at 24 h after LPS stimulation. As shown in **Figure 4.4.7a-c**, MGMT KO macrophages with BG-trained or LPS stimulation did not significantly alter cell viability compared with the WT macrophages that received the same stimulation. These results confirmed that the reduction of cytokines in MGMT KO BG-trained macrophages was not due to the decrease in cell viability.
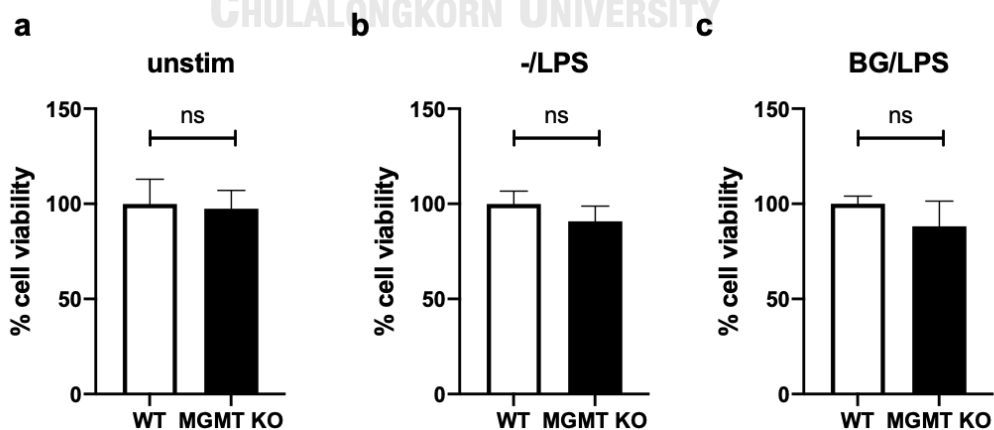
Figure 4.4.7 The viability of WT and MGMT KO macrophages after LPS stimulation

WT and MGMT KO macrophages were stimulated as in **Figure 4.4.1a**. (**a-c**) Cell viability from MTT assay of unstimulated (**a**), LPS-stimulated (**b**), or BG-primed (**c**) in WT and MGMT KO macrophages after stimulation with LPS for 24 h. The viability was normalized to the WT macrophages in each condition. ns: not statistically significant

4.4.8 *In vivo* trained immunity in WT and MGMT KO mice

As depletion of MGMT decreased the effect of trained immunity in macrophages *in vitro*, we further validated the effect of deficient MGMT in myeloid cells in WT and MGMT KO mice. *In vivo* trained immunity was induced by injection of 1 mg per mouse of BG to the mice, which was followed by injection of 10 μg of LPS at day 5 after BG-priming (**Figure 4.4.8a**). Levels of serum cytokines expression were measured at 3 h after LPS injection. As shown in **Figure 4.4.8b**, the WT mice with BG-priming significantly enhanced TNFα production compared to the WT control LPS mice (PBS/LPS), indicating that the successful induction of trained immunity was achieved. In contrast to the WT mice, depletion of MGMT significantly decreased TNFα production in BG-trained mice. The level of TNFα production from MGMT KO BG-trained mice was reduced to the level as seen in the control LPS mice. In addition, the levels of others inflammatory cytokine were measured and summarized in **Figure 4.4.8c**. Effect of trained immunity was clearly observed for IFN-γ, IL-1α, IL-1β, IL-10, IL-17A, IL-23, and IL-27 but difference in the level of these cytokines did not reach statistical significance. Most of these inflammatory cytokines were decreased in MGMT KO mice with trained immunity. Interestingly, IFN-γ was the only cytokine that the MGMT KO has training effect higher than the WT mice. This results strongly confirmed that MGMT can regulated trained immunity in both *in vitro* and *in vivo*.
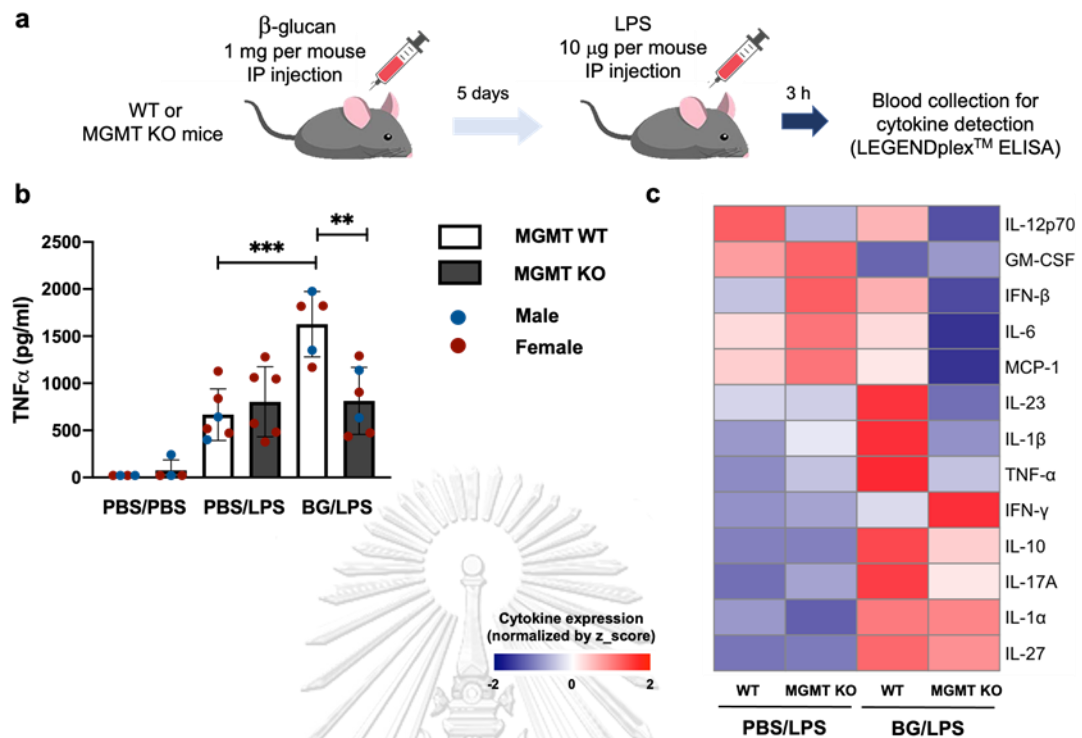
Figured 4.4.8 *In vivo* trained immunity in WT and MGMT KO mice

(**a**) Protocol to induce trained immunity in WT and MGMT KO mice and indicated time point for blood collection. (**b-c**) Level of TNFα (**b**) and others inflammatory cytokines production (**c**) was measured by multiplex ELISA in serum after 3 h of LPS injection. *, **, and *** indicate significant differences compared by two-tailed unpaired *t*-tests at $p < 0.05$, $p<0.01$ and $p<0.001$, respectively.

4.4.9 Transcriptomic analysis of trained MGMT KO macrophages

To investigate how depletion of MGMT alter the trained immunity in macrophages, we performed transcriptomic analysis of unstimulated (Unstim), BG-primed (BG24) and BG-trained (BG/LPS) macrophages. The transcriptomic data obtained from the RNA sequencing were mapped and aligned with Hisat2 and counted using the R package Rsubread, featureCounts. The PCA analysis was performed to represent the difference in the transcriptomic data of each sample. As shown in **Figure 4.4.9a**, all transcriptomic data were clustered into three groups based on the stimulation profiles. Depletion of MGMT in macrophages slightly induced difference in the transcriptomic data when compared to the WT. Then, differential expressed genes (DEGs) were compared and analyzed by DESeq2. To focus on the effect of MGMT KO in trained immunity, the expression profiles of DEGs in BG-primed and BG-trained WT and MGMT KO macrophages were normalized to the expression of unstimulated WT macrophages and represented as heatmap. As shown in **Figure 4.4.9b-d**, depletion of MGMT significantly induced specific DEGs profiles in BG-trained macrophages after the BG priming and LPS stimulation. Top 10 up-down regulated DEGs in each condition were shown in **Figure 4.4.9c-d**.
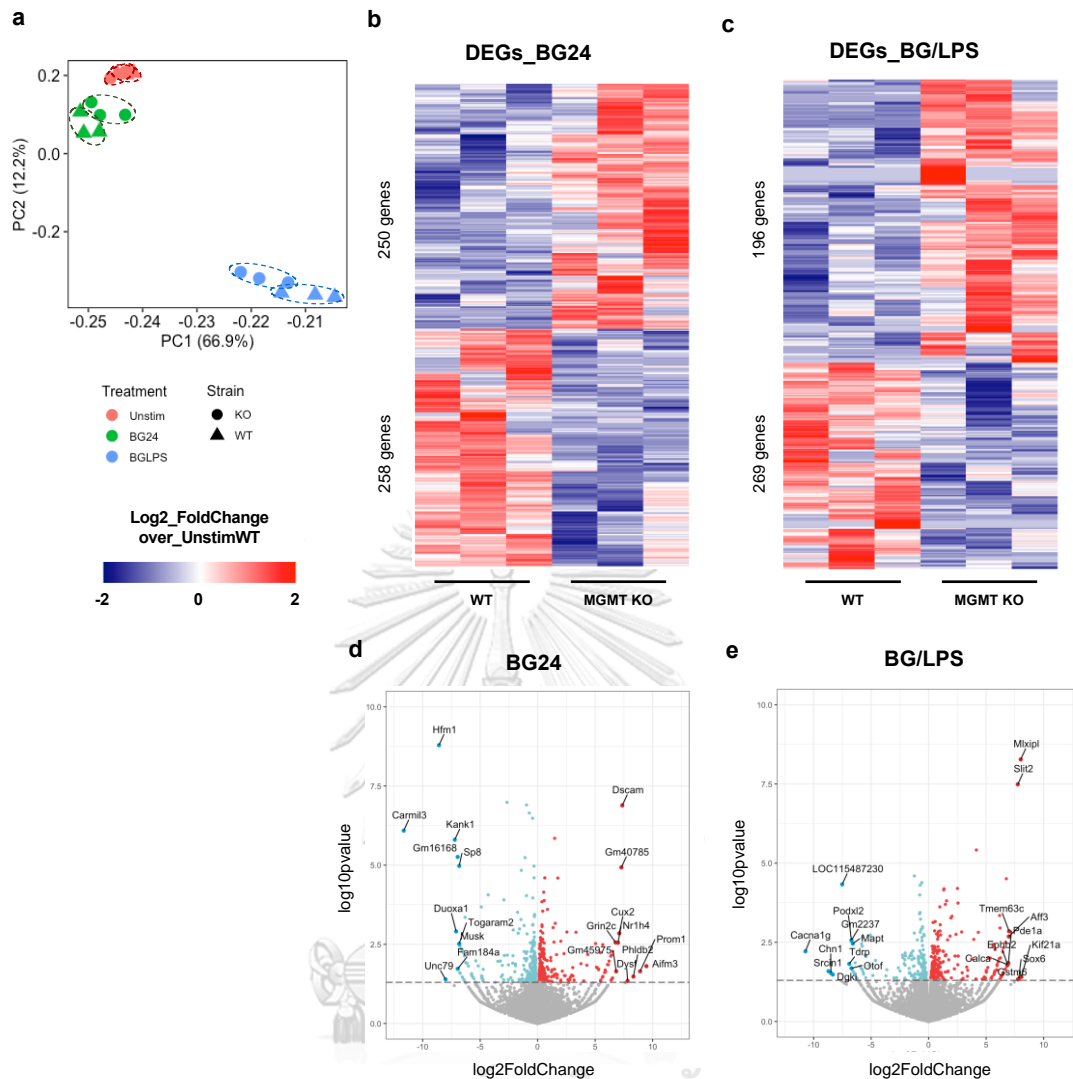
Figure 4.4.9 Transcriptomic profile of WT and MGMT KO trained macrophages

Trained immunity in WT and MGMT KO macrophages was induced as mentioned above. The indicated times of treatment for transcriptome analysis were shown in **Figure 4.4.6a**. (**a**) PCA analysis of transcriptomic profile in unstimulated, BG24 and BGLPS WT and MGMT KO macrophages are shown. (**b-c**) Heatmap of DEGs in MGMT KO macrophages after BG-priming (BG24, **b**) and LPS stimulation (BG/LPS, **c**) analyzed by DESeq2 (p-value cut off < 0.05). (**d-e**) Volcano plots between log_{10}pvalue and log_2foldchange of each DEGs in BG24 (**d**) and BGLPS (**e**) are shown.

4.4.10 Functional analysis in the transcriptomic profiles of trained MGMT KO macrophages

To further investigate the transcriptomic data of trained MGMT KO macrophages, DEGs of all conditions were compared using the Venn diagram. The up-down DEGs that expressed in both BG-primed and BG-trained MGMT KO macrophages were listed in the **Figure 4.4.10a**. The DEGs that specifically expressed in each condition (red circle) were subjected to Gene Set Enrichment Analysis (GSEA). As shown in **Figure 4.4.10b-c**, depletion of MGMT significantly increased the expression of genes involved in nuclear receptor metapathway, PI3KAKT signaling, and malignant pleural mesothelioma. On the other hands, genes involved in MAPK signaling were significantly downregulated in trained MGMT KO macrophages during LPS stimulation. As MAPK signaling is one of the TLR4 downstream signaling pathway, alteration of genes in this pathway may result in alteration of the TLR4 signaling.

a

UpKO_BG24   UpKO_BGLPS

DownKO_BG24   DownKO_BGLPS

Upregulated DEGs in BG-trained MGMT KO macrophages

- **Epigenetic Regulator** : *Prdm5*
- **Antigen processing** : *Lgmn*
- **Immune related genes** : *Aff3, Pianp, Xlr, Cyp4f18*
- **Others** : *Lins1, Tmem267, Mdm1, Ankrd55, Gm6145, Rapsn, Rab3il1, Ccdc152, Flnc*

Downregulated DEGs in BG-trained MGMT KO macrophages

- **TLR signaling** : *Treml4*
- **Integrin signaling** : *Pram1*
- **Immune response to bacterial infection** : *Lyz2*
- **Others** : *Cracdl, Ralgapa2, Rasgef1b, Cntnap1, Spns3, Mir3113, Patj*

b

c

Figure 4.4.10 Pathway analysis in MGMT KO trained macrophages

(**a**) Venn diagram compared list of up-down DEGs in BG-primed and BG-trained MGMT KO macrophages analyzed by DESeq2 (*p*-value cut off < 0.05). (**b**) GSEA analysis of

specifically expressed DEGs in BG-primed and BG-trained MGMT KO macrophages (*p*-value cut off < 0.05, FDR cut off <0.25). (**c**) Heatmap of DEGs in up-down pathway from **Figure 4.1.10b**.

4.4.11 TLR4 signaling in trained WT and MGMT KO macrophages

As MAPK signaling pathway, one of downstream TLR4 signaling cascade, was down regulated in transcriptomic data of trained MGMT KO macrophages, we hypothesized that depletion of MGMT may interfere with TLR4 signaling in BG-trained macrophages. To test this hypothesis, activation of NF-κB and MAPK pathway were investigated in BG-trained macrophages. As shown in **Figure 4.4.11a-e**, stimulation of LPS significantly activated NF-κB and MAPK signaling pathways, including ERK, p38, and SAPK/JNK, in a time-dependent manner during LPS stimulation. When compared to WT macrophages, the level of phosphorylated p38, and SAPK/JNK, was significantly lower in the trained MGMT KO macrophages. Depletion of MGMT slightly decreased NF-κB and ERK activation, but the levels did not reach statistical significance. This result is consistent with transcriptomic data in **Figure 4.4.10** and strongly indicates that depletion of MGMT interferes with TLR4 signaling in BG-trained macrophages without altering the level of TLR4 on the cell surface (**Figure 4.4.11f**).
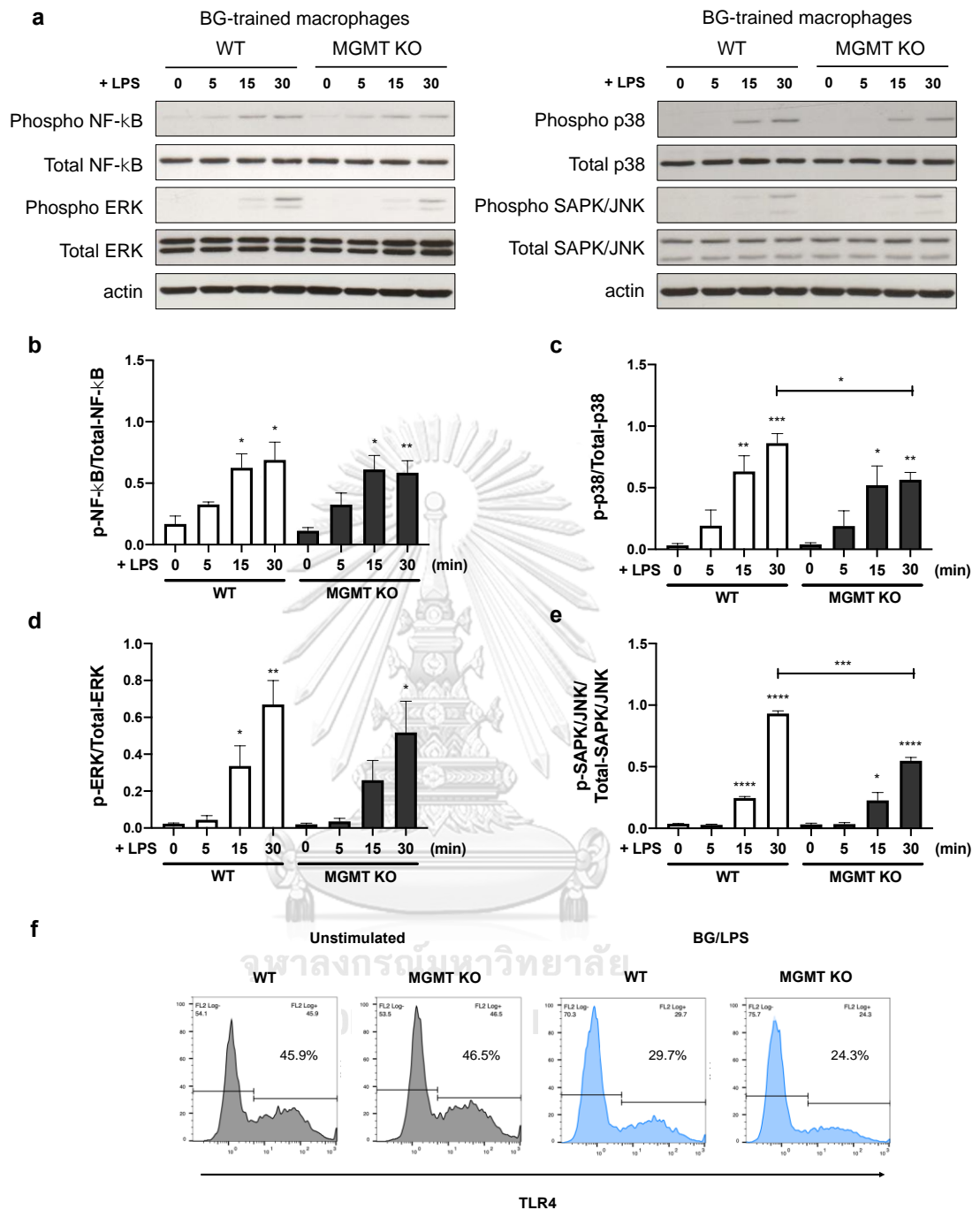
Figure 4.1.11 Decreased of NF-κB and MAPK signalings in BG-trained MGMT KO macrophages

(a) NF-κB and MAPK signaling profiles in BG-trained WT and MGMT KO macrophages were detected by Western blot assay at indicated time point after LPS stimulation. (b-e) Levels of phosphorylated NF-κB (b), p38 (c), ERK (d), and SAPK/JNK (e) were

analyzed by imageJ. The relative intensity was normalized to the total form of each protein. (**f**) Level of TLR4 expression in unstimulated and BG-trained macrophages measured by flow cytometry. *, **, and *** indicate significant differences compared by two-tailed unpaired t-tests at $p < 0.05$, $p < 0.01$ and $p < 0.001$, respectively. * over the bars represent statistical differences compared to the BG-primed WT or MGMT KO macrophages without LPS stimulation (LPS 0 min).

4.4.12 AKT/mTOR signaling profile in BG-trained WT and MGMT KO macrophages

As TLR4 signaling profiler decreased in MGMT KO macrophages, we hypothesized that whether the downstream signaling of Dectin-1 would also be altered in the MGMT KO macrophages. To answer this question, activation of AKT and mTOR pathway, downstream signaling pathway of Dectin-1 receptor, was investigated in BG-trained MGMT KO macrophages. Activation of AKT signaling pathway were detected as phosphorylation at Thr308. The signals were detected at early point after BG-priming, as it is upstream signals of the mTOR pathway. As shown in **Figure 4.4.12a**, phosphorylation of AKT were clearly induced in WT and MGMT KO macrophages at 4 h after BG priming in similar level. Even though there was no difference in AKT signaling between WT and KO macrophages, the activation of mTOR signaling pathway was significantly decreased in the MGMT KO macrophages (**Figure 4.4.12b**). This result reveals the possible role of MGMT in regulation of downstream signaling molecules of Dectin-1 and TLR4 receptors.
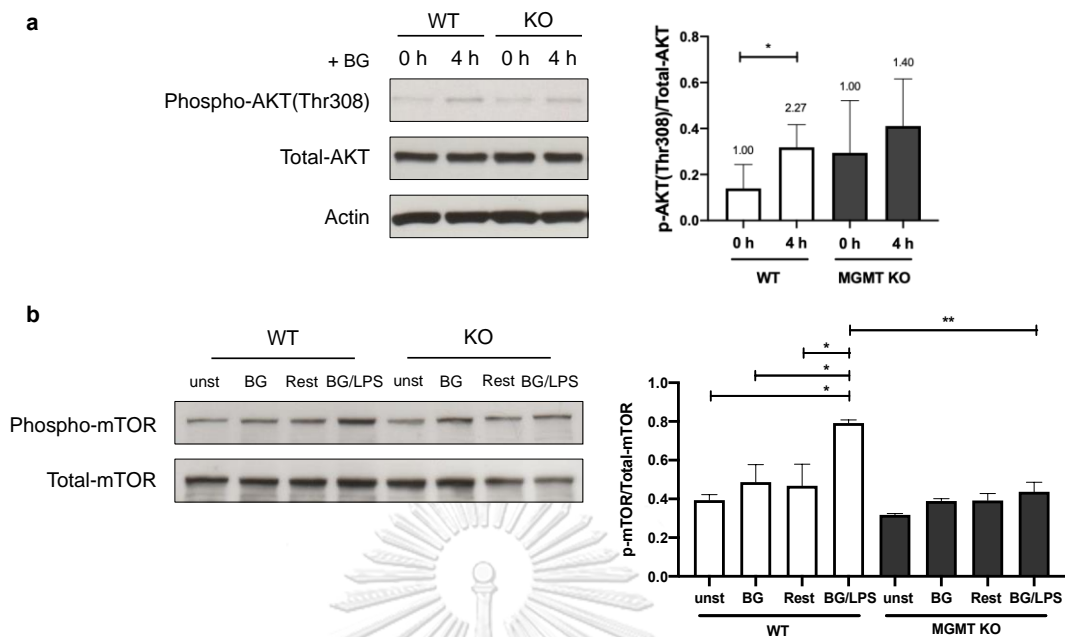
Figure 4.1.12 Decreased mTOR signaling in trained MGMT KO macrophages

(**a**) AKT signaling and the relative intensity of phosphorylated AKT in WT and MGMT KO macrophages was detected by Western blot at 4 h after BG priming. (**b**) mTOR signaling profile and relative intensity of mTOR phosphorylation in WT and MGMT KO macrophages was detected by Western blot assay after BG priming, resting and LPS stimulation. Relative intensity was analyzed by ImageJ analysis. The intensities of phosphorylated AKT and phosphorylated mTOR were normalized to the total AKT or mTOR. *, **, and *** indicate significant differences compared by two-tailed unpaired t-tests at $p < 0.05$, $p < 0.01$ and $p < 0.001$, respectively.

4.4.13 Glycolytic function in BG-trained WT and MGMT KO macrophages

As depletion of MGMT in trained macrophages resulted in decrease mTOR signaling, we asked that whether targeted deletion of MGMT alters glycolysis metabolism in trained macrophages. To clarify this point, we performed a glycolysis stress assay which detect the level of glycolysis as an extracellular acidification rate (ECAR) by Seahorse XFp Analyzer. In this experiment, the glycolytic functions were

investigated in unstimulated and BG-primed macrophages after resting for 48 h as indicated in **Figure 4.4.13a**. As shown in **Figured 4.4.13b-f**, depletion of MGMT decreased ECAR level in the BG-primed macrophages, but not in the unstimulated cells. The reduction of ECAR signals in the BG-primed MGMT KO macrophages resulted in decrease of both non-glycolytic acidification and glycolytic function, including glycolysis, glycolytic capacity, and glycolytic reserve. The reduction in glycolysis in MGMT KO during induction of trained immunity may be responsible for a decrease in the inflammatory response of trained macrophages as found in the previous experiments.
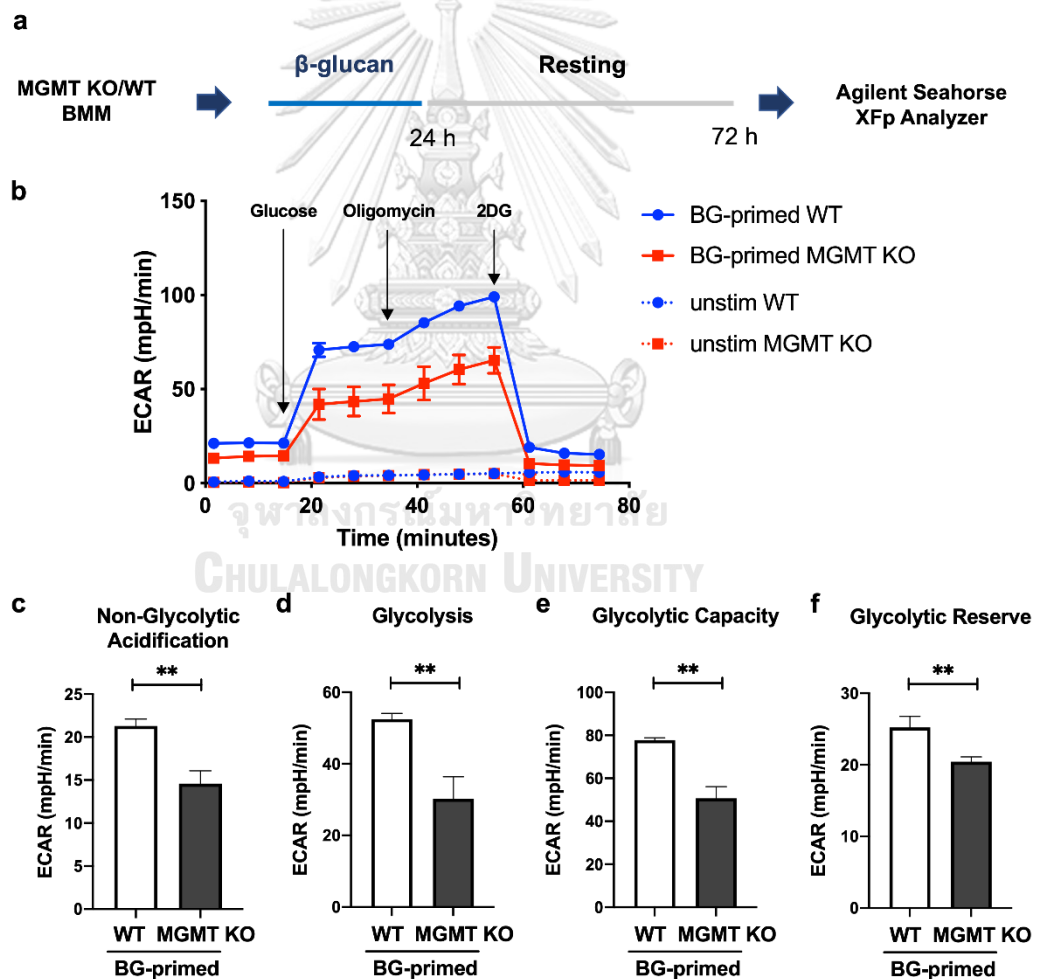
Figure 4.4.13 Glycolytic function in BG-trained WT and MGMT KO macrophages

(**a**) Protocol to induce BG-trained WT and MGMT KO macrophages. (**b**) ECAR from glycolysis stress assay in unstimulated and BG-primed WT and MGMT KO macrophages after resting for 48 h (**c-f**) ECAR from of glycol-stress analysis in BG-trained macrophages: (**d**) non-glycolytic acidification, (**e**) normal glycolysis, (**f**) glycolytic capacity, and (**g**) glycolytic reserve. *, **, and *** indicates significant difference by two-tailed unpaired *t*-test at $p < 0.05$, $p < 0.01$ and $p < 0.001$, respectively.

CHAPTER V

DISCUSSION

Innate immune response was generally believed to be nonspecific and has no memory. However, organisms lacking adaptive immune system exhibit some "memory" characteristics such as altered response to secondary infection and transplantation rejection. The innate immune memory exhibits as either enhanced or suppressed the immune response. Trained immunity and tolerance in monocytes and macrophages are part of the innate immune memory (1). These innate immune memory phenomena are governed by transcription factors, epigenetic changes and metabolic programming that result in modified responses in the subsequent encounter with the stimuli (99). Because epigenetic reprogramming plays important roles in regulating innate immune memory, in this study, we aimed to identify novel epigenetic regulators that play a role in either trained or tolerance responses, which may potentially be a novel target for the treatment of conditions caused by dysregulated innate immune memory.

LPS tolerance accompanied by gene-specific chromatin modification that results in either suppression of gene transcription (including inflammatory genes) of subset of tolerized genes and gene activation (including antimicrobial effector genes) or subset of non-tolerized genes (**Figure 4.1.5** and (14)). Upstream signaling molecules such as phosphatase SHIP-1 participate in reducing the phosphorylation of signal transduction molecules downstream of TLR (100). In tolerized genes, histone deacetylation and certain lysine methylation cooperate to induce the state of transcriptional silencing (101). In our screening assay, various inhibitors showed inhibitory effects against LPS tolerance by increasing TNFα production after repeated LPS stimulation (**Figure 4.2.2**, (98)). Inhibitors targeting histone-modifying enzymes are a major group of inhibitors that reverse LPS tolerance. Several suppressive targets identified in our screening have been characterized in previous studies, such as

HDAC1 and HDAC3 (39), HDAC6 (59), and G9a and GLP (33, 34). Most of these inhibitors showed their effects when added during LPS stimulation after LPS priming. This result suggests that these molecules may function to rapidly modify epigenetic states that influence responses to LPS stimulation during the tolerance phase.

Interestingly, Interestingly, EZH2 inhibitor EPZ011989 inhibit activity of PRC2 histone methyltransferase enhanced TNFα production when added during the priming or stimulation (98). EZH2 is a catalytic subunit of a large PRC2 protein complex that regulates the mono-, di, and trimethylation of the repressive histone mark H3K2. EZH2 also methylates non-histone protein substrates such as the transcription factor GATA4 (102, 103). The wide ranges of the substrates of PRC2/EZH2 imply that PRC2/EZH2 may regulate multiple steps during LPS tolerance. The detailed mechanism how EZH2 regulates LPS tolerance is currently being investigated by our group.

Interestingly, inhibitors of histone demethylase, OG-L002, JIB-04 and ML-324, only showed an effect when added during LPS stimulation, but not during the LPS priming. This result indicated that histone methylation may be essential for maintaining repressive chromatin for TNFα expression during LPS stimulation but not during LPS priming. The results from our screening assay showed that inhibitor function during LPS stimulation may open a window for reversing LPS tolerance after the first tolerogenic exposure that may be useful for rescuing the immune paralysis observed in the conditions such as sepsis (98, 104).

We also validated the impact of LSD1 inhibition on LPS tolerance by pharmacological and genetic approaches which yielded consistent outcomes (98). Both approaches showed that LSD1 plays a positive role in regulating LPS tolerance. LSD1 is the key enzyme that mediates demethylation of mono- and di-methylated lysine, specifically H3K4 and H3K9 among others (61). LSD1 functions downstream of LPS/TLR4 and controls acute inflammatory response during sepsis in myeloid cells.

Deletion of LSD1 resulted in severe cytokine storm and lethality in sepsis (62). In this study, we found that, pharmacological inhibition of LSD1 during LPS stimulation, but not LPS priming, rescued the LPS tolerance phenotype by enhancing both TNFα and IL-6 (**Figure 4.3.1 and 4.3.2**). Although LSD1 expression increased during the early step of LPS tolerance (**Figure 4.3.3**), silencing of *Lsd1* expression before induction of LPS tolerance significantly increased *Il1b* expression but not for *Tnf* and *Il6* expression (**Figure 4.3.5**). Different cytokine profiles may be due to the difference in time point of inhibition or silencing. Inhibition of LSD1 by 40 μM of OGL002 during LPS stimulation induced the highest TNFα production, which is equal to the level obtained from single LPS stimulation (**Figure 4.3.2**). This indicates the effective suppression of LPS tolerance by inhibitor treatment during LPS stimulation. Although LSD1 expression decreased at 48 h after resting and 24 h after LPS stimulation when compared to the priming step, LSD1 may increase at the early time point during LPS stimulation in tolerance macrophages. However, we could not detect the changes in H3K4me3 level associated with the promoter of *Tnf* upon LSD1 inhibition during LPS stimulation whereas H3K4me3 level was reduced in the *Il6* promoter (**Figure 4.3.4**). This result may indicate that LSD1 may mediate demethylation of other histone marks that have a combined effect on LPS tolerance. Alternatively, LSD1 may regulate enhancer chromatin that collaboratively suppress gene expression. Other LSD1 substrate(s) that may play a crucial role in regulating LPS tolerance include H3K9, H3K27, H3K36, and H3K79 (61).

Interestingly, Aurora kinases inhibitors showed suppressive effect against LPS tolerance. Aurora kinases are well characterized in regulating mitotic processes, and their inhibition results in cytokinesis failure and is one of the targets for cancer therapy (105). Because priming with LPS did not induce cell proliferation (**Appexdix C Figure C1**, (98))., Aurora kinases may regulate LPS tolerance through other mechanisms not related to cell cycle regulation, such as epigenetic regulation.

Among the three subtypes of Aurora kinases, Aurora kinase B has been reported to regulate the deposition of some repressive histone marks, such as phosphorylation of H3S10, H3S28 and H3K9me3 (54, 106). In our study, Aurora kinase B was the only isoform that significantly changed its phosphorylation level during LPS tolerance. Increased phosphorylation of Aurora kinase B during the resting period of LPS tolerance may regulate the deposition of these repressive histone marks (**Appexdix C Figure C2**, (98)). In addition to its roles during cell division and epigenetic regulation, Aurora kinase A participates in early signaling during T cell activation by regulating CD3z-containing vesicle trafficking (107). In one report, Aurora kinase A regulated M1 macrophage polarization by suppressing NF-κB activation and switched macrophages toward the M2 phenotype (55). How these groups of enzymes regulate LPS tolerance needs further investigation.

In trained immunity, BG stimulation through Dectin1, Akt/mTOR and HIF-1α induced metabolic changes coupled with epigenetic reprogramming (**Figure 4.1.4**, (1, 7, 40)). This complicated regulatory network results in higher transcription of the subset of trained genes, including *Tnf, Il1b* and *Il6* (**Figures 4.1.2**, (18, 40, 74)). In addition to BG, other microbial stimuli, such as BCG vaccination, and nonmicrobial stimuli, such as oxidized LDL, can also induce trained immunity in monocytes and macrophages (1, 5). Different trained stimuli utilize the common molecular mechanisms with some distinctive features for inducing trained immune responses. In this study, we used TNFα as a readout for the BG-trained response in macrophages because TNFα is one of the best characterized representative markers that is under the control of the trained immune response. To our surprise, only three compounds showed positive hit in our screening assay that have an effect on the BG-trained immune response (**Figure 4.2.1e**, (98)). An inhibitor of the histone methyltransferase SETD7, PFI-2 HCl, has a suppressive effect on trained immunity when added during the BG priming but not during stimulation. A lysine methyltransferase, SETD7, has

multiple histone and non-histone substrates that have been explored for targeted treatments of conditions, such as cancer and obesity (108). Methylation of H3K4 mediated by SETD7 is associated with increased gene expression. A recent report identified SETD7 as a key enzyme that increases oxidative phosphorylation in BG-trained macrophages by upregulating key enzymes in the TCA cycle (41). This result supports the validity of an unbiased screening approach in our study (98).

In addition to SETD7, the other two compounds lomeguatrib and carboplatin showed enhancing effects on BG-trained immunity (98). These two inhibitors have not been previously investigated with trained immunity. Lomeguatrib is a specific inhibitor of O^6-methylguanine-DNA methyltransferase (MGMT). MGMT is a DNA repair protein that functions during DNA damage caused by alkylating agents and plays a role in conferring resistance to cancer cells against some cancer chemotherapies (109). Expression MGMT expression increased after priming with BG (**Figure 4.4.3**) and inhibition or silencing of MGMT expression during the priming results in increased the effect of trained immunity (**Figure 4.4.1 and 4.4.2**). This result implies the role of MGMT in regulation of trained immunity. As the well documented function of MGMT is to mediate repair of O^6-MeG DNA scar from alkylating agents, loss of MGMT function may lead to accumulation of the O^6-MeG DNA and interfere with gene expression related to trained immunity. Besides alkylating agents, O^6-MeG may arise from the endogenous source such as S-adenosyl methionine (SAM) and endogenous N-nitroso compounds (NOC) from food (110, 111). Further experiments are required to investigate whether accumulation of the O^6-MeG scar and its endogenous causative agents can affect trained immunity in macrophages.

In addition to its role in cancer, MGMT has been linked to inflammation, as hypermethylation of its promoter is associated with chronic inflammatory diseases and chronic infectious diseases (69, 71, 72, 112). To further confirm the effect of MGMT, mice with myeloid specific deletion of MGMT (MGMT KO) was generated.

Although MGMT knockout mice are susceptible to the lethal effect of alkylating agents (113), specific deletion of MGMT in myeloid cells did not affect growth and general phenotypes of the mice (**Appendix Figure C3**). Unexpectedly, targeted deletion of MGMT results in decreased trained immunity (**Figure 4.4.5 and 4.4.6**). Together with the results of using inhibitor, the effect of MGMT in trained immunity seems to depend on the specific time point and duration of inhibition. These results indicate that although transient interfering of MGMT function enhances the effect of trained immunity, MGMT may still require for maintaining the inflammatory response during trained immunity in macrophages. The reduction of cytokines production also observed when induced trained immunity *in vivo* which most of cytokines were decreased in myeloid specific MGMT KO mice. However, IFN-γ was the only cytokine that show the training effect in MGMT KO mice. As macrophages can produce a low level of IFN-γ, the increase of IFN-γ production may produce form others immune cells which require further experiment to validate this effect.

To clarify how MGMT regulates trained immunity, transcriptomic analysis was performed in MGMT KO macrophages. Depletion of MGMT the dampened numerous signaling pathways, including MAPK and mTOR signaling in trained macrophages (**Figure 4.4.10-4.4.12**). As metabolic shift of glycolysis is regulated by mTOR pathway, glycolytic function was also decreased in MGMT KO macrophages with trained immunity (**Figure 4.4.13**). Decrease of glycolytic function may interfere with the deposition of specific epigenetic marks during trained immunity (40). This emphasized the unexpected role of MGMT beyond its role as DNA repair.

Since MGMT is not a transcription factor, it may regulate gene expression by interacting with other proteins. The possible MGMT-interacting proteins were identified in previous study. Metabolic enzyme pyruvate kinase and proteins related to epigenetic regulation such as SETs and several histone proteins are potential

interacting proteins with MGMT (114). This finding highlights the role of MGMT in epigenetic and metabolic regulation in trained immunity.

Based on our transcriptomic data, depletion of MGMT increased the expression of gene in the nuclear receptor metapathway, as shown in **Figure 4.4.10c**. Among these, nuclear receptor subfamily 1 group H member 4 (*Nr1h4*) or farnesoid X receptor (FXR) highly upregulate in trained MGMT KO macrophages. FXR is a bile acid receptor that negatively regulates several metabolic pathways such as lipid metabolism, gluconeogenesis, and glycolysis (115-118). Moreover, activation of FXR also interfere downstream signaling of TLR4 by several mechanisms such as interfere the binding of MAPK-AP1 transcription factor (116, 119) and prevent the clearance of nuclear receptor corepressor 1 (NCoR1) complex (120-122) in the promoter of inflammatory genes during TLR4 activation. These indicated that expression of MGMT may interfere with the FXR function. Further experiments are required to confirm the effect of FXR in BG-trained MGMT KO macrophages. As trained immunity is tightly regulated by histone modification, we also investigated the profile of histone modifying enzyme in BG-trained MGMT KO macrophages (**Appendix Figure C5**). Interestingly, several H3K4 modifying enzymes downregulated in MGMT KO macrophages during trained immunity. Furthermore, the epigenetic regulator PR domain zinc figure protein 5 (*Prdm5*) significantly increased in BG-trained MGMT KO macrophages. This protein can promote transcription repression by recruitment of G9a/GLP histone methyltransferase and HDAC1 (123, 124). These resultsindicated that depletion of MGMT may interfere with histone modification during trained immunity.

As inhibition and silencing of *Mgmt* expression during BG priming yielded opposite outcomes on TNFα production when compared to the results obtained from MGMT KO macrophages, the effect of MGMT in trained immunity depends on specific time point and duration of inhibition. During BG-priming, MGMT may interfere with signaling and inflammatory proteins. Based on our transcriptome data, loss of

MGMT expression increase chimaerin-1 (*Chn1*) during BG-priming (**Figure 4.4.10a**). Chimaerin has been reported to promote inflammation in many cancers tissue (125-127). Hence, loss of MGMT expression may promote the enhancing effect of trained immunity as found in inhibitor treatment and siRNA silencing. Although transient interference with MGMT function enhanced the effect of trained immunity, it may still be necessary for maintaining the inflammatory response during trained immunity in macrophages. Loss of MGMT expression during LPS stimulation in BG-trained macrophages resulted in downregulation of MAPK signaling pathway which may decrease the effect of trained immunity. Moreover, expression of chimaerin-1 also decreased in MGMT KO macrophages during LPS stimulation which may collaboratively regulate the decrease of inflammatory response in BG-trained MGMT KO macrophages.

To our surprise, several DNA/RNA synthesis inhibitors showed inhibitory effects against LPS tolerance and enhancing effects against the BG-trained immune response (98). Among this is the platinum derivative carboplatin which often used as chemotherapeutics against cancers. They induce cancer cell death by various mechanisms (128). However, the cell cycle and cell death have not been investigated in terms of training or tolerance in macrophages, but it is possible that innate immune memory is tightly coupled with epigenetic modification and cell cycle/cell death. As shown in our report publication which focused on the effect of carboplatin on LPS tolerance, the treatment of carboplatin interferes with the expression of several epigenetic machinery, including repression of H3K9 methyltransferase Suv39h1 and H3K9 reader protein Hp1, and enhanced expression of H3K9 demethylase Kdm4d. This mode of action is partially responsible for a decrease in H3K9 modification and enhancing cytokine expression during LPS-tolerized macrophages (98, 129).

To cluster the targets identified by our screening, we uncovered clusters of protein networks of the inhibitor targets identified in this study using the STRING database (**Figure 4.2.3**, (98)). For LPS tolerance response, histone modification and chromatin modifying enzymes formed a large cluster with targets identified in this study such as LSD1, PRMT3, PRMT5, EZH2, JMJD2, HDAC6 and SIRT1. Most of these interactions are experimentally determined. Proteins involved in base-excision repair (PARP1/2) and cell division (Aurora kinase A/B/C) formed small clusters that linked to the histone modification cluster via EZH2, SIRT1 and HDAC6. For the BG-trained response, two clusters of proteins in chromatin organization and cellular response to DNA damage were linked together via TRP53 and SETD7. Although TRP53 was not identified in our screening, methylation of TRP53 by SETD7 (Set7/9) has been reported in cancer settings (130). Thus, BG-trained immunity may involve in modification by methyltransferase of non-histone substrates (131). Some of the links shown here are based on the curated database and require further experimental prove for the physical/functional interactions in innate immune memory.

Tolerance and trained innate immune memory are tightly regulated, and the interaction between the two events has been reported at multiple levels. BG treatment is able to revert the epigenetic states conditioned by LPS tolerance, and trained immunity may be a mechanistic link between sepsis and atherosclerosis (24, 132). Recent emerging evidence has pointed to the critical roles of innate immune memory in various pathological conditions, including chronic inflammatory diseases and cancer. The use of epigenetic modifying compounds provides potential interventions for such diseases. Furthermore, our screening results provide new unappreciated key enzymes/pathways that may regulate training and tolerance in macrophages.

CHAPTER IV

CONCLUSION

- This study identified several new epigenetic regulators of innate immune memory including Aurora kinase, histone methyltransferase EZH2, PRMT3 and PRMT5, histone demethylase LSD1 and JMJD2, and histone deacetylase HDAC6 and SIRT1, which play a crucial role during LPS tolerance.

- Besides epigenetic proteins, DNA repair enzymes, such as PARP (for LPS tolerance) and MGMT (for trained immunity), were also found to be a novel non-epigenetic regulator of innate immune memory.

Table 6.1 Novel regulator proteins of innate immune memory identified by inhibitor screening

Novel Targets Identified by Inhibitor Screening	
Tolerance	Trained Immunity
• Aurora kinase • Histone methyltransferase: EZH2, PRMT3 and PRMT5 • Histone Deacetylase HDAC6 and SIRT1 • Histone demethylase: LSD1 and JmjD2 • DNA repair: PARP	• DNA repair enzyme: MGMT

Role of LSD1 in regulation of LPS tolerance

- Inhibition of LSD1 during repeated LPS stimulation suppressed LPS tolerance by enhancing both TNFα and IL-6 expression.

- The silencing of *Lsd1* expression before LPS priming increased the expression of *Il1b* during LPS tolerance, but not for *Tnf* and *Il6* expression.

- The level of active histone mark H3K4me3 on the *Tnf* and *Il6* promoter did not increase by LSD1 inhibition.
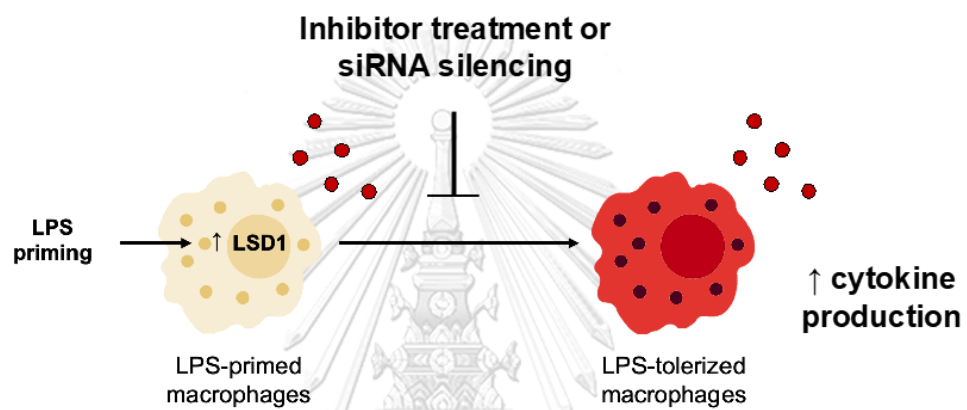
Figure 6.1 Role of LSD1 in regulation of LPS-tolerized macrophages

Effect of MGMT in regulation of trained Immunity

- A DNA repair enzyme MGMT was identified as a novel regulator of trained immunity.

- Inhibition or silencing of MGMT enhanced the effect of trained immunity by increasing both TNFα and IL-6 production.

- Depletion of MGMT resulted in suppress the effect of trained immunity in both *in vitro* and *in vivo* model.

- MGMT regulated trained immunity by interfering with downstream TLR4 signaling molecules such as p38 and SAPK/JNK, mTOR signaling and glycolytic function.
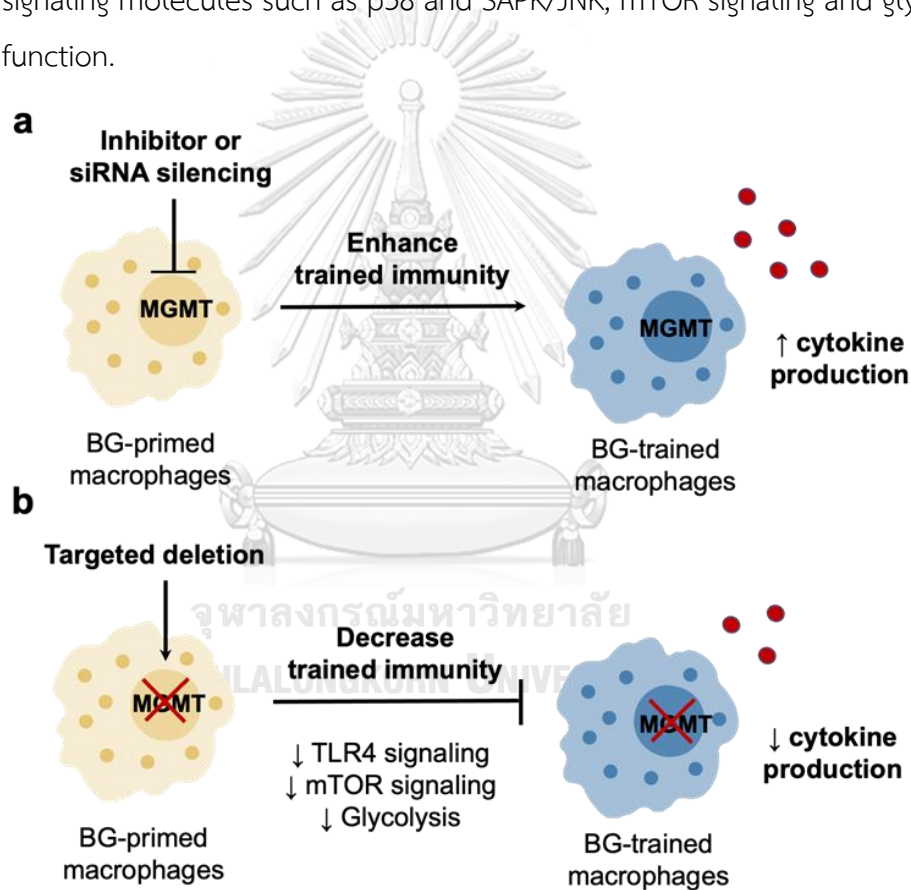
Figure 6.2 Role of MGMT in regulation of BG-trained macrophages (**a**) Transient inhibition or silencing of MGMT function during BG priming enhanced the effect of trained immunity. (**b**) Depletion of MGMT interfered TLR4 and mTOR signaling, which leads to decreased glycolysis and affects the trained immunity.

APPENDIX A

REGENTS USED IN THIS STUDY

1. Reagents for tissue culture

1.1 Serum inactivation

Commercial fetal bovine serum (FBS) and hourse serum which were kept at -20 °C was thawed at 4 °C for overnight and inactivated at 56 °C for 30 min. in water bath before use. The inactivate serum was aliquoted and stored at -20 °C.

1.2 Dulbecco's Modified Eagle (DMEM) complete media

FBS (Gibco)	4 mL
1 M HEPES (HyClone)	0.4 mL
100 mM Sodium Pyruvate (HyClone)	0.4 mL
10,000 unit/mL Pen/Strep (Invitrogen)	0.4 mL
DMEM high glucose (HyClone)	34.8 mL
Total	40 mL

1.3 Bone Marrow Macrophages differentiation media (BMM media)

Hourse serum (Hyclone)	2 mL
L929 condition media	8 mL
DMEM complete media	30 mL
Total	40 mL

To prepare L292 conditioned medium (contain M-CSF as a growth factor), 2×10^6 of L929 cells were grown in 10 cm TC plates (Corning^{TM}) in 8 mL DMEM complete media. After 4 days, the medium was collected, centrifuged, and filtered through 0.2 μm. L929 cells were collected by trypsinization (0.25% Trypsin) for further use. After 4 days of culture, L929 from one plate yield approximately 10×10^6 cells. The conditioned medium should be used with in 2 weeks.

1.4 20% DMSO Freezing media

DMSO	2 mL
FBS	8 mL
Total	10 mL

1.5 1x PBS buffer

10x PBS (Apsaiagent)	5 mL
Sterile water (Apsaiagent)	45 mL
Total	50 mL

2. Reagents for SDS-PAGE and Western blot assay

2.1 Ripa lysis buffer (500 mM NaCl, High salt)

1 M NaCl	500 µl
1 M Tris-HCl pH 7.4	50 µl
0.5 M EDTA	10 µl
20% SDS	5 µl
10% Sodium deoxychlorate	50 µl
Nonidet	10 µl
Sterile 18.2Ω water	375µl
Total	1 mL

2.2 Ripa lysis buffer (150 mM NaCl)

1 M NaCl	150 µl
1 M Tris-HCl pH 7.4	50 µl
0.5 M EDTA	10 µl
20% SDS	5 µl
10% Sodium deoxychlorate	50 µl
Nonidet	10 µl
Sterile 18.2Ω water	725µl
Total	1 mL

2.3 Separating gel

	8% gel	10% gel	15% gel
Sterile 18.2Ω water	4.236 mL	3.836 mL	3.436 mL
40% Acrylamide and Bis-acrylamide solution	1.6 mL	2 mL	2.4 mL
1.5 M Tris-HCl pH 8.8	2 mL	2 mL	2 mL
10% SDS	0.08 mL	0.08 mL	0.08 mL
10% Ammonium persulphate	0.08 mL	0.08 mL	0.08 mL
TEMED	0.004 mL	0.004 mL	0.004 mL
Total	8 mL	8 mL	8 mL

2.4 5% stacking gel

Sterile 18.2Ω water	1.204 mL
40% Acrylamide and Bis-acrylamide solution	0.25 mL
1 M Tris-HCl pH 6.8	0.504 mL
10% SDS	0.02 mL
10% Ammonium persulphate	0.02 mL
TEMED	0.002 mL
Total	2 mL

2.5 2x Laemmli buffer (SDS loading dye)

1 M Tris-HCl pH 6.8	1 mL
10% SDS	4 mL
99.5% glycerol	2 mL
Bromophenol blue	0.001 g
Sterile 18.2Ω water	2 mL
Total	9 mL

The 2x loading dye was filtered through 0.45 μm, aliquoted and stored at -20 °C until use. β-mercaptoethanol was add to 10% final concentration before use.

2.6 5x running buffer

Trisma base	15.1 g
Glycine	94 g
SDS	5 g
18.2Ω water was added to adjust volume into	1000 mL

2.7 1x transfer buffer

Trisma base	5.08 g
Glycine	2.9 g
SDS	0.37 g
18.2Ω water was added to adjust volume into	800 mL
Absolute methanol	200 mL
Total	1000 mL

2.8 10x PBS pH 7.4

NaCl	80 g
KCl	2 g
Na_2HPO_4	14.4 g
KH_2PO_4	2.4 g
18.2Ω water was added to adjust volume into	1000 mL

The buffer was autoclaved and diluted to 1x with deionized water before use.

2.9 ECL substrate

90 mM of Coumaric acid was dissolved in 10 ml DMSO, aliquoted and kept at -20 °C.

250 mM of Luminol was also dissolved in 10 ml DMSO, aliquoted and kept at -20 °C.

2.10 Substrate solution A

100 mM Tris-HCl pH 8.5	2.5 mL
90 mM coumaric acid	11 µl
250 mM luminol	22.5 µl

2.11 Substrate solution B

100 mM Tris-HCl pH 8.5	2.5 mL
30% H_2O_2	1.5 µl

3. Reagents and PCR condition for genotyping
3.1 Tissue digestion buffer

	concentration
50 mM KCl	50 mM
10 mM Tris-HCl	10 mM

Adjust pH to 9.0

The buffer was autoclaved and keep in 4 °C.

4 mg/mL Proteinase K and 0.1 % Triton X-100 were added before use.

3.2 PCR mixture

Genomic DNA	1 µl
10 µM forward primer	1 µl
10 µM reverse primer	1 µl
Taq polymerase	12.5 µl
DNase/RNase free water	9.5 µl
Total	25 µl

APPENDIX B

LIST OF COMPONDS IN EPIGENETIC COMPOUNDS LIBRARY

Appendix Table B1 List of compounds in the Epigenetic Compounds Library

(Selleckchem, USA) used in this study

List No.	Catalog Number	Product Name
1	S1004	Veliparib (ABT-888)
2	S1007	Roxadustat (FG-4592)
3	S1030	Panobinostat (LBH589)
4	S1045	Trichostatin A (TSA)
5	S1047	Vorinostat (SAHA, MK0683)
6	S1048	Tozasertib (VX-680, MK-0457)
7	S1053	Entinostat (MS-275)
8	S1060	Olaparib (AZD2281, Ku-0059436)
9	S1085	Belinostat (PXD101)
10	S1087	Iniparib (BSI-201)
11	S1090	Abexinostat (PCI-24781)
12	S1095	Dacinostat (LAQ824)
13	S1096	Quisinostat (JNJ-26481585) 2HCl
14	S1098	Rucaparib (AG-014699,PF-01367338) phosphate
15	S1100	MLN8054
16	S1103	ZM 447439
17	S1107	Danusertib (PHA-739358)
18	S1122	Mocetinostat (MGCD0103)
19	S1129	SRT1720 HCl
20	S1132	INO-1001 (3-Aminobenzamide)
21	S1133	Alisertib (MLN8237)
22	S1134	AT9283
23	S1143	AG-490 (Tyrphostin B42)
24	S1147	Barasertib (AZD1152-HQPA)
25	S1154	SNS-314 Mesylate
26	S1168	Valproic acid sodium salt (Sodium valproate)
27	S1171	CYC116
28	S1181	ENMD-2076
29	S1194	CUDC-101
30	S1200	Decitabine
31	S1216	PFI-1 (PF-6405761)
32	S1233	2-Methoxyestradiol (2-MeOE2)
33	S1249	JNJ-7706621

34	S1327	Ellagic acid
35	S1378	Ruxolitinib (INCB018424)
36	S1393	Pirarubicin
37	S1396	Resveratrol
38	S1422	Droxinostat
39	S1451	Aurora A Inhibitor I
40	S1454	PHA-680632
41	S1463	Ofloxacin
42	S1484	MC1568
43	S1509	Norfloxacin
44	S1515	Pracinostat (SB939)
45	S1529	Hesperadin
46	S1541	Selisistat (EX 527)
47	S1782	Azacitidine
48	S2012	PCI-34051
49	S2018	ENMD-2076 L-(+)-Tartaric acid
50	S2158	KW-2449
51	S2162	AZD1480
52	S2170	Givinostat (ITF2357)
53	S2178	AG-14361
54	S2179	Gandotinib (LY2784544)
55	S2198	SGI-1776 free base
56	S2214	AZ 960
57	S2219	Momelotinib (CYT387)
58	S2244	AR-42
59	S2391	Quercetin
60	S2554	Daphnetin
61	S2627	Tubastatin A HCl
62	S2686	NVP-BSK805 2HCl
63	S2692	TG101209
64	S2693	Resminostat
65	S2718	TAK-901
66	S2719	AMG-900
67	S2736	Fedratinib (SAR302503, TG101348)
68	S2740	GSK1070916
69	S2759	CUDC-907
70	S2770	MK-5108 (VX-689)
71	S2779	M344
72	S2789	Tofacitinib (CP-690550,Tasocitinib)
73	S2796	WP1066

74	S2804	Sirtinol
75	S2806	CEP-33779
76	S2818	Tacedinaline (CI994)
77	S2821	RG108
78	S2851	Baricitinib (LY3009104, INCB028050)
79	S2867	WHI-P154
80	S2886	PJ34
81	S2902	S-Ruxolitinib (INCB018424)
82	S2919	IOX2
83	S3001	Clevudine
84	S3147	Entacapone
85	S4125	Sodium Phenylbutyrate
86	S4246	Tranylcypromine (2-PCPA) HCl
87	S4294	Procainamide HCl
88	S5001	Tofacitinib (CP-690550) Citrate
89	S7029	AZD2461
90	S7036	XL019
91	S7041	CX-6258 HCl
92	S7062	Pinometostat (EPZ5676)
93	S7070	GSK J4 HCl
94	S7079	SGC 0946
95	S7088	UNC1215
96	S7104	AZD1208
97	S7110	(+)-JQ1
98	S7113	Zebularine
99	S7120	3-deazaneplanocin A (DZNeP) HCl
100	S7152	C646
101	S7189	I-BET-762
102	S7229	RGFP966
103	S7231	GSK2801
104	S7233	Bromosporine
105	S7234	IOX1
106	S7237	OG-L002
107	S7238	NVP-TNKS656
108	S7256	SGC-CBP30
109	S7265	MM-102
110	S7276	SGI-1027
111	S7281	JIB-04
112	S7292	RG2833 (RGFP109)
113	S7294	PFI-2 HCl

114	S7295	RVX-208
115	S7296	ML324
116	S7300	PJ34 HCl
117	S7304	CPI-203
118	S7305	MS436
119	S7315	PFI-3
120	S7324	TMP269
121	S7353	EPZ004777
122	S7360	OTX015
123	S7373	UNC669
124	S7438	ME0328
125	S7473	Nexturastat A
126	S7476	MG149
127	S7541	Decernotinib (VX-509)
128	S7555	4SC-202
129	S7570	UNC0379
130	S7572	A-366
131	S7574	GSK-LSD1 2HCl
132	S7581	GSK J1
133	S7582	Anacardic Acid
134	S7591	BRD4770
135	S7605	Filgotinib (GLPG0634)
136	S7610	UNC0631
137	S7611	EI1
138	S7616	CPI-169
139	S7618	MI-2 (Menin-MLL Inhibitor)
140	S7619	MI-3 (Menin-MLL Inhibitor)
141	S7620	GSK1324726A (I-BET726)
142	S7625	Niraparib (MK-4827) tosylate
143	S7641	Remodelin
144	S7656	CPI-360
145	S7680	SP2509
146	S7681	OF-1
147	S7748	EPZ015666(GSK3235025)
148	S7767	AZ6102
149	S7795	ORY-1001 (RG-6016) 2HCl
150	S7796	GSK2879552 2HCl
151	S7804	GSK503
152	S7805	EPZ011989
153	S7832	SGC707

154	S7835	I-BRD9
155	S8001	Ricolinostat (ACY-1215)
156	S8004	ZM 39923 HCl
157	S8005	SMI-4a
158	S8006	BIX 01294
159	S8038	UPF 1069
160	S8043	Scriptaid
161	S8049	Tubastatin A
162	S8056	Lomeguatrib
163	S8057	Pacritinib (SB1518)
164	S8096	Mirin
165	S8111	GSK591
166	S8112	MS023
167	S8146	Mitomycin C
168	S8179	BI-7273
169	S8180	PF-CBP1 HCl
170	S8195	Oclacitinib
171	S8209	HLCL-61 HCL
172	S8323	ITSA-1 (ITSA1)
173	S1149	Gemcitabine HCl
174	S1215	Carboplatin
175	S1373	Daptomycin
176	S1384	Mizoribine
177	S1648	Cytarabine
178	S1826	Nedaplatin
179	S1995	Procarbazine HCl
180	S7419	Blasticidin S HCl
181	S8197	APTSTAT3-9R

APPENDIX C

SUPPLEMENTARY RESULTS
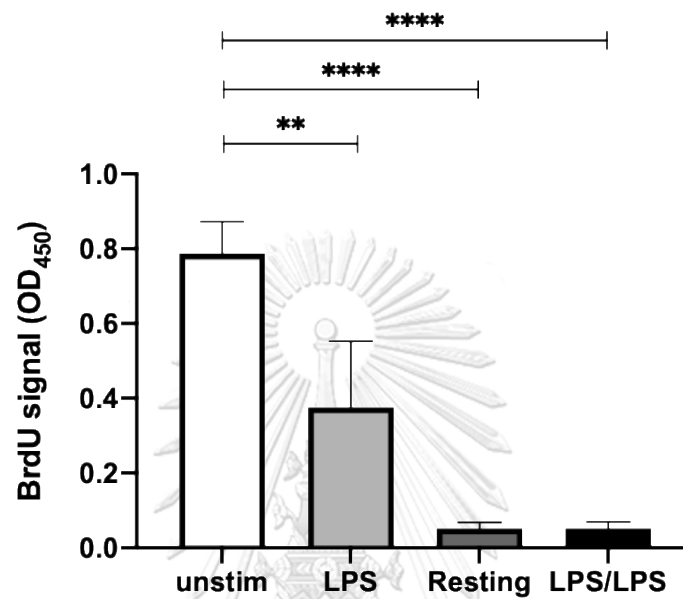
Appendix Figure C1 Cell proliferation in LPS-tolerant macrophages.

BMMs were treated as indicated for LPS-tolerant macrophages. Proliferation was measured by BrdU uptake. *, **, *** and **** indicate statistically significant difference by one-way ANOVA with Dunnett's multiple comparison test at $p< 0.05$, $p<0.01$, $p<0.001$ and $p<0.0001$, respectively.
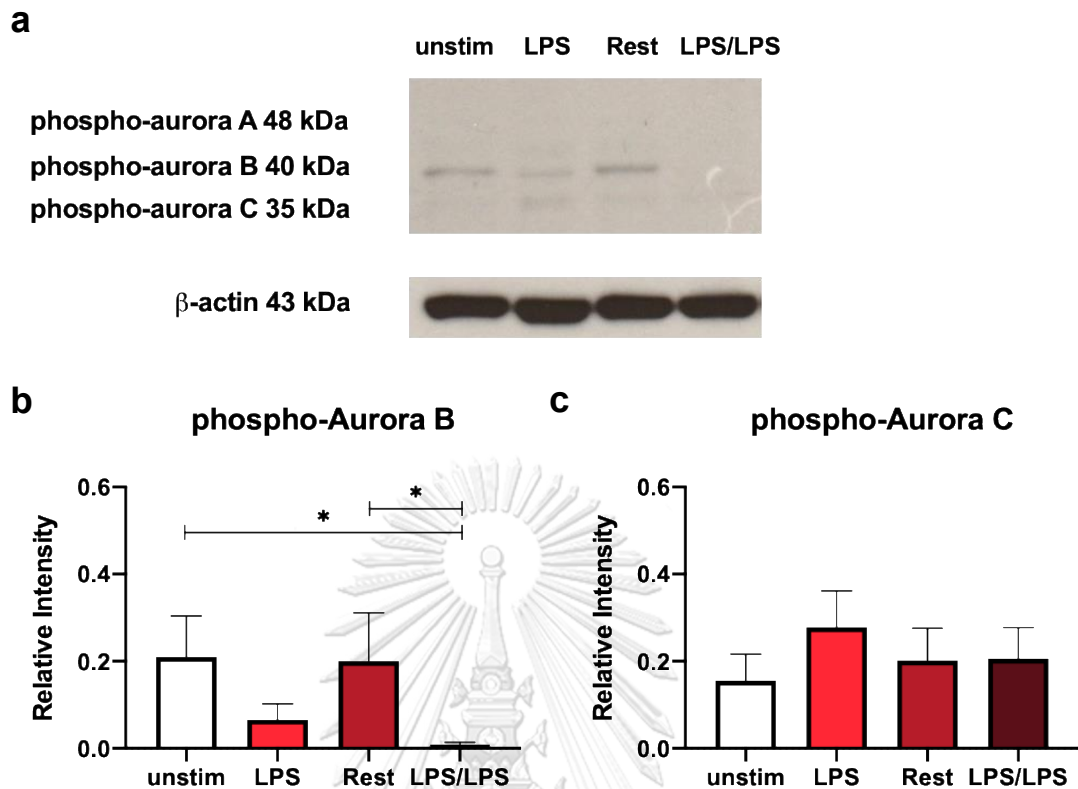
Appendix Figure C2 Expression profiles of Aurora kinase during LPS tolerance

(**a-c**) Phosphorylation of Aurora kinases was analyzed by Western blot. The relative intensity from Western blot was quantitated by ImageJ analysis and normalized to β-actin. *, **, *** and **** indicate significant differences compared by one-way ANOVA with Dunnett's multiple comparison test (a) and two-tailed unpaired t-test (d) at $p<$ 0.05, $p<0.01$, $p<0.001$ and $p<0.0001$, respectively.

a

b

Weight

Appendix Figure C3 General phenotype of WT and MGMT KO mice

(**a**) General phenotype of littermate control (WT) mice and MGMT KO at 8 weeks of age. (**b**) Weight of WT and MGMT KO mice measured at 8 weeks.

a

WT   MGMT KO

b   **c**
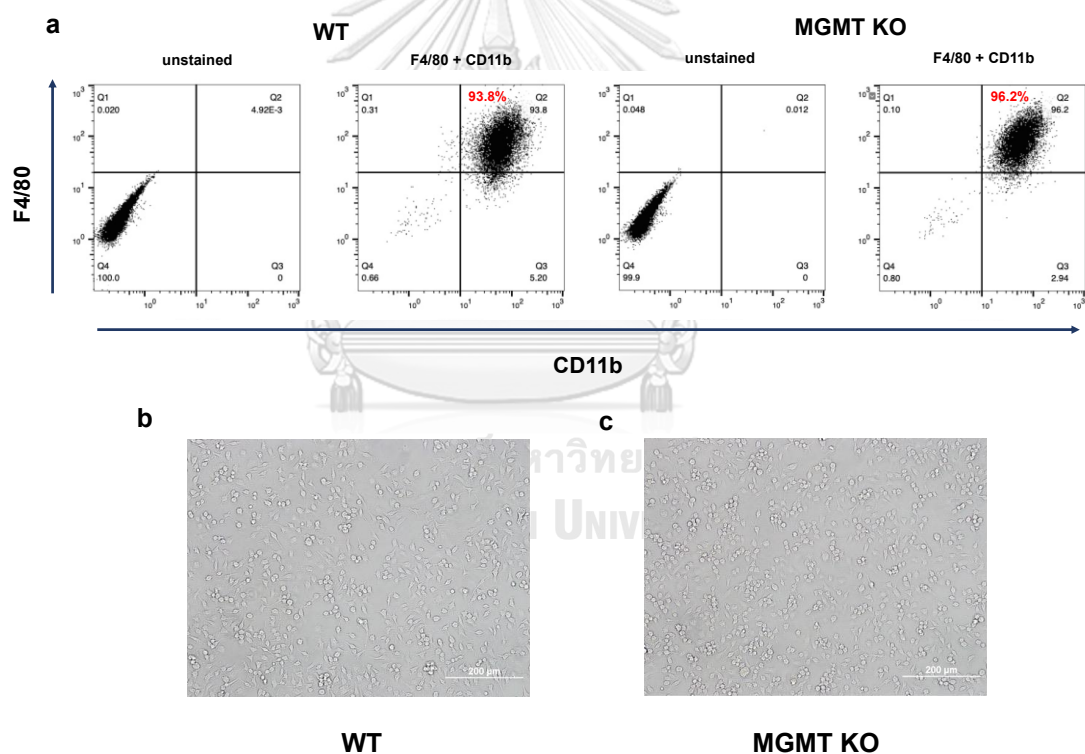
WT   MGMT KO

Appendix Figure C4 Purity of bone marrow derived macrophages of WT and MGMT KO mice

(**a**) Characterization of BMDMs by CD11b and F4/80 positive cells analyzed by flow cytometry. (**b-c**) Morphology of WT (**b**) and MGMT KO (**c**) macrophages after differentiation
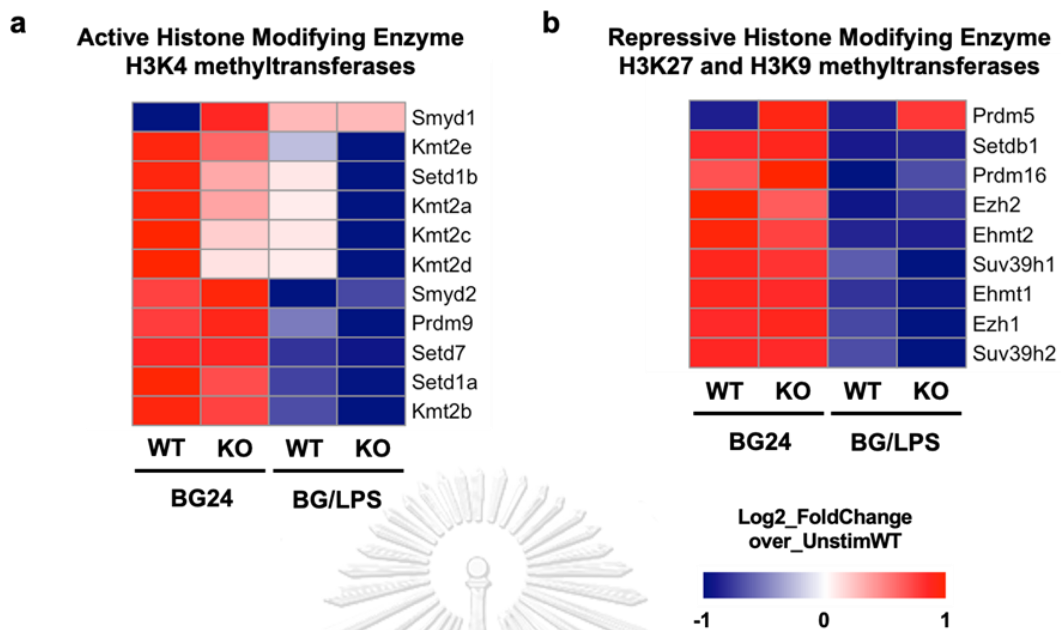
Appendix Figure C5 Expression profiles of epigenetic modifying enzyme in MGMT KO

macrophages

(**a-b**) Expression of active (**a**) and repressive (**b**) histone modifying enzyme during BG-

priming and LPS stimulation in WT and MGMT KO macrophages.

REFERENCES

1.   Netea MG, Dominguez-Andres J, Barreiro LB, Chavakis T, Divangahi M, Fuchs E, et al. Defining trained immunity and its role in health and disease. Nat Rev Immunol. 2020;20(6):375-88.

2.   Netea MG, Joosten LA, Latz E, Mills KH, Natoli G, Stunnenberg HG, et al. Trained immunity: A program of innate immune memory in health and disease. Science. 2016;352(6284):aaf1098.

3.   Netea MG, Quintin J, van der Meer JW. Trained immunity: a memory for innate host defense. Cell Host Microbe. 2011;9(5):355-61.

4.   Topfer E, Boraschi D, Italiani P. Innate Immune Memory: The Latest Frontier of Adjuvanticity. J Immunol Res. 2015;2015:478408.

5.   van der Heijden C, Noz MP, Joosten LAB, Netea MG, Riksen NP, Keating ST. Epigenetics and Trained Immunity. Antioxid Redox Signal. 2018;29(11):1023-40.

6.   Divangahi M, Aaby P, Khader SA, Barreiro LB, Bekkering S, Chavakis T, et al. Trained immunity, tolerance, priming and differentiation: distinct immunological processes. Nat Immunol. 2021;22(1):2-6.

7.   Fanucchi S, Dominguez-Andres J, Joosten LAB, Netea MG, Mhlanga MM. The Intersection of Epigenetics and Metabolism in Trained Immunity. Immunity. 2020.

8.   Durrant WE, Dong X. Systemic acquired resistance. Annu Rev Phytopathol. 2004;42:185-209.

9.   Moret Y, Siva-Jothy MT. Adaptive innate immunity? Responsive-mode prophylaxis in the mealworm beetle, Tenebrio molitor. Proc Biol Sci. 2003;270(1532):2475-80.

10.   Pham LN, Dionne MS, Shirasu-Hiza M, Schneider DS. A specific primed immune response in Drosophila is dependent on phagocytes. PLoS Pathog. 2007;3(3):e26.

11.   Arts RJW, Carvalho A, La Rocca C, Palma C, Rodrigues F, Silvestre R, et al. Immunometabolic Pathways in BCG-Induced Trained Immunity. Cell Rep. 2016;17(10):2562-71.

12.   Garly ML, Martins CL, Bale C, Balde MA, Hedegaard KL, Gustafson P, et al. BCG

scar and positive tuberculin reaction associated with reduced child mortality in West Africa. A non-specific beneficial effect of BCG? Vaccine. 2003;21(21-22):2782-90.

13. Benn CS, Netea MG, Selin LK, Aaby P. A small jab - a big effect: nonspecific immunomodulation by vaccines. Trends Immunol. 2013;34(9):431-9.

14. Foster SL, Hargreaves DC, Medzhitov R. Gene-specific control of inflammation by TLR-induced chromatin modifications. Nature. 2007;447(7147):972-8.

15. Jing J, Yang IV, Hui L, Patel JA, Evans CM, Prikeris R, et al. Role of macrophage receptor with collagenous structure in innate immune tolerance. J Immunol. 2013;190(12):6360-7.

16. Goh C, Knight JC. Enhanced understanding of the host-pathogen interaction in sepsis: new opportunities for omic approaches. Lancet Respir Med. 2017;5(3):212-23.

17. Kleinnijenhuis J, Quintin J, Preijers F, Joosten LA, Ifrim DC, Saeed S, et al. Bacille Calmette-Guerin induces NOD2-dependent nonspecific protection from reinfection via epigenetic reprogramming of monocytes. Proc Natl Acad Sci U S A. 2012;109(43):17537-42.

18. Quintin J, Saeed S, Martens JHA, Giamarellos-Bourboulis EJ, Ifrim DC, Logie C, et al. Candida albicans infection affords protection against reinfection via functional reprogramming of monocytes. Cell Host Microbe. 2012;12(2):223-32.

19. van der Valk FM, Bekkering S, Kroon J, Yeang C, Van den Bossche J, van Buul JD, et al. Oxidized Phospholipids on Lipoprotein(a) Elicit Arterial Wall Inflammation and an Inflammatory Monocyte Response in Humans. Circulation. 2016;134(8):611-24.

20. Bekkering S, Quintin J, Joosten LA, van der Meer JW, Netea MG, Riksen NP. Oxidized low-density lipoprotein induces long-term proinflammatory cytokine production and foam cell formation via epigenetic reprogramming of monocytes. Arterioscler Thromb Vasc Biol. 2014;34(8):1731-8.

21. Bekkering S, Arts RJW, Novakovic B, Kourtzelis I, van der Heijden C, Li Y, et al. Metabolic Induction of Trained Immunity through the Mevalonate Pathway. Cell. 2018;172(1-2):135-46 e9.

22. Garcia-Valtanen P, Guzman-Genuino RM, Williams DL, Hayball JD, Diener KR. Evaluation of trained immunity by beta-1, 3 (d)-glucan on murine monocytes in vitro and duration of response in vivo. Immunol Cell Biol. 2017;95(7):601-10.

23.   Schrum JE, Crabtree JN, Dobbs KR, Kiritsy MC, Reed GW, Gazzinelli RT, et al. Cutting Edge: Plasmodium falciparum Induces Trained Innate Immunity. J Immunol. 2018;200(4):1243-8.

24.   Novakovic B, Habibi E, Wang SY, Arts RJW, Davar R, Megchelenbrink W, et al. beta-Glucan Reverses the Epigenetic State of LPS-Induced Immunological Tolerance. Cell. 2016;167(5):1354-68 e14.

25.   Ifrim DC, Quintin J, Joosten LA, Jacobs C, Jansen T, Jacobs L, et al. Trained immunity or tolerance: opposing functional programs induced in human monocytes after engagement of various pattern recognition receptors. Clin Vaccine Immunol. 2014;21(4):534-45.

26.   Lachmandas E, Boutens L, Ratter JM, Hijmans A, Hooiveld GJ, Joosten LA, et al. Microbial stimulation of different Toll-like receptor signalling pathways induces diverse metabolic programmes in human monocytes. Nat Microbiol. 2016;2:16246.

27.   Armstrong L. Epigenetic. New York: Garland Science, Taylor & Francis Group, LLC; 2013.

28.   Bannister AJ, Kouzarides T. Regulation of chromatin by histone modifications. Cell Res. 2011;21(3):381-95.

29.   Saeed S, Quintin J, Kerstens HH, Rao NA, Aghajanirefah A, Matarese F, et al. Epigenetic programming of monocyte-to-macrophage differentiation and trained innate immunity. Science. 2014;345(6204):1251086.

30.   Ostuni R, Piccolo V, Barozzi I, Polletti S, Termanini A, Bonifacio S, et al. Latent enhancers activated by stimulation in differentiated cells. Cell. 2013;152(1-2):157-71.

31.   Fanucchi S, Fok ET, Dalla E, Shibayama Y, Borner K, Chang EY, et al. Publisher Correction: Immune genes are primed for robust transcription by proximal long noncoding RNAs located in nuclear compartments. Nat Genet. 2019;51(2):364.

32.   Fanucchi S, Fok ET, Dalla E, Shibayama Y, Borner K, Chang EY, et al. Immune genes are primed for robust transcription by proximal long noncoding RNAs located in nuclear compartments. Nat Genet. 2019;51(1):138-50.

33.   Chen X, El Gazzar M, Yoza BK, McCall CE. The NF-kappaB factor RelB and histone H3 lysine methyltransferase G9a directly interact to generate epigenetic silencing in endotoxin tolerance. J Biol Chem. 2009;284(41):27857-65.

34.   El Gazzar M, Yoza BK, Chen X, Hu J, Hawkins GA, McCall CE. G9a and HP1 couple histone and DNA methylation to TNFalpha transcription silencing during endotoxin tolerance. J Biol Chem. 2008;283(47):32198-208.

35.   Lehnertz B, Ueda Y, Derijck AA, Braunschweig U, Perez-Burgos L, Kubicek S, et al. Suv39h-mediated histone H3 lysine 9 methylation directs DNA methylation to major satellite repeats at pericentric heterochromatin. Curr Biol. 2003;13(14):1192-200.

36.   Zhang T, Cooper S, Brockdorff N. The interplay of histone modifications - writers that read. EMBO Rep. 2015;16(11):1467-81.

37.   Das J, Verma D, Gustafsson M, Lerm M. Identification of DNA methylation patterns predisposing for an efficient response to BCG vaccination in healthy BCG-naive subjects. Epigenetics. 2019;14(6):589-601.

38.   Verma D, Parasa VR, Raffetseder J, Martis M, Mehta RB, Netea M, et al. Anti-mycobacterial activity correlates with altered DNA methylation pattern in immune cells from BCG-vaccinated subjects. Sci Rep. 2017;7(1):12305.

39.   Sun R, Hedl M, Abraham C. Twist1 and Twist2 Induce Human Macrophage Memory upon Chronic Innate Receptor Treatment by HDAC-Mediated Deacetylation of Cytokine Promoters. J Immunol. 2019;202(11):3297-308.

40.   Cheng SC, Quintin J, Cramer RA, Shepardson KM, Saeed S, Kumar V, et al. mTOR- and HIF-1alpha-mediated aerobic glycolysis as metabolic basis for trained immunity. Science. 2014;345(6204):1250684.

41.   Keating ST, Groh L, van der Heijden C, Rodriguez H, Dos Santos JC, Fanucchi S, et al. The Set7 Lysine Methyltransferase Regulates Plasticity in Oxidative Phosphorylation Necessary for Trained Immunity Induced by beta-Glucan. Cell Rep. 2020;31(3):107548.

42.   Gillen J, Ondee T, Gurusamy D, Issara-Amphorn J, Manes NP, Yoon SH, et al. LPS Tolerance Inhibits Cellular Respiration and Induces Global Changes in the Macrophage Secretome. Biomolecules. 2021;11(2).

43.   Zhang D, Tang Z, Huang H, Zhou G, Cui C, Weng Y, et al. Metabolic regulation of gene expression by histone lactylation. Nature. 2019;574(7779):575-80.

44.   Mills EL, Ryan DG, Prag HA, Dikovskaya D, Menon D, Zaslona Z, et al. Itaconate is an anti-inflammatory metabolite that activates Nrf2 via alkylation of KEAP1. Nature.

2018;556(7699):113-7.

45. Kawasaki T, Kawai T. Toll-like receptor signaling pathways. Front Immunol. 2014;5:461.

46. Bohannon JK, Hernandez A, Enkhbaatar P, Adams WL, Sherwood ER. The immunobiology of toll-like receptor 4 agonists: from endotoxin tolerance to immunoadjuvants. Shock. 2013;40(6):451-62.

47. Sly LM, Rauh MJ, Kalesnikoff J, Song CH, Krystal G. LPS-induced upregulation of SHIP is essential for endotoxin tolerance. Immunity. 2004;21(2):227-39.

48. Liu ZJ, Liu XL, Zhao J, Shi YJ, Yan LN, Chen XF, et al. The effects of SOCS-1 on liver endotoxin tolerance development induced by a low dose of lipopolysaccharide are related to dampen NF-kappaB-mediated pathway. Dig Liver Dis. 2008;40(7):568-77.

49. Guha M, Mackman N. LPS induction of gene expression in human monocytes. Cell Signal. 2001;13(2):85-94.

50. Sato S, Takeuchi O, Fujita T, Tomizawa H, Takeda K, Akira S. A variety of microbial components induce tolerance to lipopolysaccharide by differentially affecting MyD88-dependent and -independent pathways. Int Immunol. 2002;14(7):783-91.

51. Yadav M, Schorey JS. The beta-glucan receptor dectin-1 functions together with TLR2 to mediate macrophage activation by mycobacteria. Blood. 2006;108(9):3168-75.

52. Carmena M, Earnshaw WC. The cellular geography of aurora kinases. Nat Rev Mol Cell Biol. 2003;4(11):842-54.

53. Willems E, Dedobbeleer M, Digregorio M, Lombard A, Lumapat PN, Rogister B. The functional diversity of Aurora kinases: a comprehensive review. Cell Div. 2018;13:7.

54. Sabbattini P, Canzonetta C, Sjoberg M, Nikic S, Georgiou A, Kemball-Cook G, et al. A novel role for the Aurora B kinase in epigenetic marking of silent chromatin in differentiated postmitotic cells. EMBO J. 2007;26(22):4657-69.

55. Ding L, Gu H, Gao X, Xiong S, Zheng B. Aurora kinase a regulates m1 macrophage polarization and plays a role in experimental autoimmune encephalomyelitis. Inflammation. 2015;38(2):800-11.

56. Zhang X, Wang Y, Yuan J, Li N, Pei S, Xu J, et al. Macrophage/microglial Ezh2 facilitates autoimmune inflammation through inhibition of Socs3. J Exp Med. 2018;215(5):1365-82.

57.   Rajan A, Shi H, Xue B. Class I and II Histone Deacetylase Inhibitors Differentially Regulate Thermogenic Gene Expression in Brown Adipocytes. Sci Rep. 2018;8(1):13072.

58.   Adcock IM. HDAC inhibitors as anti-inflammatory agents. Br J Pharmacol. 2007;150(7):829-31.

59.   Beurel E. HDAC6 regulates LPS-tolerance in astrocytes. PLoS One. 2011;6(10):e25804.

60.   Manni W, Jianxin X, Weiqi H, Siyuan C, Huashan S. JMJD family proteins in cancer and inflammation. Signal Transduct Target Ther. 2022;7(1):304.

61.   Perillo B, Tramontano A, Pezone A, Migliaccio A. LSD1: more than demethylation of histone lysine residues. Exp Mol Med. 2020;52(12):1936-47.

62.   Wang J, Saijo K, Skola D, Jin C, Ma Q, Merkurjev D, et al. Histone demethylase LSD1 regulates hematopoietic stem cells homeostasis and protects from death by endotoxic shock. Proc Natl Acad Sci U S A. 2018;115(2):E244-E52.

63.   Fulton MD, Brown T, Zheng YG. Mechanisms and Inhibitors of Histone Arginine Methylation. Chem Rec. 2018;18(12):1792-807.

64.   Kim JH, Yoo BC, Yang WS, Kim E, Hong S, Cho JY. The Role of Protein Arginine Methyltransferases in Inflammatory Responses. Mediators Inflamm. 2016;2016:4028353.

65.   Litt M, Qiu Y, Huang S. Histone arginine methylations: their roles in chromatin dynamics and transcriptional regulation. Biosci Rep. 2009;29(2):131-41.

66.   Rose M, Burgess JT, O'Byrne K, Richard DJ, Bolderson E. PARP Inhibitors: Clinical Relevance, Mechanisms of Action and Tumor Resistance. Front Cell Dev Biol. 2020;8:564601.

67.   Pazzaglia S, Pioli C. Multifaceted Role of PARP-1 in DNA Repair and Inflammation: Pathological and Therapeutic Implications in Cancer and Non-Cancer Diseases. Cells. 2019;9(1).

68.   Gerson SL. MGMT: its role in cancer aetiology and cancer therapeutics. Nat Rev Cancer. 2004;4(4):296-307.

69.   Teuber-Hanselmann S, Worm K, Macha N, Junker A. MGMT-Methylation in Non-Neoplastic Diseases of the Central Nervous System. Int J Mol Sci. 2021;22(8).

70.   Mokarram P, Kavousipour S, Sarabi MM, Mehrabani G, Fahmidehkar MA, Shamsdin SA, et al. MGMT-B gene promoter hypermethylation in patients with

inflammatory bowel disease - a novel finding. Asian Pac J Cancer Prev. 2015;16(5):1945-52.

71.   Guzman L, Depix MS, Salinas AM, Roldan R, Aguayo F, Silva A, et al. Analysis of aberrant methylation on promoter sequences of tumor suppressor genes and total DNA in sputum samples: a promising tool for early detection of COPD and lung cancer in smokers. Diagn Pathol. 2012;7:87.

72.   Su PF, Lee TC, Lin PJ, Lee PH, Jeng YM, Chen CH, et al. Differential DNA methylation associated with hepatitis B virus infection in hepatocellular carcinoma. Int J Cancer. 2007;121(6):1257-64.

73.   Xiaoming Zhang LK, Antonio M. Lerario,Marissa L. Dubbelaar, Nieske Brouwer, Evelyn M. Wesseling, Erik W.G.M. Boddeke, Bart J.L. Eggen, Susanne M. Kooistra. Epigenetic regulation of innate immune memory in microglia. bioRxiv2021.

74.   Mourits VP, Wijkmans JC, Joosten LA, Netea MG. Trained immunity as a novel therapeutic strategy. Curr Opin Pharmacol. 2018;41:52-8.

75.   Mulder WJM, Ochando J, Joosten LAB, Fayad ZA, Netea MG. Therapeutic targeting of trained immunity. Nat Rev Drug Discov. 2019;18(7):553-66.

76.   Sanchez-Ramon S, Conejero L, Netea MG, Sancho D, Palomares O, Subiza JL. Trained Immunity-Based Vaccines: A New Paradigm for the Development of Broad-Spectrum Anti-infectious Formulations. Front Immunol. 2018;9:2936.

77.   Livak KJ, Schmittgen TD. Analysis of relative gene expression data using real-time quantitative PCR and the 2(-Delta Delta C(T)) Method. Methods. 2001;25(4):402-8.

78.   Szklarczyk D, Gable AL, Lyon D, Junge A, Wyder S, Huerta-Cepas J, et al. STRING v11: protein-protein association networks with increased coverage, supporting functional discovery in genome-wide experimental datasets. Nucleic Acids Res. 2019;47(D1):D607-D13.

79.   Shi J, Hua L, Harmer D, Li P, Ren G. Cre Driver Mice Targeting Macrophages. Methods Mol Biol. 2018;1784:263-75.

80.   Kim D, Paggi JM, Park C, Bennett C, Salzberg SL. Graph-based genome alignment and genotyping with HISAT2 and HISAT-genotype. Nat Biotechnol. 2019;37(8):907-15.

81.   Liao Y, Smyth GK, Shi W. featureCounts: an efficient general purpose program for assigning sequence reads to genomic features. Bioinformatics. 2014;30(7):923-30.

82.   Liao Y, Smyth GK, Shi W. The Subread aligner: fast, accurate and scalable read mapping by seed-and-vote. Nucleic Acids Res. 2013;41(10):e108.

83.   Subramanian A, Tamayo P, Mootha VK, Mukherjee S, Ebert BL, Gillette MA, et al. Gene set enrichment analysis: a knowledge-based approach for interpreting genome-wide expression profiles. Proc Natl Acad Sci U S A. 2005;102(43):15545-50.

84.   Mootha VK, Lindgren CM, Eriksson KF, Subramanian A, Sihag S, Lehar J, et al. PGC-1alpha-responsive genes involved in oxidative phosphorylation are coordinately downregulated in human diabetes. Nat Genet. 2003;34(3):267-73.

85.   Liberzon A, Subramanian A, Pinchback R, Thorvaldsdottir H, Tamayo P, Mesirov JP. Molecular signatures database (MSigDB) 3.0. Bioinformatics. 2011;27(12):1739-40.

86.   Liberzon A, Birger C, Thorvaldsdottir H, Ghandi M, Mesirov JP, Tamayo P. The Molecular Signatures Database (MSigDB) hallmark gene set collection. Cell Syst. 2015;1(6):417-25.

87.   Viceconte N, Burguillos MA, Herrera AJ, De Pablos RM, Joseph B, Venero JL. Neuromelanin activates proinflammatory microglia through a caspase-8-dependent mechanism. J Neuroinflammation. 2015;12:5.

88.   Minashima T, Campbell KA, Hadley SR, Zhang Y, Kirsch T. The role of ANK interactions with MYBBP1a and SPHK1 in catabolic events of articular chondrocytes. Osteoarthritis Cartilage. 2014;22(6):852-61.

89.   Lai CF, Lin SL, Chiang WC, Chen YM, Wu VC, Young GH, et al. Blockade of cysteine-rich protein 61 attenuates renal inflammation and fibrosis after ischemic kidney injury. Am J Physiol Renal Physiol. 2014;307(5):F581-92.

90.   Palaga T, Buranaruk C, Rengpipat S, Fauq AH, Golde TE, Kaufmann SHE, et al. Notch signaling is activated by TLR stimulation and regulates macrophage functions. European Journal of Immunology. 2008;38(1):174-83.

91.   Magner WJ, Kazim AL, Stewart C, Romano MA, Catalano G, Grande C, et al. Activation of MHC class I, II, and CD40 gene expression by histone deacetylase inhibitors. J Immunol. 2000;165(12):7017-24.

92.   Syed KM, Joseph S, Mukherjee A, Majumder A, Teixeira JM, Dutta D, et al. Correction: Histone chaperone APLF regulates induction of pluripotency in murine fibroblasts (doi:10.1242/jcs.194035). J Cell Sci. 2018;131(8).

93.   Kin NW, Chen Y, Stefanov EK, Gallo RL, Kearney JF. Cathelin-related antimicrobial peptide differentially regulates T- and B-cell function. Eur J Immunol. 2011;41(10):3006-16.

94.   Hwang I, Cao D, Na Y, Kim DY, Zhang T, Yao J, et al. Far Upstream Element-Binding Protein 1 Regulates LSD1 Alternative Splicing to Promote Terminal Differentiation of Neural Progenitors. Stem Cell Reports. 2018;10(4):1208-21.

95.   Wongchana W, Lawlor RG, Osborne BA, Palaga T. Impact of Notch1 Deletion in Macrophages on Proinflammatory Cytokine Production and the Outcome of Experimental Autoimmune Encephalomyelitis. J Immunol. 2015;195(11):5337-46.

96.   Saz-Leal P, Del Fresno C, Brandi P, Martinez-Cano S, Dungan OM, Chisholm JD, et al. Targeting SHIP-1 in Myeloid Cells Enhances Trained Immunity and Boosts Response to Infection. Cell Rep. 2018;25(5):1118-26.

97.   Hu L, Yu Y, Huang H, Fan H, Hu L, Yin C, et al. Epigenetic Regulation of Interleukin 6 by Histone Acetylation in Macrophages and Its Role in Paraquat-Induced Pulmonary Fibrosis. Front Immunol. 2016;7:696.

98.   Benjaskulluecha S, Boonmee A, Pattarakankul T, Wongprom B, Klomsing J, Palaga T. Screening of compounds to identify novel epigenetic regulatory factors that affect innate immune memory in macrophages. Sci Rep. 2022;12(1):1912.

99.   Rodriguez RM, Suarez-Alvarez B, Lopez-Larrea C. Therapeutic Epigenetic Reprogramming of Trained Immunity in Myeloid Cells. Trends Immunol. 2019;40(1):66-80.

100.   Xiong Y, Medvedev AE. Induction of endotoxin tolerance in vivo inhibits activation of IRAK4 and increases negative regulators IRAK-M, SHIP-1, and A20. J Leukoc Biol. 2011;90(6):1141-8.

101.   Seeley JJ, Ghosh S. Molecular mechanisms of innate memory and tolerance to LPS. J Leukoc Biol. 2017;101(1):107-19.

102.   Duan R, Du W, Guo W. EZH2: a novel target for cancer treatment. J Hematol Oncol. 2020;13(1):104.

103.   Luo Y, Fang Y, Kang R, Lenahan C, Gamdzyk M, Zhang Z, et al. Inhibition of EZH2 (Enhancer of Zeste Homolog 2) Attenuates Neuroinflammation via H3k27me3/SOCS3/TRAF6/NF-kappaB (Trimethylation of Histone 3 Lysine 27/Suppressor

of Cytokine Signaling 3/Tumor Necrosis Factor Receptor Family 6/Nuclear Factor-kappaB) in a Rat Model of Subarachnoid Hemorrhage. Stroke. 2020;51(11):3320-31.

104.   Cheng SC, Scicluna BP, Arts RJ, Gresnigt MS, Lachmandas E, Giamarellos-Bourboulis EJ, et al. Broad defects in the energy metabolism of leukocytes underlie immunoparalysis in sepsis. Nat Immunol. 2016;17(4):406-13.

105.   Bavetsias V, Linardopoulos S. Aurora Kinase Inhibitors: Current Status and Outlook. Front Oncol. 2015;5:278.

106.   Le LT, Vu HL, Nguyen CH, Molla A. Basal aurora kinase B activity is sufficient for histone H3 phosphorylation in prophase. Biol Open. 2013;2(4):379-86.

107.   Blas-Rus N, Bustos-Moran E, Perez de Castro I, de Carcer G, Borroto A, Camafeita E, et al. Aurora A drives early signalling and vesicle dynamics during T-cell activation. Nat Commun. 2016;7:11389.

108.   Batista IAA, Helguero LA. Biological processes and signal transduction pathways regulated by the protein methyltransferase SETD7 and their significance in cancer. Signal Transduct Target Ther. 2018;3:19.

109.   Yu W, Zhang L, Wei Q, Shao A. O(6)-Methylguanine-DNA Methyltransferase (MGMT): Challenges and New Opportunities in Glioma Chemotherapy. Front Oncol. 2019;9:1547.

110.   De Bont R, van Larebeke N. Endogenous DNA damage in humans: a review of quantitative data. Mutagenesis. 2004;19(3):169-85.

111.   Fahrer J, Kaina B. O6-methylguanine-DNA methyltransferase in the defense against N-nitroso compounds and colorectal cancer. Carcinogenesis. 2013;34(11):2435-42.

112.   Zhang BG, Hu L, Zang MD, Wang HX, Zhao W, Li JF, et al. Helicobacter pylori CagA induces tumor suppressor gene hypermethylation by upregulating DNMT1 via AKT-NFkappaB pathway in gastric cancer development. Oncotarget. 2016;7(9):9788-800.

113.   Glassner BJ, Weeda G, Allan JM, Broekhof JL, Carls NH, Donker I, et al. DNA repair methyltransferase (Mgmt) knockout mice are sensitive to the lethal effects of chemotherapeutic alkylating agents. Mutagenesis. 1999;14(3):339-47.

114.   Niture SK, Doneanu CE, Velu CS, Bailey NI, Srivenugopal KS. Proteomic analysis of human O6-methylguanine-DNA methyltransferase by affinity chromatography and

tandem mass spectrometry. Biochem Biophys Res Commun. 2005;337(4):1176-84.

115.   Schaap FG, Trauner M, Jansen PL. Bile acid receptors as targets for drug development. Nat Rev Gastroenterol Hepatol. 2014;11(1):55-67.

116.   Fiorucci S, Biagioli M, Zampella A, Distrutti E. Bile Acids Activated Receptors Regulate Innate Immunity. Front Immunol. 2018;9:1853.

117.   Trabelsi MS, Daoudi M, Prawitt J, Ducastel S, Touche V, Sayin SI, et al. Farnesoid X receptor inhibits glucagon-like peptide-1 production by enteroendocrine L cells. Nat Commun. 2015;6:7629.

118.   Cariou B, Staels B. FXR: a promising target for the metabolic syndrome? Trends Pharmacol Sci. 2007;28(5):236-43.

119.   Fiorucci S, Antonelli E, Rizzo G, Renga B, Mencarelli A, Riccardi L, et al. The nuclear receptor SHP mediates inhibition of hepatic stellate cells by FXR and protects against liver fibrosis. Gastroenterology. 2004;127(5):1497-512.

120.   Mencarelli A, Renga B, Migliorati M, Cipriani S, Distrutti E, Santucci L, et al. The bile acid sensor farnesoid X receptor is a modulator of liver immunity in a rodent model of acute hepatitis. J Immunol. 2009;183(10):6657-66.

121.   Vavassori P, Mencarelli A, Renga B, Distrutti E, Fiorucci S. The bile acid receptor FXR is a modulator of intestinal innate immunity. J Immunol. 2009;183(10):6251-61.

122.   Yao J, Zhou CS, Ma X, Fu BQ, Tao LS, Chen M, et al. FXR agonist GW4064 alleviates endotoxin-induced hepatic inflammation by repressing macrophage activation. World J Gastroenterol. 2014;20(39):14430-41.

123.   Duan Z, Person RE, Lee HH, Huang S, Donadieu J, Badolato R, et al. Epigenetic regulation of protein-coding and microRNA genes by the Gfi1-interacting tumor suppressor PRDM5. Mol Cell Biol. 2007;27(19):6889-902.

124.   Porter LF, Galli GG, Williamson S, Selley J, Knight D, Elcioglu N, et al. A role for repressive complexes and H3K9 di-methylation in PRDM5-associated brittle cornea syndrome. Hum Mol Genet. 2015;24(23):6565-79.

125.   Li JP, Zeng SH, Zhang YH, Liu YJ. Bioinformatics-based analysis of the association between the A1-chimaerin (CHN1) gene and gastric cancer. Bioengineered. 2021;12(1):2874-89.

126.   Rourke JL, Dranse HJ, Sinal CJ. Towards an integrative approach to

understanding the role of chemerin in human health and disease. Obes Rev. 2013;14(3):245-62.

127. Hong SN, Joung JG, Bae JS, Lee CS, Koo JS, Park SJ, et al. RNA-seq Reveals Transcriptomic Differences in Inflamed and Noninflamed Intestinal Mucosa of Crohn's Disease Patients Compared with Normal Mucosa of Healthy Controls. Inflamm Bowel Dis. 2017;23(7):1098-108.

128. Rebe C, Demontoux L, Pilot T, Ghiringhelli F. Platinum Derivatives Effects on Anticancer Immune Response. Biomolecules. 2019;10(1).

129. Boonmee A, Benjaskulluecha S, Kueanjinda P, Wongprom B, Pattarakankul T, Palaga T. The chemotherapeutic drug carboplatin affects macrophage responses to LPS and LPS tolerance via epigenetic modifications. Sci Rep. 2021;11(1):21574.

130. Kurash JK, Lei H, Shen Q, Marston WL, Granda BW, Fan H, et al. Methylation of p53 by Set7/9 mediates p53 acetylation and activity in vivo. Mol Cell. 2008;29(3):392-400.

131. Zhang X, Huang Y, Shi X. Emerging roles of lysine methylation on non-histone proteins. Cell Mol Life Sci. 2015;72(22):4257-72.

132. Bekkering S, Joosten LA, Netea MG, Riksen NP. Trained innate immunity as a mechanistic link between sepsis and atherosclerosis. Crit Care. 2014;18(6):645.

VITA

NAME	Salisa Benjaskulluecha
DATE OF BIRTH	30 March 1995
PLACE OF BIRTH	Bangkok, Thailand
INSTITUTIONS ATTENDED	2013-2016
	Bachelor of Science (Second Class Honors)
	Department of Microbiology, Faculty of Science,
	Chulalongkorn University
	2017-present
	Doctor of Philosophy Program in Medical Microbiology,
	Interdisciplinary Program, Graduate School,
	Chulalongkorn University
HOME ADDRESS	15/27 Nalin Residence, Hathairat Rd., Bang chan, Klong samwa,
	Bangkok, Thailand, 10510
PUBLICATION	1. Laopanupong T, Prombutara P, Kanjanasirirat P, Benjaskulluecha S, Boonmee A, Palaga T, et al. Lysosome repositioning as an autophagy escape mechanism by Mycobacterium tuberculosis Beijing strain. Sci Rep. 2021;11(1):4342.
	2. Boonmee A, Benjaskulluecha S, Kueanjinda P, Wongprom B, Pattarakankul T, Palaga T. The chemotherapeutic drug carboplatin affects macrophage responses to LPS and LPS tolerance via epigenetic modifications. Sci Rep. 2021;11(1):21574.
	3. Benjaskulluecha S, Boonmee A, Pattarakankul T, Wongprom B, Klomsing J, Palaga T.

Screening of compounds to identify novel epigenetic regulatory factors that affect innate immune memory in macrophages. Sci Rep. 2022;12(1):1912.

AWARD RECEIVED

1. The 100th Anniversary Chulalongkorn University Fund for Doctoral Scholarship (2017-2022)

2. The FIMSA Travel Awards at the 48th Annual Meeting of JSI December 11-13, 2019. Hamamatsu, Japan

3. The 90th Anniversary Chulalongkorn University Fund (Ratchadaphiseksomphot Endowment Fund, 2020)

4. Oral Presentation Immunology Award at The 38th Annual Hybrid Meeting of The Allergy, Asthma & Immunology Association of Thailand 30 March 2022